The Dissertation Committee for Charles Aaron Seipp Certifies that this is the approved version of the following dissertation:

Guanidinium-Based Receptors for Anion Separations

Committee:

Jonathan Sessler, Supervisor

Bruce Moyer

Eric Anslyn

Sean M. Kerwin

Stephen F. Martin

Simon Humphrey

Guanidinium-Based Receptors for Anion Separations

by

Charles Aaron Seipp, B.A.; M.A.

Dissertation

Presented to the Faculty of the Graduate School of

The University of Texas at Austin

in Partial Fulfillment

of the Requirements

for the Degree of

Doctor of Philosophy

The University of Texas at Austin

May 2017

Dedication

I'd like to dedicate this work to my parents. Their understanding and support throughout my life has been instrumental to everything I've done. They sacrificed whatever it took in order to make sure I had a good life, and I appreciate that every day. Thank you Mom and Dad.

Acknowledgements

First and foremost, I owe sincere thanks to Dr. Bruce Moyer. Without him taking me under his wing, I likely would not be in a position to write these acknowledgements! His mentorship and passion for separations chemistry enabled me to become the scientist I am today.

Next, thank you Dr. Sessler for becoming my advisor in a time of need.

Thank you Dr. Radu Custelcean. You are a great mentor and friend, and you took so much of your time to help me grow even further as both a chemist and a person.

To Neil, Will, Kyle, and Alan: Thank you for being the wonderful friends you are and supporting me when needed, both in lab, at home, and out on the town. It was a privilege getting to work with you all and getting to know you as both friends and scientists over the last five years.

Guanidinium-Based Receptors for Anion Separations

Charles Aaron Seipp, Ph.D.

The University of Texas at Austin, 2017

Supervisor: Jonathan Sessler

Herein, work on guanidinium-based anion receptors and their anion separation properties are described. First, a novel receptor based on the N,N'-bis(2-pyridyl)guanidinium motif is rationally designed, synthesized, and characterized. In the solid state, X-ray crystallography shows that is has a strong conformational preference for the α,α form of the molecule. This ligand has association constants of 3.78 ± 0.12 and 2.10 ± 0.23 respectively for log K_1 and log K_2. A lipophilic form of this ligand was synthesized for extraction studies, where it performed better than commercially available Aliquat 336 for the extraction of sulfate into 1,2-DCE from water. Next, a series of bis(imino)guanidinium ligands are created that are capable of forming highly insoluble salts with many oxoanions, the most insoluble being sulfate. This leads to novel methods of separation of highly charged oxoanion species by precipitation followed by simple filtration, and its use was demonstrated on natural seawater. This methodology was adapted to the sequestration of CO_2 from ambient air, leading to an effective method for the crystallization of CO_2 as its carbonate salt from water as well as its low temperature release. Finally, future work towards the creation of iminoguanidinium-based oxoanion receptors is described.

Table of Contents

List of Tables

List of Figures

Chapter 1: Introduction

Separation

noun:

The division of something into constituent or distinct elements.

The oxford dictionary's simple definition of *separation* belies the distinct challenge of this word when applied to chemical practice.[1] Indeed, chemical separations are complicated and often times misunderstood phenomena where, through a series of physical and/or chemical manipulations one substance is separated from another. Yet, despite the complexity, separations occur in every facet of everyday life. Water is purified and rendered drinkable from sewage, and lively spirits are created through distillations and filtrations. On the outside, these processes are simple, and indeed they are when the molecular mechanics involved are ignored. It is easy to forget that all of these macroscopic changes occur due to separations taking place on a molecular level. Water purification occurs by separating undesired molecules from bulk water. These molecular impurities may be toxic chromate, arsenic, mercury, or other contaminants that would render the water undrinkable. Chemical separation via distillation is possible through exploiting differences in the boiling points of the constituents due to variation in the strengths of -intramolecular interactions. When one accounts for the intra- and inter-molecular interactions, the densities, dielectric constants, and Coulombic interactions,

chemical separations are, in the opinion of many scientists, a fascinating and diverse research area.

The breadth of the subject means that separations chemistry is composed of many sub-areas ranging from cation recognition to process design and implementation; my research efforts thus far have been focused largely on the design and synthesis of selective complexants for the binding, extraction, and precipitation of environmentally relevant oxoanions from aqueous solutions. It has been our aim to use new approaches in ligand design, from the use of intramolecular hydrogen-bond stabilized pseudo bicyclic systems to *in situ* receptor formation to create new receptors and processes that allow for effective and energy efficient methods of oxoanion separations. Before we go further into this research, it is important to take a step back and fully understand the problems at hand. Oxoanions are molecular species comprised of multiple oxygen atoms bound to a central element, with the overall structure having an inherent negative charge. Common examples include sulfate, chromate, phosphate, carbonate, and nitrate **(Figure 1.1)**.

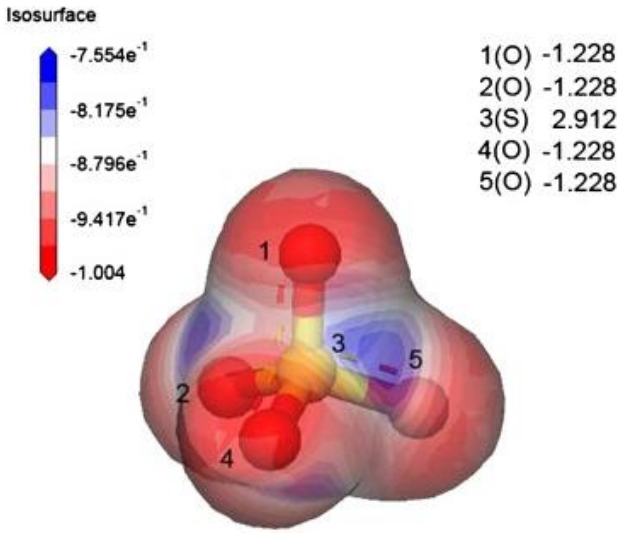

Figure 1.1: Electrostatic potential map of sulfate. Regions of electron density can be found around the edges Reused with permission from: Shim, H.; Kim, J.; Koo, K.; *J. Cryst. Growth*, **2013**, *373*, 64-68.[2]

These anions have broad implications in many relevant processes in biology and the environment. In biology, anion recognition plays a pivotal role in the Krebs cycle with ATP recognition being key in supplying the chemical potential needed to sustain cellular processes.[3] In the environment, excesses of phosphate or nitrate from agricultural run-off have been linked to occurrences of algae blooms and red tide, stripping oxygen from the water and promoting the growth of toxic dinoflagellates.[4] Additionally chromate and arsenate pollute many sources of otherwise fresh potable groundwater.

Sulfate, another oxoanion, is unique from the others mentioned as the need for effective sulfate separation is not immediately obvious. While sulfate is well known for fouling oil wells due to the formation of insoluble barium sulfate salts,[5] this troublesome oxoanion is also making nuclear waste cleanup exponentially more costly by increasing the volume of waste needing to be processed and disposed.[6] Over the last several decades, countless millions of gallons of nuclear waste have been produced and has been sitting in storage tanks awaiting processing. Just at the Hanford site alone, there are 55 million gallons of unprocessed high level waste stored there, which is estimated to cost around $100 million.[7] There are many different chemical separations used to process waste, ranging from the CSSX [8] and NGS processes[9] to remove radioactive cesium to the use of monosodium titanate[10] to remove the strontium and actinides. Even after removing the most radiotoxic and undesirable from the waste, it still must be stabilized and stored.

One of the leading methods for the stabilization and safe storage of high level nuclear waste is vitrification- this involves taking concentrated radioactive waste forms, mixing it with silica and heating it in a metal canister until a glass is formed.[7] This stable glass is then safely stored in geological repositories. Unfortunately, the presence of sulfate complicates this procedure. Sulfate has an extremely low solubility in the glass mixture, causing it to precipitate and drastically weaken the glass; this corresponds to needing to increase the volume of produced glass by 10-30%.[6] The presence of even a small amount of sulfate drastically increases the cost of the vitrification process. Unfortunately, the

Hanford site's waste contains large quantities of sulfate, with the concentration being about **0.2%** by mass.[11] It is easy to see that removing this troublesome anion from the HLW could provide substantial cost and volume reduction, providing an impetus to continue research on sulfate separation.

Unfortunately, the selective binding and separation of oxoanions, in particular those with a high charge density like sulfate, is a challenging prospect. In order to interact with oxoanions, one must be able to recognize them at the molecular level in solution. While a seemingly simple problem, the innate characteristics of oxoanions makes this a profound challenge due to their inherent charge and numerous hydrogen bond acceptors, which have a very strongly bound hydration shell in aqueous solution.[12] Sulfate, due to its extremely high charge density, has a free energy of hydration of –1080 kJ mol^{-1}.[12] Water is an excellent hydrogen bond donor, and given that the effective molarity of pure water hovers around 55 *M*, the odds are clearly not in the receptor's favor. To further complicate matters, anions are very charge diffuse and come in many different shapes and larger sizes than cations.[13] Thus, using electrostatic interactions for binding is much more difficult in the case of anions than in the case of cations. These small individual problems combine to make anion binding in solution very difficult.

The challenge of anion recognition and separation has attracted many notable scientists to the field, and their triumphs and failures have helped to develop an understanding of what

makes a good anion receptor. Many consider Simmons and Park to be the founders of the field[13], as they were some of the first to publish their work on anion receptors in 1968.[14] In this work, they reported several different receptors based on ammonium macrocycles that bound to halides **(Figure 1.2).**

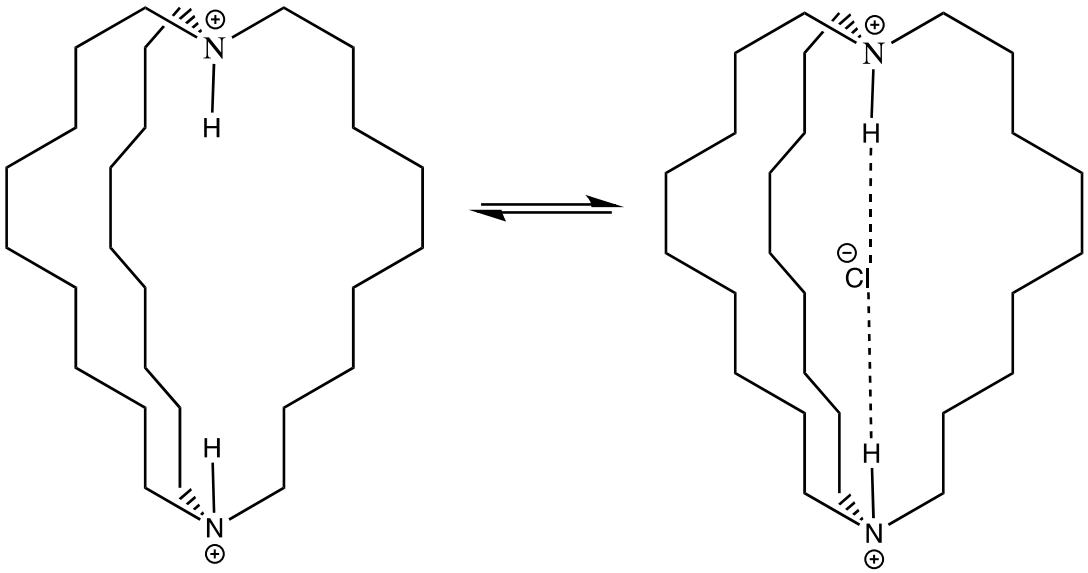

Figure 1.2: Simmons and Park's anion receptor. Chloride can be seen binding within the cleft of the macrocycle. This simplistic receptor helped to spur research within the field.

Simmons and Park used NMR spectroscopy to determine, that chloride in aqueous solution would diffuse into the receptor to form a stable complexes. A K_a of 4 M^{-1} for the chloride-ligand complex was determined via titration of a solution of the ligand in 50% deuterated trifluoroacetic acid which contained chloride and they hypothesized that the anion was likely found within the receptor. Interestingly, they casually noted that

bromide was encapsulated much less strongly than chloride and iodide showed no affinity for the ligand. Later crystal structures would confirm this hypothesis.[15] They reasoned that these bigger anions were simply too big to fit within the binding pocket of the receptor, thus there was a sort of size complementarity between the host and the guest able to bind.

It should be noted that the quantification of the binding affinity (K_a), can be related to the equilibrium concentrations of the host, guest, and formed complex. Take a ligand, L, that forms a 1:1 complex with a given analyte, A. The K_a can be determined by comparing the equilibrium concentrations of the species, where [L], [A], and [LA] refer to the concentrations of the ligand, anion, and complex respectively. (Figure **1.3**).

$$K_a = \frac{[LA]}{[L][A]}$$

Figure 1.3: The binding affinity can be related to the equilibrium concentrations of the receptor, guest, and complex.

Using this technique, the oxoanion guest is unobservable by ^{1}H-NMR and often the binding of the guest and host is very fast in comparison to the NMR time scale. This leads to an averaging of the peaks of the complex and the free guest. This makes it difficult to determine the exact concentrations by NMR. Thus, these values have to be inferred or observed indirectly which often descends into a complex mixture of mass-

balance equations, quadratics, and line fitting.[16] While Simmons and Park had to struggle with the derivation of these equations by hand, there are many modern software packages including HypNMR[17] and Pall Thordarson's fitting programs on supramolecular.org[18] that help to simplify these calculations.

While Simmons and Park's work can be considered basic when compared to modern anion receptors, it was revolutionary for its time. They proved that small, and more importantly non-biological molecules were capable of selectively binding anions and that anions could be discriminated based on size. This was a research area that had not been previously explored and their findings spurred the development of a brand new field. Soon after, future Nobel Laureate Dr. Jean-Marie Lehn made substantial contributions to the field discovering many host-guest complexes and further solidifying the concept of size complementarity.[19,20] While examining cryptand receptors and their binding to halide species, he recognized that an anion must be of the correct size to fit into a host molecule (**Figure 1.4).**

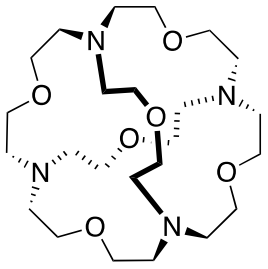

Figure 1.4: Example of one of Lehn's macro-tricyclic ammonium receptors. These interesting cryptand-like anion receptors will only bind smaller anions, like chloride, capable of fitting inside.

Lehn and his co-workers had observed that these cryptands seemed to only include anions that were of a certain size; while the ligands would bind to chloride, iodide showed little affinity due to its large size. Thus, he hypothesized, that molecules must be able to fit into the receptor in order to bind. The difference in binding depending on the size of the anion was staggering. For chloride, binding constants of log $K_a > 4.0$ were observed. Upon moving to the bigger bromide however, these dropped off to a log K_a of < 1.0. Relatively small difference in ionic radius (181 pm vs. 196 pm respectively)[21] corresponds to orders of magnitude difference in binding affinities. This work helped corroborate Park and Simmon's observation that chloride but not iodide would bind in their macrocyclic ammonium receptors. While simple in hindsight, size complementarity has significant implications in the design of anion receptors. In order to accommodate a desired anion, it must be able to fit within the binding pocket of the receptor. If the molecule is too big, it simply will not be able to fit. If it's too small, the binding interactions will not be as strong as they could if ion is of an optimal size. This has

profound implications as well on selectivity in binding. By designing a receptor with a binding pocket of a certain size, one can selectively bind oxoanions of a certain size. While discovered back in the late 1960s and early 70s, the notion of size complementarity is a huge driving force in anion recognition even today and plays a large role even in the work described herein.

While it was strongly implied by Lehn, Simmons, and Park's early work, having a complementarity shape is also of utmost important for strong binding. Lehn outlined this well in his Nobel lecture where he discussed the ability of these cryptands to recognize the tetrahedral ammonium cation. [22] As the neutral receptor, the cryptand contains four nitrogen and six oxygen binding sites. These sites are spaced perfectly apart so that the lone pair on the four amines is able to interact strongly with the four protons on the ammonium. Furthermore, the six oxygens are positioned to donate some electron density into the positively charged cation. This shape or "structural" complementarity as Lehn refers to it revolves around the receptor's ability to take a form that allows for strong interactions with the target species. While this example from Lehn focuses on a tetrahedral cation, the same principals apply to non-spherical anions as well.

While size and shape complementarity both help to increase anion affinity, another concept, *charge* complementarity is just as important. Schmidtchen and co-workers were

one of the first to explore this concept with their tetrahedral quaternary ammonium based receptors **(Figure 1.5).**[23]

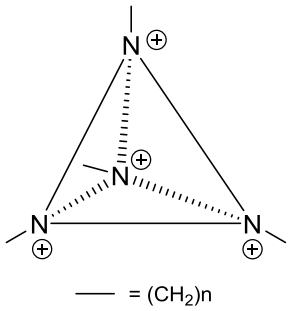

Figure 1.5: Schmitchen's charged tetrahedral anion receptor lacks hydrogen bonding, but still binds simple anions.

These receptors contained no hydrogen bonding interactions to interact with the anion, but were positively charged. This charge interacted in an attractive manner with the anionic character of the substrate, causing it to bind strongly. Now, the importance of shape complementarity should not be ignored, as the associated anion must bind within the cleft of the cationic receptor. Yet, utilizing this ion-pairing interaction was a great leap in the field. More of Schmidtchen's work as it pertains to guanidinium-based receptors will be discussed in the first chapter.

These concepts of *size*, *shape* and *charge* complementarity play a huge role in anion receptor chemistry, even today. The deeper understanding of supramolecular interactions, backed by leaps in synthetic, analytical, and computational chemistry, allows for the

rational design of anion receptors. Anion receptors can be designed and ultimately synthesized that take advantage of these favorable interactions in order to maximize the binding of the ion-receptor pair. One modern triumph demonstrating rational design was recently put forth by Yang and co-workers, where a tris(urea) scaffold was used to recognize sulfate and phosphate **(Figure 1.6 and 1.7).**[24]

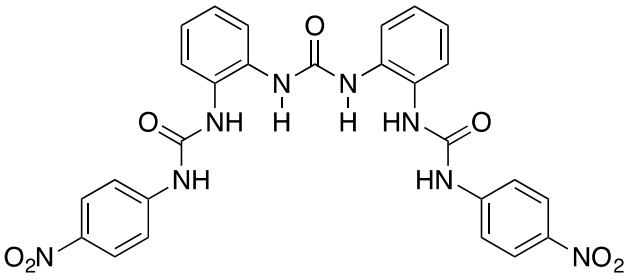

Figure 1.6: This ligand provides six coordinated hydrogen bonds that bind along the edge of sulfate and phosphate. Due to its *shape* complementarity, two can come together to fully coordinate a single sulfate.

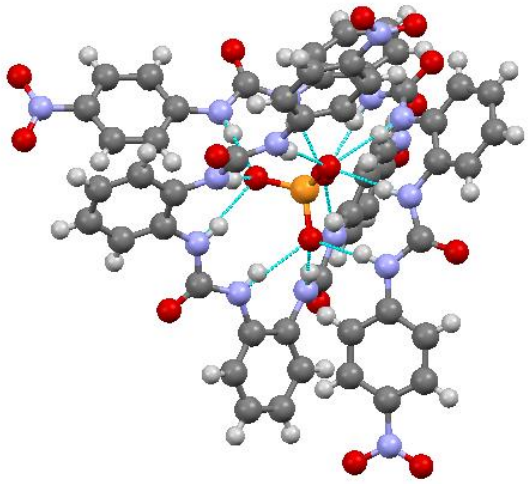

Figure 1.7: Crystal structure showing shape and charge complementarity of the tris(urea) ligand and phosphate.

These urea receptors were created so that each pair of hydrogen bonds on the urea groups would coordinate along the edge of an oxoanion. As a tetrahedral oxoanion can accept in theory a total of 12 hydrogen bonds, two of these receptors can come together to fully coordinate to the target anion. This shape and size complementarity is clearly seen in **Figure 1.7.** This receptor is a perfect example of the progress that has been made in anion receptor chemistry over the years. Knowledge of shape complementarity was used to design the ligand, the synthetic methodology was there to synthetize the target receptor, and modern analytical methods were available to quantify the results.

While this previous work has laid out many of the central tenants of ion binding and recognition, it does little to demonstrate the usefulness and utility of chemical

separations. Due to the attention this subject has received over decades there are many separation processes, and to talk about them all would require many volumes, yet a few processes stand out for both their implications and their elegance. One of these, the PUREX (**P**lutonium **U**ranium **R**edox **EX**traction) process, enables the recovery of uranium and plutonium from spent nuclear fuel.[25] While a generally clean energy source, nuclear power has the side effect of generating a highly radiotoxic waste product. Within this waste resides usable uranium in addition to other by-products (e.g. transuranics and lanthanides). This waste thus presents a twofold problem. First, this mixture itself cannot be simply reused as a fuel, the uranium must first be separated from the other by-products. Second, if this mixture were to just be discarded not only would many desirable and rare elements be lost, but also the storage of the untreated waste becomes an enormously complex issue to address. The PUREX process, and complimentary separation steps, provide chemical separations that solves these problems and turn a complex waste product, into pure and useful materials.

During the PUREX process, spent nuclear fuel is dissolved in nitric acid and filtered before being thoroughly contacted with tributylphosphate (TBP) in kerosene **(Figure 1.8)**. The TBP acts as an extractant, pulling plutonium and uranium as nitrate salts into the organic layer, separating them from the many undesirable by-products which remain in the aqueous phase. Subsequent workup and steps allow the separation of the two nuclear commodities. The PUREX process provides a convenient and economical

chemical separation to recycle the fuel while reducing the volume of waste needing to be remediated.

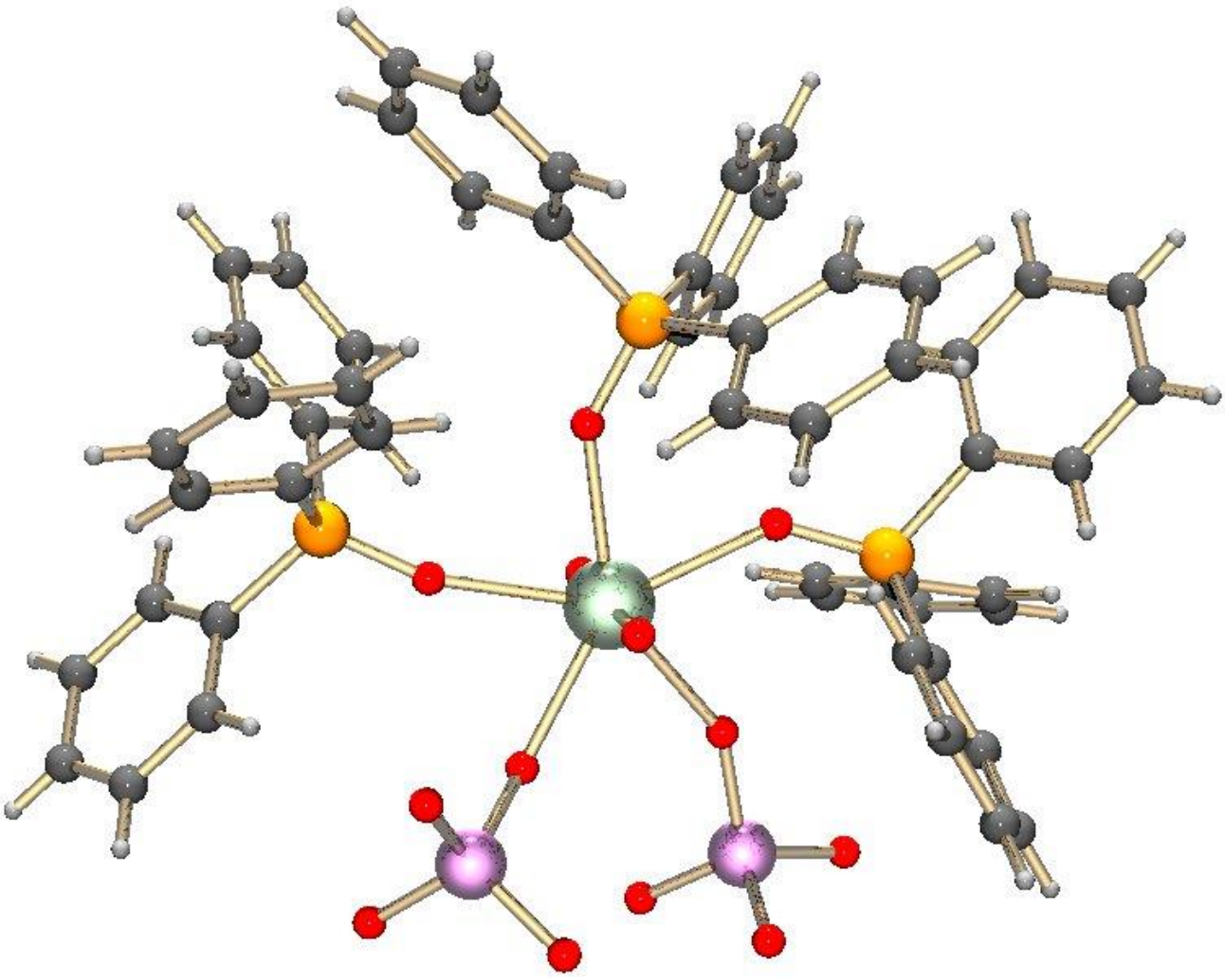

Figure 1.8: A crystal structure showing the uranium nitrate TBP complex. Image is under the public domain and used from https://en.wikipedia.org/wiki/PUREX#/media/File:Uraniumtccomplex2.jpg.

Another elegant and useful chemical separation is that of desalination. Seawater makes up the bulk of water found on our planet but is undrinkable due to the high salinity. One obvious method of purification would be distillation, but the energy cost is rather high due to the unfavorable energetics of sustained boiling. Methods such as reverse osmosis are more energetically favorable and work by applying pressure to the seawater in contact with a semipermeable membrane.[26] This membrane is designed to allow pure water to pass, but not charged solutes, meaning that only pure water is capable of flowing through. Thus, the result is drinkable water from an undrinkable source. In fact, this process is currently so efficient that the state of Israel currently generates 65% (86.5 Mm^3/day) of its fresh water via desalination of sea water.[27] This quantity is not economically achievable on this scale when using more convention methods such as distillation.

In this dissertation, two main methods of chemical separation will be discussed: solvent extraction and selective crystallization. Solvent extraction is a separations technique that utilizes two insoluble liquid phases in order to perform an extraction **(Figure 1.9)**.[28]

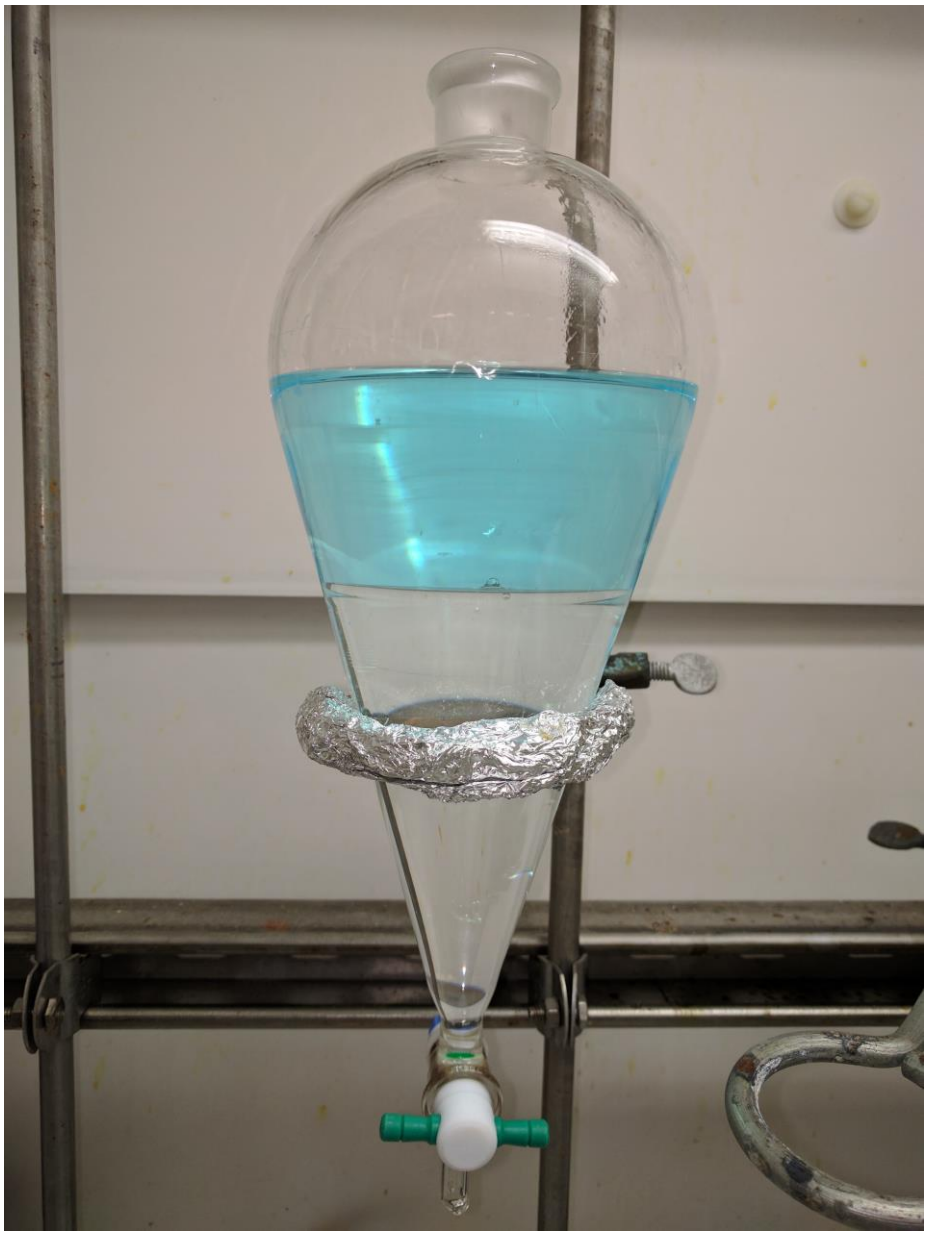

Figure 1.9: A 1000 mL separatory funnel used for bench scale liquid-liquid extractions. The top layer is composed of a copper(I)chloride and water solution, while the bottom layer is 1,2-dichloroethane, a commonly used extraction solvent. The immiscibility of the two solvents enables separations to occur.

In most cases, the oxoanion typically starts in an aqueous phase. In contact with this phase is a hydrophobic organic phase, also known as the diluent. Unfortunately, contacting these two phases without additives normally results in the oxoanion sitting exclusively in the aqueous phase, which is due in large part to the hydrophilicity of the anion. An additive that can bind and subsequently partition the oxoanion to the diluent, an extractant, is needed to afford the desired separation. When a suitable extractant is chosen, upon vigorous contacting of the two phases a majority of the desired oxoanion should be located in the diluent. The efficiency of the extraction is shown by a term called the *distribution ratio,* which compares the amount of an analyte, A, in both the organic and aqueous phase **(Equation 1)**.[28]

$$D = [A]_{org} / [A]_{aq} \quad (1)$$

The larger this ratio, the better the separation is considered to have performed. An example most chemists have seen is the extractive purification of benzoic acid, a commonly performed experiment in undergraduate laboratories. Here, benzoic acid is synthesized and remains in organic solution with impurities. To purify the compound, the organic is contacted vigorously with sodium hydroxide, deprotonating the benzoic acid and separating it into the aqueous phase with a *high D-value* due to its negative charge and newly-found insolubility in organics. The other impurities, which do not undergo

deprotonation, remain in the organic layer. The organic layer is then separated to remove the impurities. Subsequent protonation allows for recrystallization of the compound as a pure, white solid.

The previously mentioned PUREX process is often considered the golden standard of liquid/liquid extraction and demonstrates the technique perfectly.[28] Here, the aqueous phase is composed of ~5*M* nitric acid and both the targets (U and Pu) and many undersirable fission products. The diluent is typically a hydrocarbon species like kerosene, and the extractant is tributylphosphate. After the initial extraction and subsequent workups, ideally the plutonium and uranium are completely separated from one another. In the initial extraction, both the plutonium and uranium are pulled largely into the organic layer, leading to a large distribution ratio; this does little to describe the efficacy at which the plutonium and uranium are separated from each other as the D-value describes the partitioning of only a single analyte. An additional term is needed to describe how efficiently these two species are isolated from one another. This term, or the separation factor, can be written as the ratio of the two individual distribution ratios **(Equation 2)**. [28]

$$SF = D_U / D_{Pu} \qquad (2)$$

These two values, the distribution ratio and the separation factor, allow one to adequately describe the efficacy of an extraction process. While the PUREX process describes the removal of cationic species from solution, removing oxoanions is a similar proposition. The major change is that the extractant is ideally a cationic hydrogen-bond donor whereas for cations it should be an anionic hydrogen-bond acceptor.

Another approach to separations, selective precipitation / crystallization, offers the unique benefit of being both energetically efficient and operationally simple. Here, a precipitant is added to a solution containing a target species **(Figure 1.10)**.

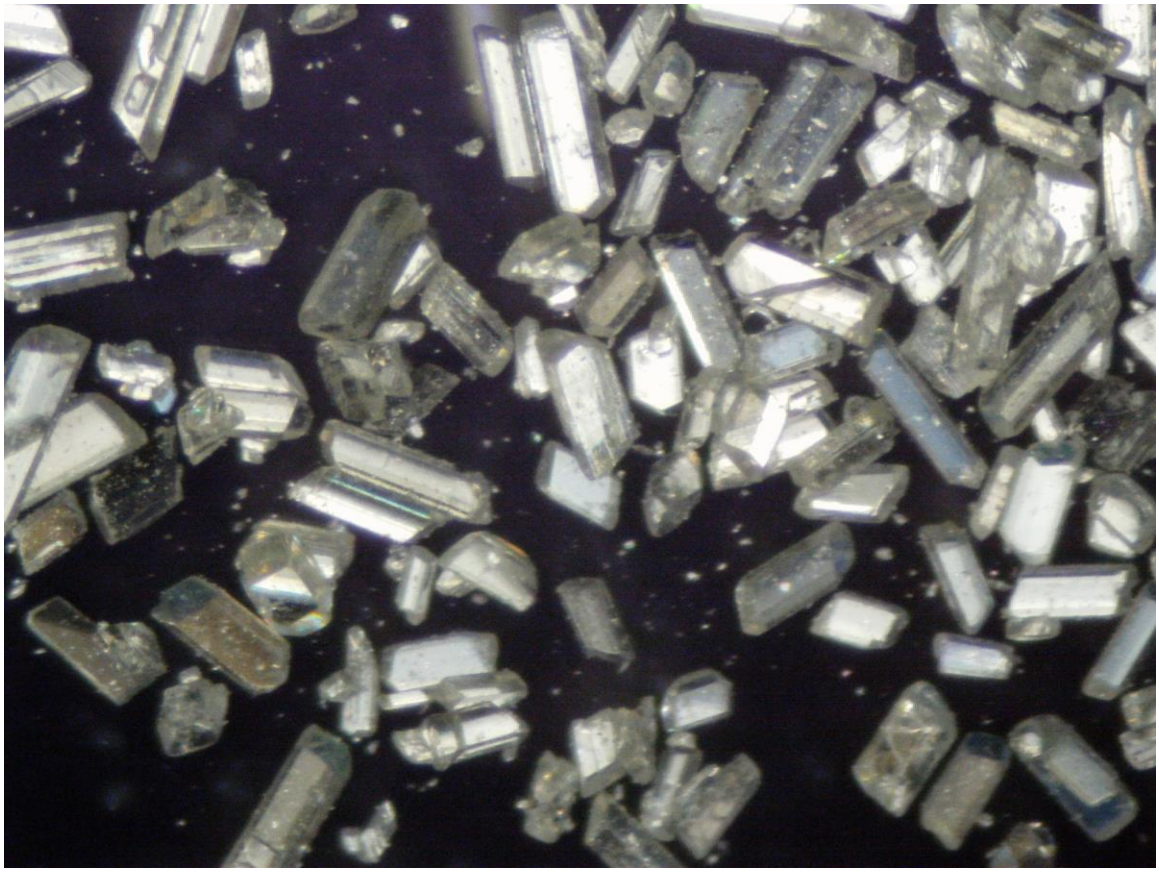

Figure 1.10: Insoluble crystals (viewed under polarized light) of an iminoguanidinium ("PyBIG"- as discussed in Chapter 3) and carbonate. These crystals average 1mm in length and are insoluble in water, enabling separation by filtration.

Upon addition, an insoluble complex is formed allowing for easy filtration of the target species. One of the most classic examples of a separation using selective precipitation is the removal of halide ions from solution using silver salts. Many silver salts are rather water-soluble but the halides, silver chloride in particular, form insoluble complexes with the K_{sp} of AgCl being 1.8×10^{-10}.[29] This corresponds to a solubility of only 5.2

milligrams in a liter of water! Compared sodium chloride, which is soluble at nearly 360 grams per liter, AgCl can be said to be completely insoluble. In fact, addition of a silver salt to a solution with chloride results in near instant and quantitative precipitation of the chloride species, which can be recovered via filtration. Depending on the purpose of the separation, it is often desirable to be able to recover the bound species. In the case of silver chloride, this is not an easy proposition, but developed processes should contain a means of recovering the analyte whether through a pH swing or a competitive process.

This dissertation focuses on the binding and separation of oxoanions using guanidinium-based ligands. Here, receptors, extractants, and precipitants have been designed for the purpose of separating oxoanions from aqueous solution. Two new approaches have been utilized. First, a pseudobicyclic system was built into a guanidinium-based receptor in order to favorably orient the molecule for binding oxoanions. As a result, a potent yet simple extractant for sulfate from sodium chloride solution was developed. Second, iminoguanidinium species were utilized to form selective precipitants for oxoanions. This work allows for energetically favorable separation of sulfate from solution and even CO_2 from air. Finally, a combination of the two approaches is currently being worked on, which we hope will allow for the creation of *in situ* formed guanidinium-based oxoanion extractants.

Chapter 2: Receptors and Extractants Based on the Pseudobicyclic N,N'-bis(2-pyridyl) Guanidinium Motif*

SUMMARY: *In Chapter 2, the design and synthesis of a pseudobicyclic guanidinium-based oxoanion receptor will be discussed. First, the synthesis, solid state structures, and solution binding ability of the host compound, N,N'-bis(2-pyridyl)guanidinium, will be described. Next, the synthesis of a lipophilic derivative for extraction studies, as well as its ability to partition sulfate is examined. As this research has already been published in the literature, only a summary will be described in the body of this text. For full papers, as well as supporting information, please see Appendix B, C, D, and E.*

2.0: BACKGROUND

As stated previously, the hydration shell and corresponding hydration energy of multivalent oxoanions make their selective binding in aqueous media quite difficult. At an effective concentration of 55 M, the sheer amount of water, coupled with its capable hydrogen bond donating ability, provides a highly competitive environment for binding. In order to overcome the negative energetics imparted by this hydration, it is necessary for a receptor to confer many strong hydrogen bonding interactions, comparable in number and strength to those lost in displacing water molecules. [30,31,32] A complementary charge on the binding group also adds Coulombic stabilization as well as provides the charge neutralization needed to form an extractable complex. Guanidinium species fit this bill rather well, as they consist of a bidentate hydrogen-bonding group with an attached

* Based on the following paper: Seipp, C.; Williams, N. J.; Bryantsev, B. S.; Custelcean R.; Moyer, B. A.; *RSC Adv.*, **2015**, 5, 107266.
For a full list of author contributions, please see **Appendix A** for a detailed and complete listing.

positive charge.[33,34] It has been demonstrated both empirically and computationally that in the case of urea groups, there exists substantial shape complementarity between the sulfate and the urea group.[35] Namely, the two hydrogen bonds coordinate perfectly along the one of the O-X-O edges of the oxoanion, allowing for a total of 12 hydrogen bonds to be made in principle to the inner coordination sphere of the sulfate molecule **(Figure 2.1)**.

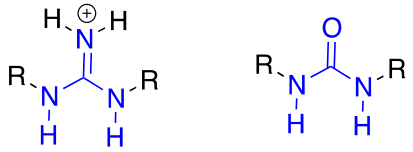

Figure 2.1: The structure of the guanidinium cation versus the structure of a urea. The analogous structure is outlined in blue.

While the tris-urea receptor could dimerize to form a complex with sulfate that was shape complementary, the ligand itself was neutral and therefore not charge complementary. Guanidiniums have very similar shape and bond lengths as the urea, making them an analogous binding group but with the added bonus of being a cationic species.[33] In the past, quaternary ammonium salts have been used to provide charge neutrality for the anion-ligand complex.[36] While these species are able to provide ionic attraction to the target species, they tend to lack specificity due to their inability to hydrogen bond. If the positive charge were directly attached to the hydrogen bond donor, such as in

guanidiniums, the added attractive force between the oppositely charged species could dramatically enhance the binding. Furthermore, as the guanidinium is capable of edge-on binding of oxoanions the receptor has inherent shape complementarity. It is for all of these reasons that we have chosen the guanidinium group as the basis for our receptor design for oxoanions.

Now, the guanidinium group is not without its faults and one problem with this otherwise ideal binding species is its conformational flexibility. Guanidiniums have the potential to exist in three different interconvertible conformations through rotation of the C-N bond **(Figure 2.2)**.[37]

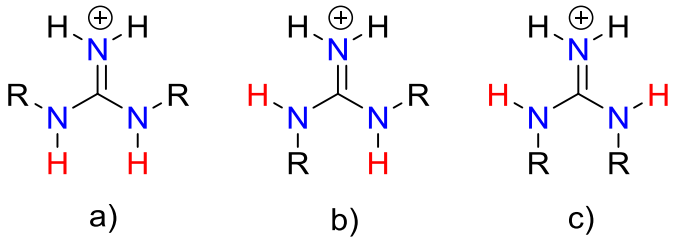

Figure 2.2: The three major conformations of *N*,*N*'-disubstituted guanidinium cations. a) **α**,**α** b) **α**,**β** c) **β**,**β.** α and β refer to the orientation of the R group relative to the NH_2^+ group.

If the central binding group can rotate, such in the case as guanidinium species, it makes it difficult to preorganize the receptor for binding. In particular, if one wants to append additional binding groups to the guanidinium frame, their orientation to form a

convergent host molecule will not be assured. Thus, limiting the conformational freedom of the species is necessary.

There have been several takes on preorganization of the guanidinium species in the past. One of the most well known examples is the bicyclic frame developed by Schmidtchen and coworkers, who introduced a series of ligands based on a triazabicyclodecene core that locks the central guanidinium in place.[38] **(Figure 2.3).**

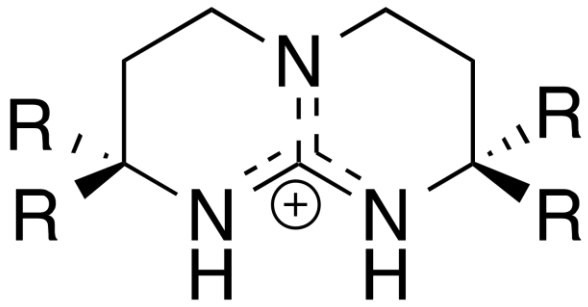

Figure 2.3: General structure of Schmidtchen's bicyclic guanidiniums. The rigid core lock the conformation of the guanidinium in place, enabling the creation of pre-organized receptors.

These ligands were appended with several different binding groups, including amides, ureas, and in one case another triazabicyclodecene group. In this regard, the bicyclic guanidinium facilitated the design of multifunctional receptors with predetermined structure. These ligands showed a very high affinity for many oxoanions, with affinities for sulfate as high as 6.8×10^6 M^{-1} in MeOD. Complementary studies by Schmidtchen *et.*

al.: by forcing the guanidinium into a single conformation that was complementary to the oxoanion, the entropic penalty for binding was drastically reduced increasing binding. Other approaches towards maximizing guanidinium preorganization includes Anslyn's use of 1,3,5-triethylphenyl groups to orient the binding guanidiniums using steric interactions[39] and Schmuck's use of carbonyl species to intramolecularly hydrogen bond guanidinium groups. **(Figure 2.4)**[40]

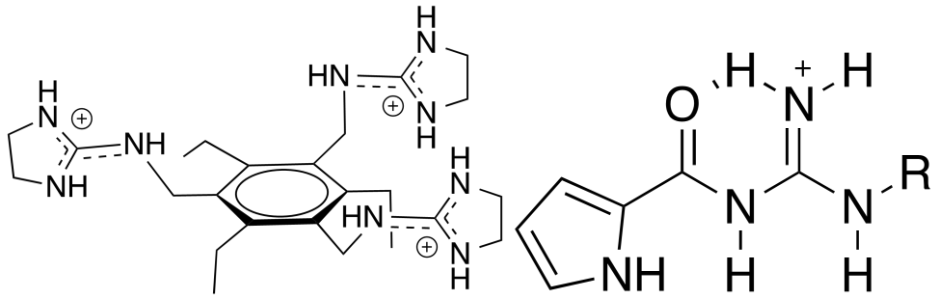

Figure 2.4: Examples of two oxoanion receptors utilizing intramolecular interactions to stabilize a specific conformation.[39,40] The guanidinium on the left utilizes a steric ratcheting effect in order to ensure that all three guanidiniums are on the same side of the ring. The receptor on the right utilizes a single intramolecular hydrogen bond to partially rigidify the system.

Preorganization of the binding species helps to limit the entropic penalty for rearrangement that normally must occur. Because of this, binding is typically more selective and stronger. Thus, anions receptors should be designed in such a way to rigidify the structure and limit the reachable conformations.

2.1: SOLID STATE STRUCTURES OF *N,N'*-BIS(2-PYRIDYL)GUANIDINIUM CHLORIDE

With the importance of limiting the available conformations of the central binding guanidinium well established, we set out to improve upon the available methods. The synthetic liability of creating many of these systems is steep, and we thought it expedient to simplify the synthesis. Our solution to this problem lays in utilizing intramolecular hydrogen bonds to form a pseudobicyclic system. We hypothesized that by adding two flanking pyridine groups, forming an *N,N*'-bis(2-pyridyl)guanidinium motif, we would be able to not only use intramolecular hydrogen bonding to favor the **α,α** orientation, but also increase the acidity of the N-H bonds making a stronger hydrogen bonding group **(Figure 2.5)**.

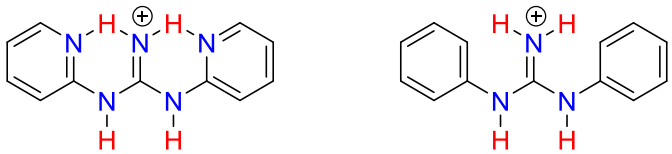

Figure 2.5: The *N,N'*-bis(2-pyridyl)guanidinium (**1**) can have two intramolecular hydrogen bonds that enhance conformational rigidity compared to bis(phenyl)guanidinium (**2**), which can undergo free rotation about the guanidinium C–N bonds.

Computational studies[41,42] (at the uB97X-D/6- 311++G(3df,3pd) level of theory) performed within the group indicated that in the presence of an anion the **α,α** orientation would be observed exclusively, while if it were unbound there would be no preference. The control, *N,N'*-bis(phenyl)guanidinium chloride **(2)**, which had no ability for intramolecular hydrogen bonding, was predicted to show no conformational preference in either of the scenarios. In order to experimentally test these results, *N,N'*-bis(2-pyridyl)guanidinium chloride **(1)** was synthesized via a four step-procedure starting with 2-aminopyridine.

2-Aminopyridine was first reacted with carbon disulfide in the presence of sulfur to give the corresponding thiourea. The product was subsequently reacted with lead carbonate and ammonia in a sealed tube to yield the free guanidinium. Precipitation of the free base from ether with anhydrous HCl gave the corresponding guanidinium in an overall high yield **(Figure 2.6)**.

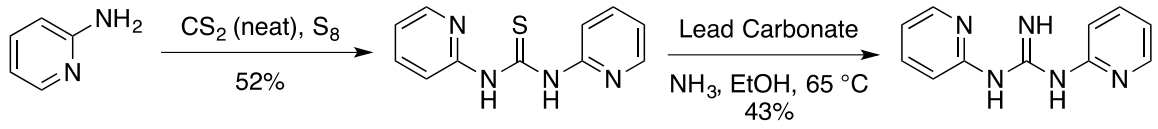

Figure 2.6: Synthetic route for the formation of BiPyG, consisting of two steps starting from 2-aminopyridine.

The synthesis, while short, was not as straightforward as it seemed it would be on paper. The initial formation of the thiourea proved to be very difficult, and despite several literature procedures existing for the formation of the compound, the molecule was not obtained in a reasonable yield.[43,44] Reaction with carbon disulfide in the presence of a base such as pyridine, triethylamine, or DMAP resulted in low and irreproducible yields. These yields typically corresponded to large amounts of unreacted starting material, with little product observed. Longer reaction times and/or higher temperatures did not seem to shift the reaction in favor of the product. Thus a stronger isothiocyanate equivalent, thiophosgene, was introduced. Despite its extreme toxicity, thiophosgene is a classic reagent for the formation of both acyclic and cyclic thioureas.[45] One of the downsides of this reagent is its reactivity—the extremely electrophilic nature of the reagent often leads to it reacting unpredictably with any nucleophilic source in the molecule. We hoped that in this case this reactivity would be a boon to our synthesis and overcome the apparent barrier to reaction that the 2-aminopyridine system faced. Unfortunately, thiophosgene at both elevated and lowered temperatures resulted in appreciable decomposition, although the decomposition products could not be identified by ^{1}H-NMR. A table of attempted reaction conditions is shown below **(Table 2.1).** Ultimately the methods of Toptschiew[46] utilizing elemental sulfur as a desulfurization agent proved effective, affording up to 52% of the target compound.

Table 2.1: Representative sample of attempted thiourea formations.

Trial:	**Reagents:**	**Conditions:**	**Result:**
1	CS_2, TEA	Reflux (neat CS_2, or ethanol, or THF)	13% yield
2	CS_2, pyridine	Reflux (neat pyridine or ethanol)	Trace yield for neat pyridine, other solvents no reaction.
3	CS_2, DMAP	Reflux (neat CS_2 or ethanol)	No reaction.
4	Thiophosgene (TP), $NaHCO_3$	0° > RT, chloroform	<10% yield, large amounts of decomposition
5	CS_2, S_8	Reflux, neat CS_2	52% yield

Even though a 52% yield was less than we were hoping, it was still surprising to us that such simple and mild reaction conditions could afford the compound where thiophosgene failed. Despite the modest yields, no other reaction conditions were discovered that gave a higher yield.

The conversion of the thiourea into the guanidine was another reaction that did not proceed as simply as hoped. In many cases, guanidinium species have been known to

form upon reaction of the parent thiourea with an activating agent, followed by displacement with the desired amine to form the desired guanidine. This activating reagent can vary from simple metal salts (mercury, lead, etc.) to alkylation with harsh methylating groups such as methyl iodide or bromoethane.[47] Unfortunately, many of these traditional reagents failed to give us the desired results (**Table 2.2).**

Table 2.2: Representative sample of attempted guanidine formations.

Trial:	**Reagents:**	**Conditions:**	**Result:**
1	Silica, $CuSO_4$, TEA, NH_4Cl	RT, THF	Starting material recovered.
2	IBX, NH_4OH	RT, THF	Unexpected cyclization of thiourea
3	Bromoethane followed by ammonia	Chloroform, then ethanol. Reflux in both steps	Starting material recovered.
4	Basic Lead Carbonate, Ammonium Hydroxide	Ethanol 65° in bomb flask	43% yield

Both desulfurization of the thiourea with copper in the presence of silica gel **(1)** as well as alkylation with bromoethane and subsequent reaction with ammonia **(3)** did not furnish the desired compound. In each of these cases, predominately unreacted starting material was left behind. Of note was the attempted desulfurization using IBX as a sulfur oxidant. While the guanidine was not formed, a unique and unexpected tetracyclic system was the

only isolated species (as the hydrogen-sulfate) salt as shown by x-ray crystallography (**Figure 2.7).**

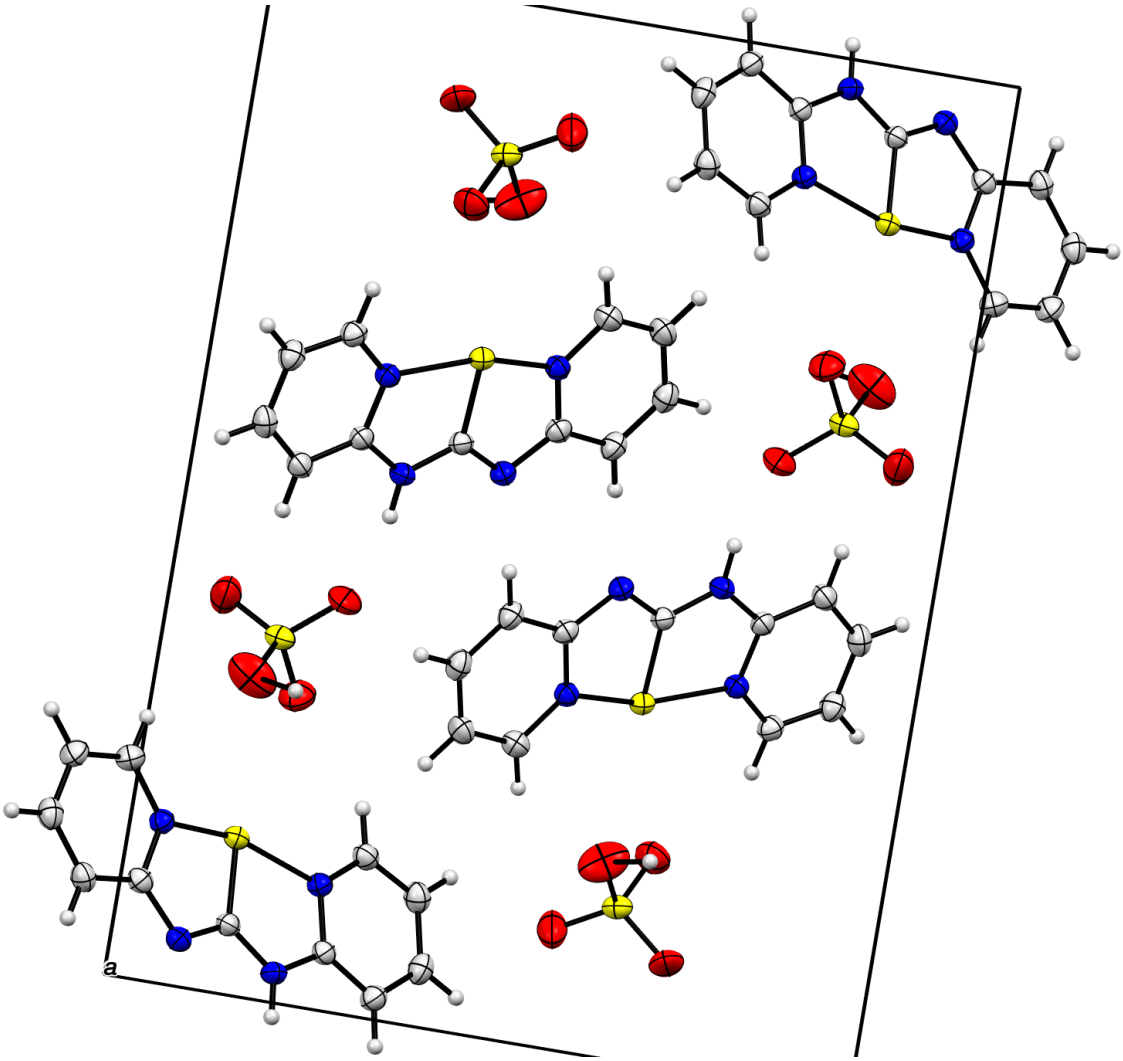

Figure 2.7: Single-crystal structure for the obtained tetracycle from the IBX oxidation of *N,N'*-bis(2-pyridyl)thiourea and subsequent crystallization in the presence of sodium sulfate. The ligand crystallized as the hydrogen-sulfate salt. Thermal ellipsoids are shown. R-Factor (%) = 5.21.

This surprising cyclization was discovered after attempting to crystallize the crude product with sodium sulfate. While certainly unexpected, this species was not entirely unknown, as it had been reported previously in the literature.[48,49] This molecule represents a rather unique motif in anion recognition, as it is a singly charged species that has both a hydrogen bond donor and acceptor build into the molecule. In theory, it should be possible for a protonated anion (such as hydrogen phosphate or hydrogen sulfate) to be recognized by this species. In this crystal however, the hydrogen sulfate anions are dimers and do not interact with the receptor in this idealized method. In the future, we may explore this work further in order to see under what conditions this mode of recognition is seen and if it can be used for selective recognition of hydrogen phosphate and hydrogen sulfate.

A more straightforward method of obtaining the desired guanidinium was sought through an Ullman-style coupling of 2-bromopyridine with guanidine nitrate. This method, first reported by Lei *et. al.*[50], was reported to give high yields of the corresponding guanidine. Unfortunately, in our hands, yields of only 10% were achieved despite multiple attempts. The precise nature of the reaction conditions was carefully controlled in order to rule out some common causes of failed metal couplings (impurities, presence of oxygen, etc). Attempts using freshly purified CuI, strictly anhydrous and anaerobic conditions, catalytic water, or freshly ground anhydrous K_3PO_4 had no affect on the observed yield, and in all cases obtained yields were under 10%, if the reaction proceeded at all.

Ultimately, the desired species was obtained in the highest yield by desulfurization with basic lead carbonate, to afford the guanidine in 43% yield. The required hydrogen chloride salt was obtained quantitatively by precipitation with anhydrous hydrogen chloride in diethyl ether.

With product in hand, we proceeded to grow single crystals via vapor diffusion of ethyl ether into methanol in order to examine the orientation of the guanidinium complexes **(Figure 2.8)**.

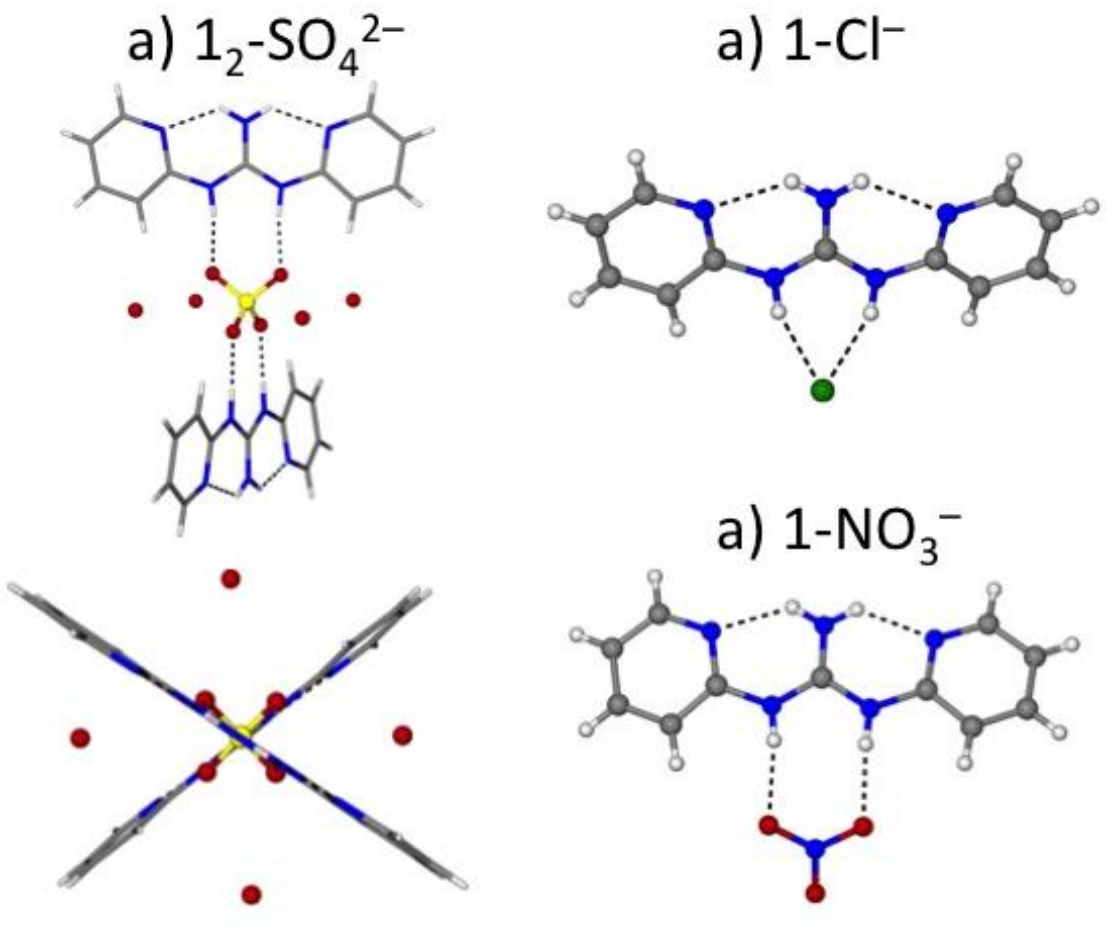

Figure 2.8: Crystal structures of 1 bound to various anions. A) Side view and top view of 1 bound to sulphate, which is additionally hydrogen bonding to four water molecules (water protons could not be located). B) 1 bound to chloride. C) 1 bound to nitrate. (*C. A. Seipp, N. J. Williams, V. S. Bryantsev, R. Custelcean and B. A. Moyer, RSC Adv., 2015,* ***5****, 10726*- Reproduced by permission of The Royal Society of Chemistry)

Luckily crystallization of the ligand proceeded rather easily in all cases. In each case, single crystals were obtained by dissolving the free guanidine in methanol, adding one equivalent of the corresponding mineral acid, and allowing diethyl ether to diffuse into

the solution. In all cases, **1** showed an **α,α** conformation while bound to an anion. This conformation was stabilized via two intramolecular N-H---N hydrogen bonds between the pyridine and the guanidinium. The final two protons able to be donated were bound firmly to the anion. While similar, all three species did show subtle differences. When **1** was bound to chloride and nitrate, a 1:1 complex was observed. In all three cases the ligand was completely planar, but in the case of nitrate the anion is bent slightly out of plane. With sulfate, the predicted 2:1 complex was observed, with four additional water molecules around the sulfate to complete its inner hydration sphere. As an interesting exception, one crystal structure was obtained where chloride was not hydrogen-bonded to the guanidinium and instead was solvated. In this case, the conformation of the ligand was α,β confirming the computational results demonstrating that it is necessary for **1** to be coordinated to an anion in order to show conformational persistence of the α,α form **(Figure 2.9)**.

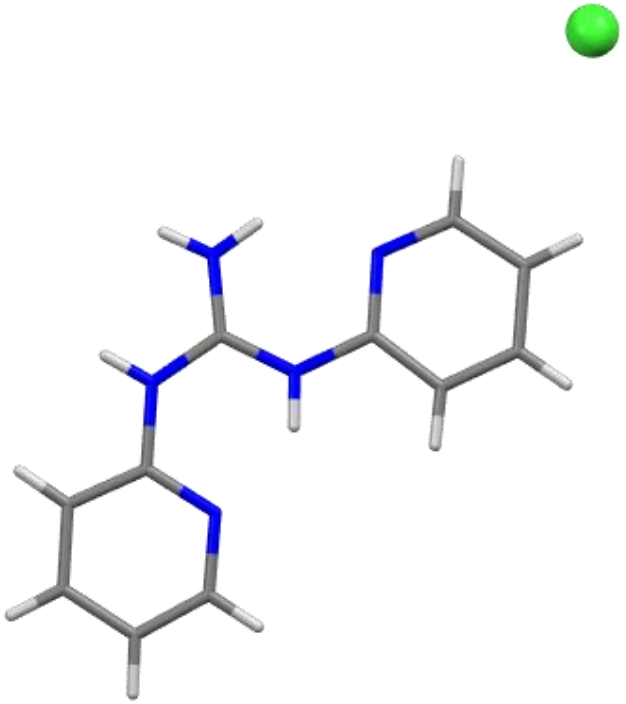

Figure 2.9: Ligand showing its conformation when not hydrogen bonding to chloride.

The observed conformational persistence of **α,α-1** upon anion binding is not seen in the bis(phenyl) control receptor **2**, which lacks the ability to intramolecularly hydrogen bond. Searching the Cambridge Crystallographic Database (CCSD) gave a plethora of examples of anion:**2** complexes, which existed in many different binding orientations **(Figure 2.10)**.

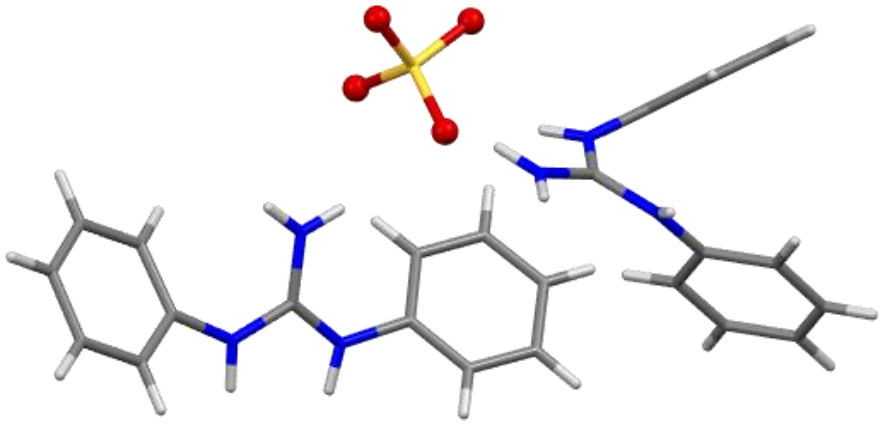

Figure 2.10: The control, *N*,*N*'-bis(phenyl)guanidinium, cannot form intramolecular hydrogen bonds and thus exists in a non-planar and random orientation.[51,52]

In the case of sulfate, **2** has multiple orientations within a single unit cell. Chloride likewise shows no preference across multiple crystal structures. Even in the case of nitrate, where the ligand is nominally in an **α,α** orientation, the ligand itself is twisted out of plane and does not show the regular planarity that **1** exhibits.

2.2: SOLUTION STATE BINDING OF *N,N'*-BIS(2-PYRIDYL)GUANIDINIUM

Crystallography is an excellent way to study ligand binding in the solid state, yet additional studies were needed to determine the efficacy of this ligand in the solution states. In order to shed light on this problem, the binding of **1** to various anions was

studied using ^{1}H-NMR spectroscopy. Initially, attempts were made to quantify the binding of the ligand in water, but this proved to be impossible. The simple, and very hydrophilic, guanidinium chloride species forms an insoluble sulfate complex (~20 mg/mL) in water. Thus, a binding constant in water was unable to be measured. The ligand does not show this property with anions other than sulfate: in the cases of nitrate, iodide, and chloride no precipitation event was observed. Furthermore, the control molecule *N,N'*-bis(2-pyridyl)guanidinium chloride did not exhibit this behavior.

Choosing the solvent for measuring the binding constant was a challenging endeavor. We had initially wanted to measure the binding constant in water as this would allow us to better understand what would be occurring in liquid-liquid extraction conditions. Unfortunately, due to the aforementioned precipitation this was no longer a reality. Often in these studies, chloroform or dichloromethane are used as solvents. While this would provide us with a meaningful comparison our issue with chloroform was three-fold. First, chloroform is an aprotic solvent that is hydrophobic. Due to this, binding constants are rather large, as the solvent cannot solvate the anionic species. We did not want to overstate the binding efficacy of our compound by choosing a solvent in which strong binding was forced. Second, our starting ligand is a guanidinium chloride and is not soluble in chloroform. Finally, chloroform decomposes over time to form trace amounts of phosgene and hydrochloric acid. We were concerned that these might influence our observed results. Thus, a 90% methanol and 10% water system was chosen to measure

the binding constant as this represented a protic solvent system that was able to solvate both our starting receptor and the corresponding sulfate species. While not as competitive as solvent systems containing more water, it represents a commonly used yet moderately challenging system in which to bind anions (unlike other commonly used aprotic solvents such as chloroform). The results of the binding studies are summarized in **Table 2.3.**

Table 2.3: Binding constants of various anions determined by ^{1}H-NMR (90% CD_3OD and 10% H_2O)

Anion	log K_1	log K_2
Chloride	< -0.5	-
Nitrate	< 1	-
Sulfate	3.78 ± 0.12	2.10 ± 0.23

The assumed equilibrium model of binding sulfate is shown in **Figure 2.13, Eq. 1**. For a simple receptor, the logK_a values of **1** binding to sulfate in 90% CD_3OD and 10% H_2O were quite large, considering the nature of the competitive protic solvent, and were estimated to be to be 3.78 ± 0.12 and 2.10 ± 0.23, respectively, for log K_1 and log K_2.[53] **1** is only capable of donating two hydrogen bonds and one positive charge per ligand, yet it is still capable of tightly binding sulfate. Furthermore, these solvent conditions are highly

competitive. Sulfate has an extremely high hydration energy, and for such a simple ligand to out-compete the swamping concentration of polar solvents is noteworthy.[54,55] Whether this is due to the increased hydrogen-bond donating ability of **1** from the attached pyridines, the shape complementarity, or other entropic benefits pertaining to desolvation[56] is still a question under investigation. Unfortunately, due to the weak binding of **2** to sulfate as well as the overlapping shifts of the aromatic protons, we were unable to determine an exact binding constant for **2** to sulfate; however, we were able to put the upper bound of its binding affinity around an order of magnitude less than that shown by **1**.

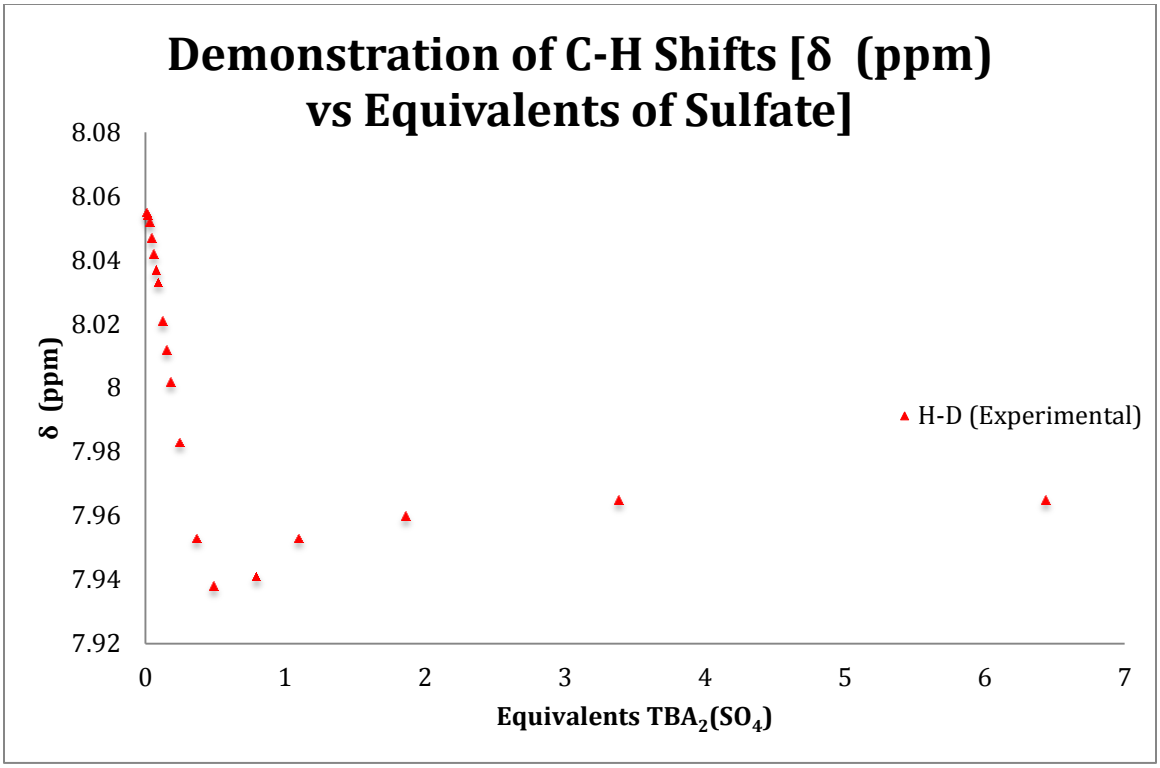

Figure 2.11: C-H shift of N,N'-bis(2-pyridyl)guanidinium with increasing amounts of sulfate present.

Evidence for 2:1 solution binding of **1** can be found by examining the responses chemical shifts of the aromatic protons of the receptor upon being titration with tetrabutylammonium sulfate **(Figure 2.11)**. The initial formation of the 2:1 complex is seen due to the upfield shift in the aromatic signals of the ^{1}H-NMR spectrum. This shift continues until one hits exactly 0.5 equivalents of added sulfate. As excess sulfate is added past this critical point, the signal shifts downfield until a plateau is reached. This plateau corresponds to the 1:1 complex.

Given the difficulty of binding sulfate in competitive solution there are relatively few examples with which to compare our ligand. Two relevant ligands are the aforementioned triazabicyclodecene guanidiniums reported by Schmidtchen and Berger.[57] **(Figure 2.12)**

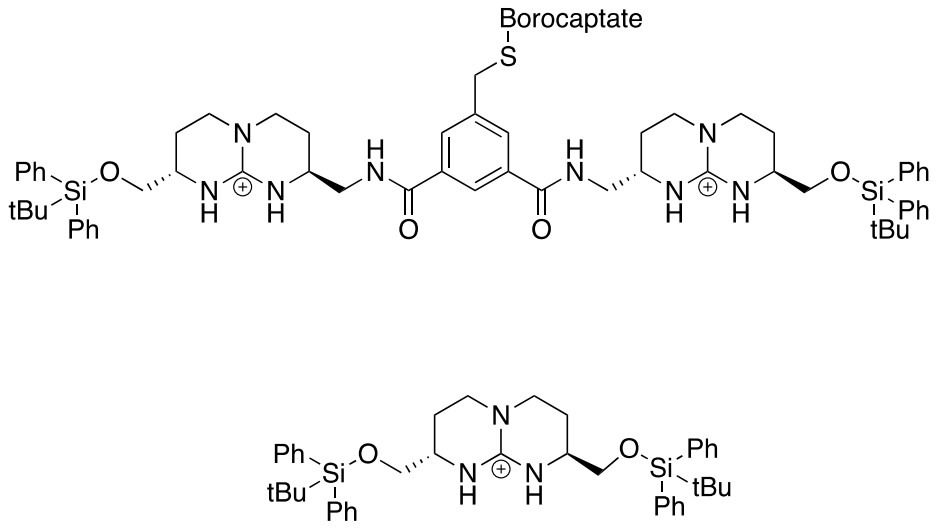

Figure 2.12: Bicyclic guanidinium ligands made by Schmidtchen and Berger utilizing a rigid triazabicyclodecene core.

The two simplest monoguandinium species reported show no binding in DMSO, and modest binding in MeOD (K_a = 313 and 553 M^{-1}). The more complex diguanidinium receptors show a large binding constant (6.8 x 10^6 M^{-1}) in MeOD. Both of these receptors were based on the synthetically difficult bicyclic core, while our receptor, **1,** is a simple pseudobicyclic species. While **1** has a higher affinity for sulfate in more competitive solution than Schmidtchen's reported monoguanidinium ligand, it binds much less

strongly than the diguanidinium receptor. Given the simplistic nature of our species and its outstanding performance relative to the other monoguanidinium, the benefit of the added pyridyl groups is clear. One point of future research is whether or this observed affinity is due to the intramolecular locking, the electron-withdrawing nature of the pyridines, or some combination of both.

The selectivity of the ligand was probed by examining the binding of the monovalent anions, nitrate and chloride **(Figure 2.13, Model 2).** These two anions were shown to bind weakly with an estimated log*K* values of < 1 M^{-1} and -0.5 respectively. These results are interesting as chloride has a higher charge density and is thus empirically seen to bind more strongly to both neutral and charged anion receptors.[58,59] Here, these trends are reversed. It is likely that the shape complementarity provided by the bidentate guanidinium affects the observed affinity.

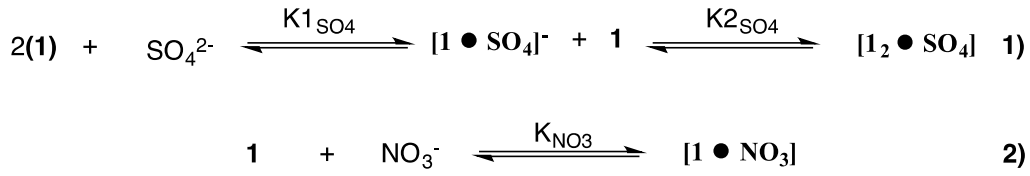

Figure 2.13: Proposed binding models for *N,N'*-bis(2-pyridyl)guanidinium, nitrate and sulfate.

2.3: Synthesis and Extraction Studies of a Lipophilic Derivative

We were very interested to apply this research towards creating a workable solvent extraction system. While a potent anion receptor, **1** is extremely hydrophilic (est. cLogP = -0.88) necessitating the modification of the molecule. In performing liquid-liquid extraction, one typically would like to partition the oxoanion selectively into a water immiscible, inexpensive diluent such as kerosene using a very "greasy" extractant. Sufficiently lipophilic guanidiniums[60] ensure that the guanidinium salt resides in the organic phase, wherein it can be expected to function as an anion exchanger. As such, it resembles commercial anion exchangers like Aliquat 336 except that the guanidinium cation can donate hydrogen bonds leading to recongnition of the O–X–O edges of oxoanions.

Simple guanidinium salts, by nature of their positive charge tend to be quite water-soluble. For this receptor to be a useful extractant, a significant hydrocarbon bulk would need to be added to it. To this aim, two dodecyl chains were added to the receptor in order to aid its partitioning into a nonpolar diluent. (**Figure 2.14)**.

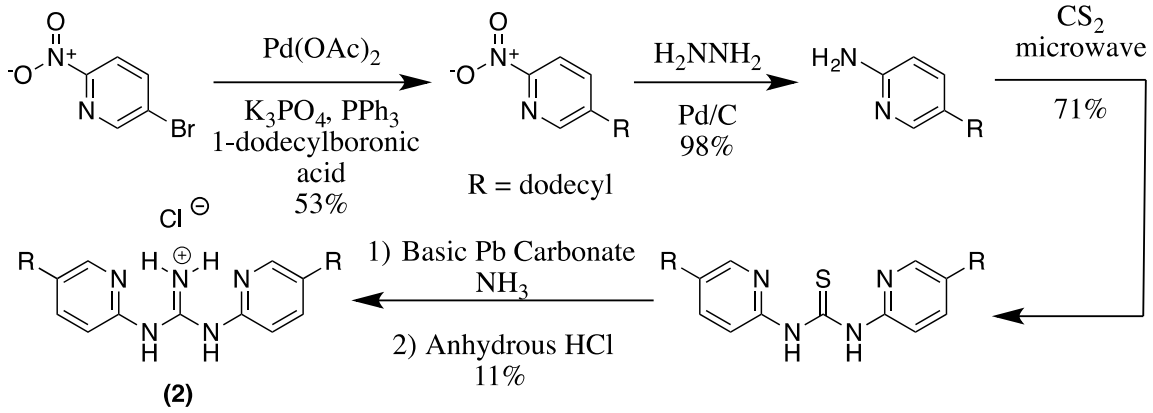

Figure 2.14: The synthesis of the lipophilic derivative of the bis(2-pyridyl)guanidinium.

Synthesis of **2** commenced via an sp^3-sp^2 Suzuki coupling to a severely electron-deficient 2-substituted nitropyridine. While sp^3-sp^2 couplings are known to be difficult at times, modern synthetic methodology has given us a toolbox that can be applied in such cases.[61,62] Yet, despite our best, and numerous, efforts, getting the reaction to proceed in a timely and high yielding fashion was difficult (**Table 2.4**).

Table 2.4: Representative sample of attempted Suzuki coupling conditions.

Trial:	Reagents:	Conditions:	Result:
1	$Pd(dppf)Cl_2$, K_2CO_3	3:1 Dioxane water	No reaction.
2	$NiCl_2(dppp)$ K_3PO_4	Dioxane, reflux	No reaction.
3	$Pd(dppf)Cl_2$, K_3PO_4	Dioxane reflux	Trace yield.
4	$Pd(dppf)Cl_2$, K_3PO_4	3:1 Dioxane /water, reflux	<15% yield.
5	$Pd(OAc)_2$, SPHOS, various bases	3:1 Dioxane / water, reflux	<15% yield
6	$Pd(OAc)_2$, PPh_3, K_3PO_4	3:1 Dioxane / water, reflux	Average 53% yield.

In all, nearly 80 different Suzuki reactions were screened, with none proving to be better than condition **6**. These trials did inform us of some of the peculiarities of this reaction. First, Buchwald ligands did not seem to have any positive effect on the yield of the reaction. Highest yields were seen exclusively with K_3PO_4, while other, weaker bases did not seem to afford a transformation. Even stronger bases such as sodium hydroxide were not attempted. The best catalyst appeared to be the combination of a palladium(II) source ($Pd(OAc)_2$ or $Pd(Cl)_2$) and triphenylphosphine as a phosphine ligand. Finally, dioxane/water as solvent appeared to give the best and most consistent yield. While anhydrous dioxane did afford the desired compound, the presence of water seemed to drastically improve the yields.

While a 53% yield was enough to continue the project, more efficient conditions were desired. We chose to investigate additional routes to the product, hoping to improve the overall yield of the net transformation **(Figure 2.15, Table 2.5).**

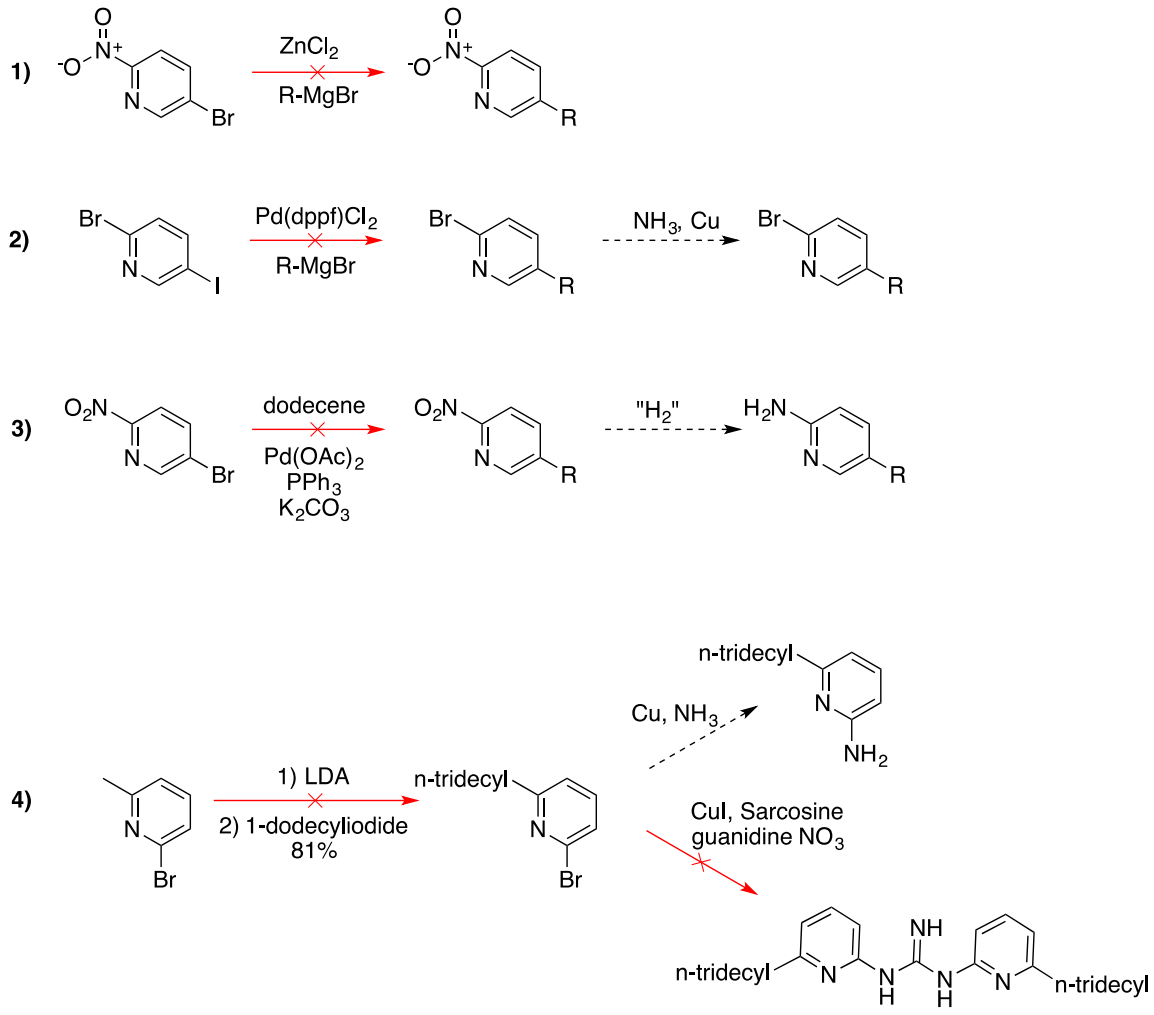

Figure 2.15: Many other synthetic pathways were attempted in order to circumvent the difficulties faced in the synthesis of the lipophilic extractant.

Table 2.5: Representative sample of other synthetic pathways attempted.

Trial:	Reagents:	Conditions:	Result:
1	$ZnCl_2$, octylMgBr	THF, RT > reflux	No reaction.
2	2-Bromo-5-iodopyridine, octylMgBr, $Pd(dppf)Cl_2$	Stirred on ice, then heated to reflux.	Decomposition to multiple unidentifiable products.
3	Dodecene, $Pd(Ac)_2$, PPh_3, K_2CO_3	Dioxane, reflux	Mixture of products. Not further pursued.
4	6-Alkyl-2-bromopyridine, CuI, sarcosine	Acetonitrile, reflux	No pure obtained product.

Negishi couplings **(1)**, were used in an attempt to furnish direct access to the nitro- or amino- alkyl pyridine through the use of an organozinc reagent. Unfortunately, in all attempted Negishi couplings no coupling product was detected. Another alternative route involved the Kumada coupling **(2)** of an alkyl Grignard reagent, followed by subsequent copper catalyzed amination. It was hoped that the difference in reactivity between the bromo and the iodo group would allow for selective alkylation of the 5 position of the pyridine ring. This would leave behind a functional 2-bromopyridine handle for subsequent amination. Unfortunately, no attempted Kumada coupling afforded any detected alkylated product. As Grignard reagents are known to interact with nitro- groups, this did not come to us as a complete surprise.[63] Addition of the Grignard at cryogenic

temperatures did not improve the reaction. Another attempt of alkylating the pyridine ring was through a Heck Coupling. One advantage of this method is that the corresponding 1-dodecene is extremely cheap and commercially available so a lower yield would be acceptable in exchange for the scalability of the reaction. While Heck coupling with dodecene **(3)** appeared to give some product (isolated as a mixture of compounds), there did not appear to be a worthwhile difference between the Heck and the optimal Suzuki coupling so further exploration and optimization of this reaction ceased.

As a final effort, 6-tridecyl-2-bromopyridine was synthesized in one step from 2,6-dibromopyridine and subjected to Ullman-like conditions. In the first reaction, a 2% yield (<15mg) of a product was obtained by preparative TLC that, while crude, had a proton NMR spectrum that looked reasonable for the expected proton spectru, of the desired product. Unfortunately, this product could not be re-obtained for complete characterization—this reaction failed to reproduce these observed results over many attempts. Different batches of solvent were used, freshly dried and/or purified reagents, different glassware / stirbars (cleaned in both acidic and basic conditions), as well as different temperatures screened, and nothing afforded more of the product. This here remains a potential avenue of research as this reaction had been shown to work with the non-alkylated derivative and potentially once with the alkylated derivative, yet needs optimization to achieve higher yields and any semblance of reproducibility.

With the Suzuki-coupling problem solved, we turned to the rest of the synthesis. Reduction of 5-*n*-dodecyl-2-nitropyridine proceeded easily in the presence of hydrazine and Pd/C. Unfortunately, the excitement over the ease of this step quickly faded as the subsequent thiourea formation was difficult to fully optimize **(Table 2.6)**. Sulfur catalysis (8), while effective on 2-aminopyridine, only afforded a trace amount of the desired product. Thus, we were forced to screen many additional conditions. Of note, thiophosgene (1) achieved a modest and reproducible yield, whereas with 2-aminopyridine it afforded predominately decomposition. This observation lead me to believe that the alkyl groups, through probably a steric or miscellization effect, drastically slowed down the reaction rates. Given that reaction rates can often be improved by increasing reagent concentrations and temperatures, microwave conditions were chosen (9). While harsh (approximately 60 degrees over the auto-ignition temperature of CS_2), in a sealed and strictly anaerobic environment this reaction afforded the desired product in a 71% yield and allowed for quantitative recovery of unreacted starting material.

Table 2.6: Representative sample of attempted thiourea formations.

Trial:	Reagents:	Conditions:	Result:
1	TP, $NaHCO_3$	Chloroform, RT	40% yield
2	CS_2 (1 eq), pyridine	Reflux	Trace yield.
3	CS_2, DMAP	Reflux	No reaction.
4	CS_2, Pyridine	Reflux	No reaction.
5	Thiocarbonyl diimidazole	RT	Decomposition
7	CS_2 neat	Reflux	Trace yield
8	CS_2 neat, sulfur	Reflux	Trace yield
9	CS_2 neat	Microwave at >149°	71% yield, clean reaction

The guanylation proceeded in a 10.5% yield using identical conditions as those used for the unalkyalted derivative**.** Several additional reaction conditions were tried in an attempt to increase the observed yield (**Table 2.7).** Alkylation with either bromoethane or methyl iodide followed by reaction with ammonia did not furnish the desired compound. No evidence for methylation of the pyridines were observed. A new reaction condition utilizing cyanogen bromide (4) was attempted but decomposition of the starting material was observed. Furthermore, given the highly toxic nature of cyanogen bromide this reaction was not repeated. Sadly, other conditions that would increase this yield to a more workable amount were not found.

Table 2.7: Representative sample of attempted guanidine formations.

Trial:	Reagents:	Conditions:	Result:
1	Bromoethane, then ammonia	Chloroform then ethanol, reflux	No reaction
2	Methyliodide, then ammonia	Chloroform then ethanol, reflux	No reaction
3	Basic Lead carbonate, ammonium hydroxide	EtOH, 65° in bomb flask	10.5 % yield
4	Cyanogen bromide, 5-alkyl-2-aminopyridine	RT > Reflux in ethanol	Decomposition

Overall, the synthesis proceeded in four linear steps to give the desired product in a modest 3.8% yield. This new receptor has an estimated cLog*P* of 11.76, and despite being positively charged was soluble in 1,2-dichloroethane. Quantification of the ability of this receptor to extract sulfate was determined by beta-scintillation counting. A solution of sodium sulfate in aqueous sodium chloride was spiked with a small amount of $Na_2{}^{35}SO_4$ and allowed to thoroughly contact with solutions of varying concentrations of ligand in 1,2-DCE. Due to the presence of the radiolabeled sulfate, the concentration of sulfate in each phase was able to be determined by beta-scintillation counting. The distribution ratios of the partitioning of SO_4^{2-} into 1,2-dichloroethane from sodium chloride solution are shown in **Figure 2.16.**

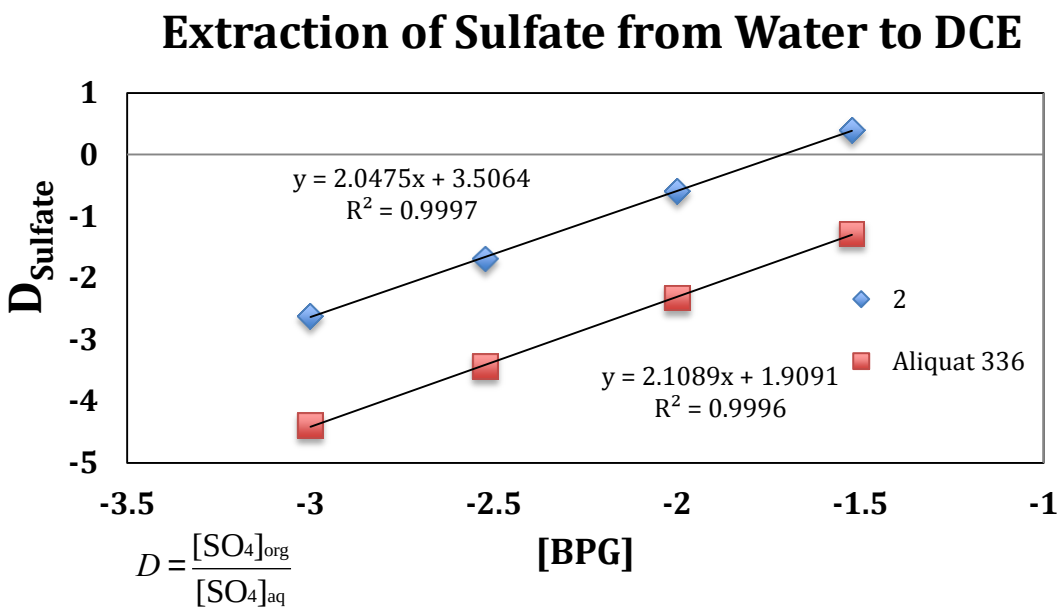

Figure 2.16: Extraction data for 2 partitioning sulfate from water into 1,2-dichloroethane.

The experiment shows that **2** exhibits D_{SO4} values in the range of 0.002 to 2.5 at relatively low concentrations (1–30 mM). A *D* value of greater than one is indicative of separation (more sulfate is being pulled out of the aqueous solution than is remaining), thus at 30 mM this ligand is able to extract sulfate. For comparison, *N*,*N*'-bis(4-tetradecylphenyl)guanidinium chloride **(3)** was synthesized as a control due to its lack of pyridine rings. Unfortunately, this molecule was not soluble in 1,2-dichloromethane and could not be used as a meaningful comparison. Therefore, commercially available Aliquat 336 was used as a control. The lipophilic guanidinium receptor **2** exhibits higher extraction strength than this commercially available extractant, which we attribute to the

hydrogen-bond donating ability of the guanidinium group. Due to the fact that the aqueous phase was composed of an excess of sodium chloride, **2** appears to be a competent extractant of sulfate even when competing against high concentrations of chloride. This is in strong accordance with the binding constants observed with **1**.

This work has provided a new guanidinium-based sulfate binding motif that is capable of forming conformation-stabilizing intramolecular hydrogen bonds, a type of intramolecular self-assembly stabilizing the desired receptor conformation. This pseudobicyclic system is unique, in that a linear molecule is able to behave as a rigid system. Furthermore, this motif proves to be a selective sulfate extractant, even out performing commercially available derivatives. Future work will involve appending additional convergent hydrogen-bond donors to enhance selectivity and affinity for target anions. Additional lipophilic groups will also be explored in order to maximize the distribution ratio of sulfate. More about this future work, and the current progress on it, will be discussed briefly in Chapter 4.

Chapter 3: Crystallization Agents Based on Bis(Imino)Guanidiniums*

SUMMARY: *In Chapter 3, the design and synthesis of iminoguanidinium-based crystallization agents will be discussed. First, the first generation receptor based off of the glyoxal linker (GBAH) will be examined. This molecule is capable of forming very insoluble oxoanion salts. Second, the second generation receptor based off of terephthaladehyde (BBIG) will be explored. This ligand is more planar than the first, and forms a much more insoluble sulfate salt. It is capable of quantitatively stripping sulfate from seawater. Third, a 2,6-pyridinecarboxaldehyde based ligand (PyBIG) will be discussed. PyBIG is much more efficient at sulfate removal from seawater. Finally, applying PyBIG towards direct air capture of CO_2 is explored. In all cases, detailed structural analysis is performed by X-ray crystallography. For full papers, as well as supporting information, please see Appendix F, G, and H.*

3.0: Background

As stated briefly earlier, selective crystallization offers a unique and energy efficient way of performing separations. By simply adding a precipitant to a complex solution, a subsequent filtration can quantitatively remove an analyte from solution. In contrast to solvent extraction, which requires expensive contactors and organic solvents, crystallization provides an operationally simple way to perform separations with no additional diluent.

* Based on the following papers: Custelcean, R., Williams, N. J., Seipp, C. A. *Angew. Chem. Int. Ed.* **2015.** *54*, 10525-10529.; Custelcean, R., Williams, N. J., Seipp, C. A., Ivanov, A. S., Bryantsev, V. S. *Chem. Eur. J.* **2016,** 1997-2003.; Seipp, C.A.; Williams, N.K.; Kidder, M.K.; Custelcean. R.*; Angew. Chem. Int. Ed.* **2017,** 1042. For a full list of author contributions, please see **Appendix A** for a detailed and complete listing.

While a rare occurrence, insoluble sulfate salts do in fact appear in nature. $BaSO_4$, $PbSO_4$, Ag_2SO_4, $SrSO_4$, and $RaSO_4$ range from slight insolubility (Ag_2SO_4, K_{sp} = 1.2 x 10^{-5})[64] to complete insolubility ($RaSO_4$, K_{sp} = 1 x $10^{-10.38}$)[65] Man made examples of these types of complex are much less common. The traditional belief was that in order to crystallize sulfate from aqueous solution, one must strip sulfate of its hydration sphere. This amounts to nearly -1080 kJ mol^{-1} of energy that must be over come. Custelcean *et. al.* have previously designed urea based ligands that form insoluble capsules in contact with sulfate **(Figure 3.1)**.[66,67,68]

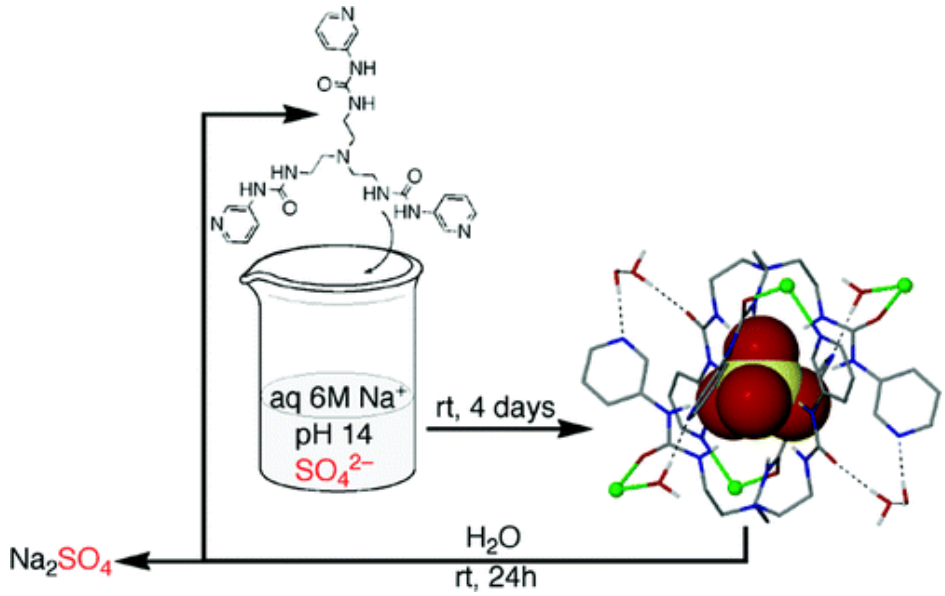

Figure 3.1: Custelcean's sulfate precipitating ligand. It completely dehydrates sulfate and precipitates the encapsulated oxoanion. (Reprinted with permission from Custelcean, R.; Sloop, F. V.; Rajbanshi, A.; Wan, S.; Moyer, B. A. *Crystal Growth & Design* **2015**, *15* (1), 517–522. Copyright 2015 American Chemical Society.)

The formed complex donates 12 hydrogen bonds to the sulfate from six urea groups, coordinatively saturating the oxoanion. Due to the neutral nature of the ligand, $Na_2(H_2O)_4^{2+}$ clusters are incorporated into the complex to provide a neutral charge. Overall, the process takes around 24 hours but converts a mixture ~6 M NaOH, sodium sulfate, and ligand into ~90% of the sulfate complex.

There exist a few limitations with this system however. First, it is a kinetically slow process slightly complicating possible industrial use. Second, it needs an excess of sodium to function. In pure water, the complex dissociates back into the free ligand and

aqueous sodium sulfate. Admittedly, this property could be useful for nuclear waste separations, where highly basic and sodium rich waste streams would allow this ligand to function while providing an easy form of ligand regeneration. Having a precipitation agent that could work without excess sodium present would however be useful.

Anions are known to exist in anion water clusters, where the anion is coordinated by a a discrete sphere of hydration **(Figure 3.2)**

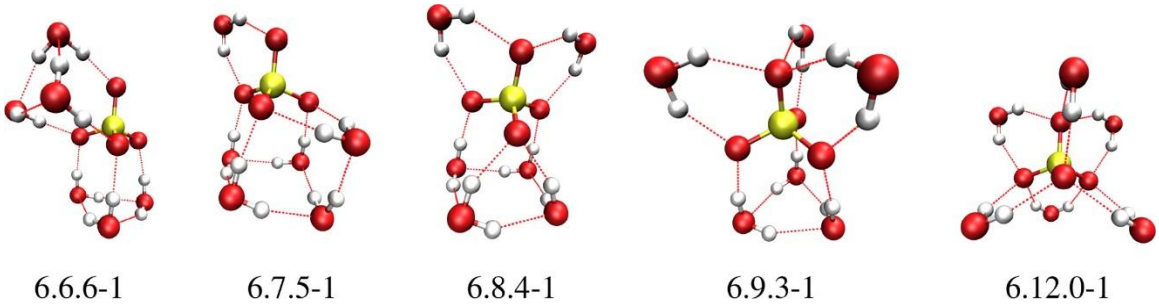

Figure 3.2: Potential sulfate-water clusters as calculated. (Reprinted with permission from Mardirossian, N.; Lambrecht, D.; McCaslin, L.; Xantheas, S.; Head-Gordon, M.; *Jour. Chem. Theory and Comp.*, **2013,** 1368. Copyright **2013** American Chemical Society.)[69]

Our group had postulated that it might be possible to recognize these discrete clusters with receptors. This would offer the benefit of no longer having to remove the waters of hydration prior to binding and would open up new avenues to receptor design. We are happy to report that we have developed a series of imino(guanidinium) based compounds that are able to not only accomplish recognition of oxoanion water clusters, but also

selectively separate those oxoanions from solution via crystallization with unprecedented levels of observed complex insolubility.

3.1: PRECIPITATION OF OXOANIONS USING GBAH

Serendipity played a large role in this area for us, and two key discoveries lead to very fruitful research. It was first noticed that during titrations of aqueous N,N'-bis(2-pyridyl)guanidinium chloride with sulfate that addition of a small amount of sulfate lead to precipitation of the sulfate complex. **(Figure 3.3).**

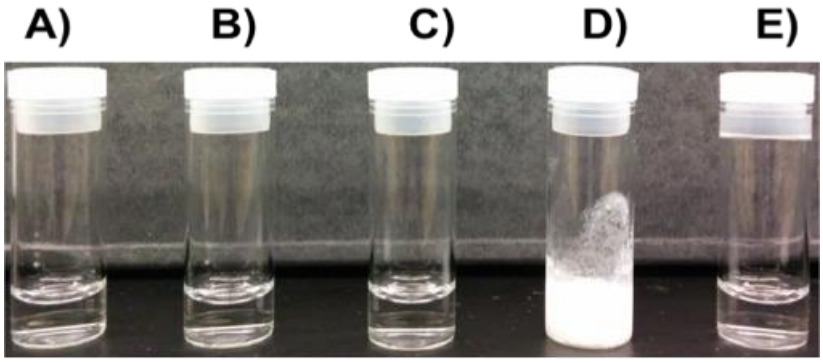

Figure 3.3: Vials of **1** (N,N'-bis(2-pyridyl)guanidinium) and various aqueous salts. A) **1** + NaI, B) **1** + NaCl, C) **1** + $NaNO_3$, D) **1** + Na_2SO_4, E) **2** + Na_2SO_4. (*C. A. Seipp, N. J. Williams, V. S. Bryantsev, R. Custelcean and B. A. Moyer, RSC Adv., 2015, **5**, 10726*- Reproduced by permission of The Royal Society of Chemistry)

The $\mathbf{1}_2$-SO_4 complex was calculated to have a solubility of ~20 mg/mL, much less than a typical organic sulfate. Simultaneously, it was observed that glyoxal, when allowed to react with aminoguanidinium chloride in aqueous solution, formed a bis(iminoguanidinium) (GBAH) compound *in situ* which would precipitate a large variety of oxoanions. In stark contrast to $\mathbf{1}_2$-SO_4, the sulfate salt of this bis(iminoguanidinium) compound was orders of magnitude less soluble—the K_{sp} of which was calculated by UV-Vis titrations to be $3.2(5) \times 10^{-7}$ (7.26×10^{-4} M). In fact, all of the oxoanions tested had extremely low solubilities **(Table 3.1).**

Table 3.1: Aqueous solubilities of the GBAH salts.

Complex	Solubility (M)
GBAH-SO_4	$7.2(6) \times 10^{-4}$
GBAH-Cl	0.88(8)
GBAH-NO_3	$1.2(2) \times 10^{-3}$
GBAH-CLO_4	$1.36(1) \times 10^{-2}$

While relative solubilities are correlated with separation factors, a more stringent experiment was devised. A series of competitive crystallization experiments were formed where GBAH was formed *in situ* in an aqueous solution of anions **(Table 3.2).**

Table 3.2: Results of the competitive crystallizations.

Experiment:	Anion Mixture (M)	Complex Formed (GBAH-X):
1	SO_4^{2-} (0.25), ClO_4^- (0.25)	SO_4
2	SO_4^{2-} (0.25), Cl^- (0.25)	SO_4
3	SO_4^{2-} (0.25), NO_3^- (0.25)	SO_4 (26%) NO_3 (74%)
4	NO_3^- (0.25), ClO_4^- (0.25)	NO_3
5	SO_4^{2-} (0.07), ClO_4^- (0.07), Cl^- (0.07), NO_3^- (0.07)	SO_4 (24%) NO_3 (76%)

As can be seen from the results, complete selectivity for sulfate was observed when the competition was between sulfate and perchlorate or sulfate and chloride. When nitrate or chloride was present, 74% and 76% of the recovered species was the nitrate and chloride salt respectively. Typically, one sees selectivity that follows the trend of the Hoffmeister bias; that is, more hydrophobic anions are typically more easily separated from the aqueous phase. In this case though, sulfate (hydrophilic) is separated in preference to perchlorate (hydrophobic) while nitrate (hydrophobic) is precipitated more readily than sulfate (hydrophilic). Thus, there appears to be additional factors that determine the relative solubilities and rates of crystallizations. In order to better understand the observed solubility trends, single crystal structures were obtained (**Figure 3.4**).

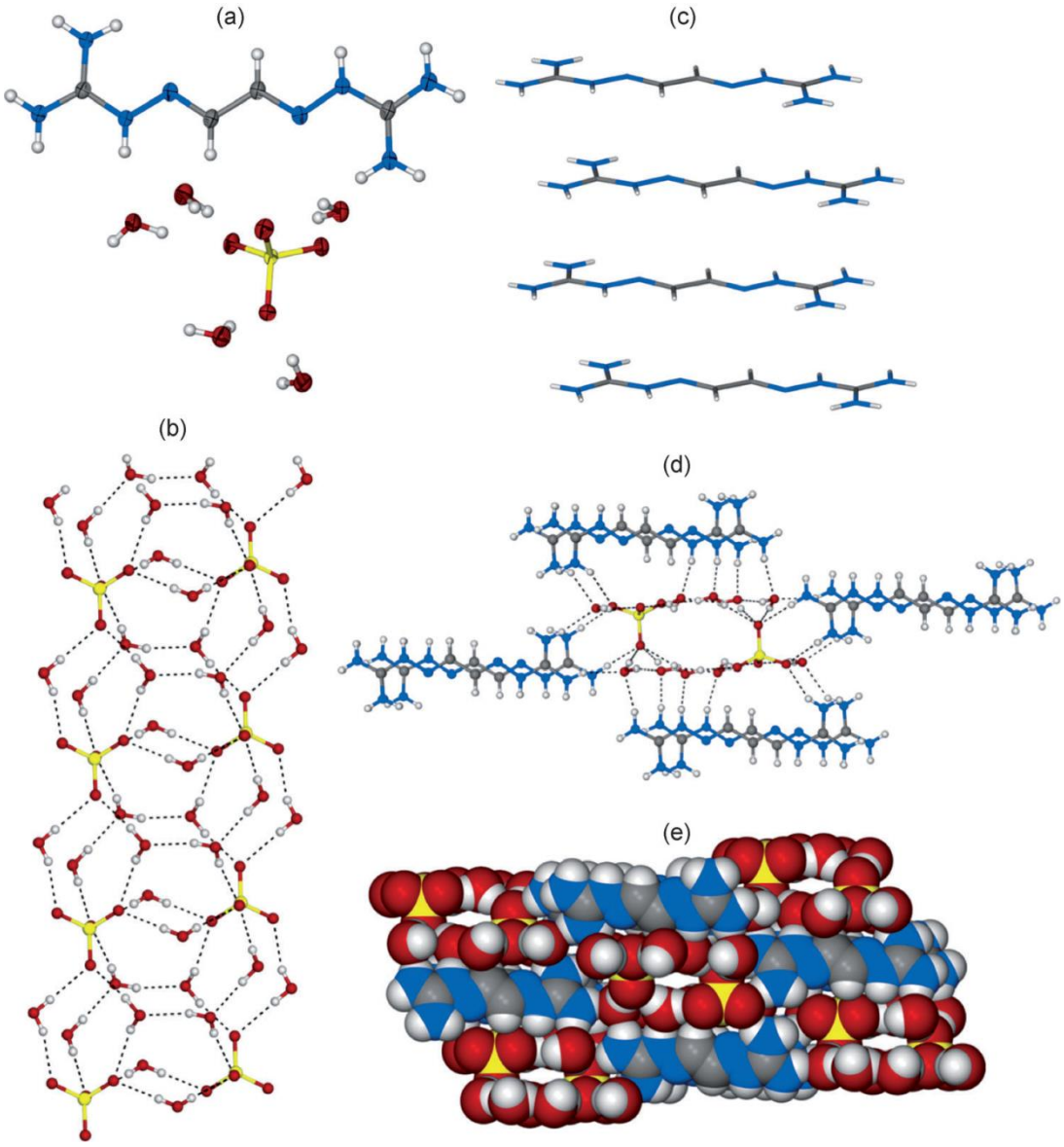

Figure 3.4: X-ray crystal structure of the GBAH-SO_4^{2-} salt. a) GBAH cation and the $SO_4(H_2O)_5^{2-}$ cluster. b) Hydrogen-bonded sulfate water clusters clusters. c) Stacking of the GBAH cations.d) Hydrogen bonding of the sulfate–water clusters by the cationic GBAH stacks. e) Space-filling representation of the crystal packing. (*Used with permission from John Wiley and Sons and Angwandte Chemie and is taken from: Custelcean, R., Williams, N. J., Seipp, C. A. Angew. Chem. Int. Ed. 54, 10525-10529 (2015).*)

The crystal structure of the SO_4^{2-} complex was surprising in that it wasn't bound to sulfate directly, but one dimension $[SO_4(H_2O)_5^{2-}]$ clusters that formed along the crystallographic *b* axis. The waters around sulfate contribute eight short hydrogen bonds, with an average hydrogen bond length of 2.015 angstroms. It is typically assumed that in order to bind an oxoanion strongly, the anion must undergo dehydration which imparts a significant entropic cost. Here, we see that this is not necessarily the case. By recognizing the cluster, the entropic penalty can be ignored. The other, less-soluble, complexes do not have this anion-water cluster motif. While it cannot be said with certainty that the hydration of sulfate contributes to the observed insolubility, we surmise that the two observations may be correlated. Another interesting feature of the crystal structures are the close packing of the individual cations. The guanidinium species form stacks with interplanar distances alternating between 3.10 and 3.20 angstroms. As all of these complexes were much less soluble than their aminoguanidinium counterparts, we also suspect that the favorable stacking of the cation species may also contribute to the observed insolubility.

3.2: CRYSTALLIZATION OF OXOANIONS USING BBIG

We hypothesized that enabling further intramolecular interactions through the introduction of planar aromatic groups, would further decrease the solubility of the system. To this aim, BBIG was synthesized **(Figure 3.5).**

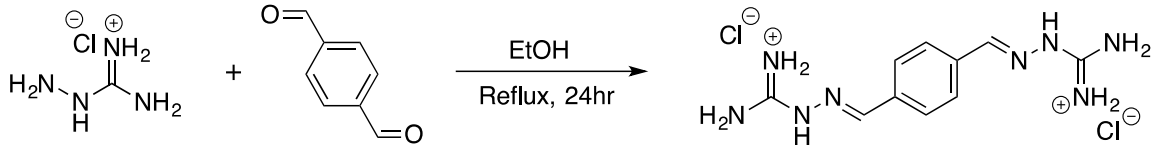

Figure 3.5: Representative synthesis of BBIG from terepthaladehyde and aminoguanidinium chloride.

Much like the previous ligand, BBIG could either be formed *in situ* and reacted with present anions or could be isolated as the HCl salt, and used as a precipitant. Single crystals were grown and analyzed via X-ray diffraction **(Figure 3.6).**

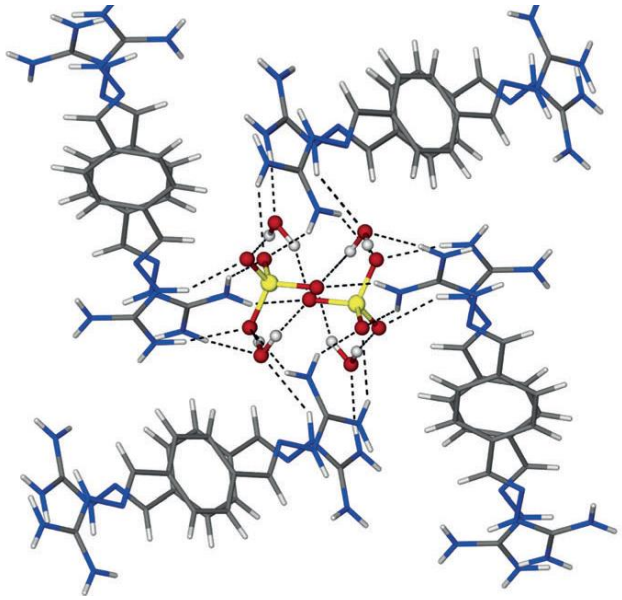

Figure 3.6: Crystal structure showing BBIG binding to a sulfate water cluster. *Used with permission from John Wiley and Sons and Angwandte Chemie and is taken from:* Custelcean, R., Williams, N. J., Seipp, C. A., Ivanov, A. S., Bryantsev, V. S. *Chem. Eur. J.* **22**, 1997-2003 (2016).

Once again, a sulfate water cluster was observed, this time with a stoichiometry of $[(SO_4)_2(H_2O)_4]^{4-}$. Each sulfate receives four water hydrogen bonds as well as seven guanidinium hydrogen bonds, nearly completing its coordination sphere. The cations are stacked in an antiparallel fashion similar to GBAH, with a mean interplanar distance of 3.39 angstroms. The calculated solubility of the complex was $1.6(2)x10^{-5}$ M, nearly an order of magnitude lower than that of GBAH. The nitrate complex mirrors closely the structure seen in GBAH. No waters of hydration are present and the cations stack in a parallel fashion. The solubility of this complex is $6.5(5)x10^{-4}$, an order of magnitude lower than that of the sulfate complex.

To demonstrate the real-world applicability of such a ligand, we decided to test its separation of sulfate from seawater. Seawater is also a highly complex natural mixture of various ionic species, and selective removal of sulfate is therefore a challenging task. The results of this experiment are shown in **Table 3.3**.

Table 3.3: Separation of Sulfate from Gulf Stream Seawater. Initial sulfate concentration 33 mM. Residual sulfate measured by β liquid scintillation counting.

BBIG [equiv]	Residual [SO_4^{2-}] [mM]	% Sulfate Removed
1	3.5	88
1.1	1.6	95
1.5	0.3	99
2	0.3	99

Surprisingly, with only 1.5 equivalents of BBIG, over 99% of sulfate was removed. No additional gain was seen when additional amounts of BBIG were added. A complete

recovery cycle was demonstrated by regenerating of the ligand with sodium hydroxide. The original ligand was obtained in a 93% yield.

3.3: CRYSTALLIZATION OF OXOANIONS USING PYBIG

Our initial reaction to the insolubility of the BBIG complex was slight disappointment—while the results were impressive we still failed to create an organic sulfate salt less soluble than barium sulfate. We wanted to know if it would be possible to fine tune the structure of the ligand in order to further increase the insolubility, perhaps even beating $Ra(SO_4)_2$ the most insoluble sulfate salt. The guanidinium group contains two highly polarized and strong hydrogen bond donors that are complementary to sulfate, but these hydrogen bonds can be made even stronger via the addition of electron withdrawing groups, making the hydrogens more acidic. Pyridines, as used in the formation of receptor **1** in the first chapter, are extremely electron deficient and should render the hydrogens highly acidic. A pyridine group was added as the central linker to the molecule, creating PyBIG **(Figure 3.7)**. We hoped that these stronger hydrogen bonds would create a stronger sulfate complex, and lead to even greater levels of insolubility.

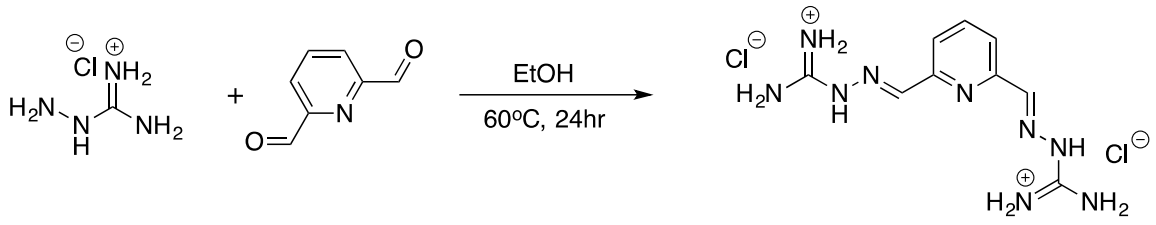

Figure 3.7: Representative synthesis of PyBIG-Cl.

PyBIG was synthesized starting from pyridine dimethanol. While Swern oxidation gave access to the product, despite multiple washing and purifications the compound smelled with such intensity that my colleagues, and myself, were unwilling to work with it. Thus, an alternative synthesis was devised utilizing Dess Martin Periodinane as a gentle oxidant (**Figure 3.8**).

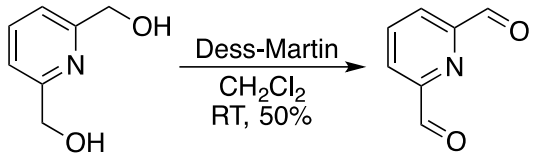

Figure 3.8: Synthesis of the required dialdehyde using Dess-Martin Periodinane.

Single crystals of PyBIG and its complex with SO_4^{2-}, CrO_4^{2-}, SeO_4^{2-}, HPO_4^{-}, and Cl^{-} were obtained from aqueous solution, and their crystal structures were gathered and compared **(Figure 3.9).**

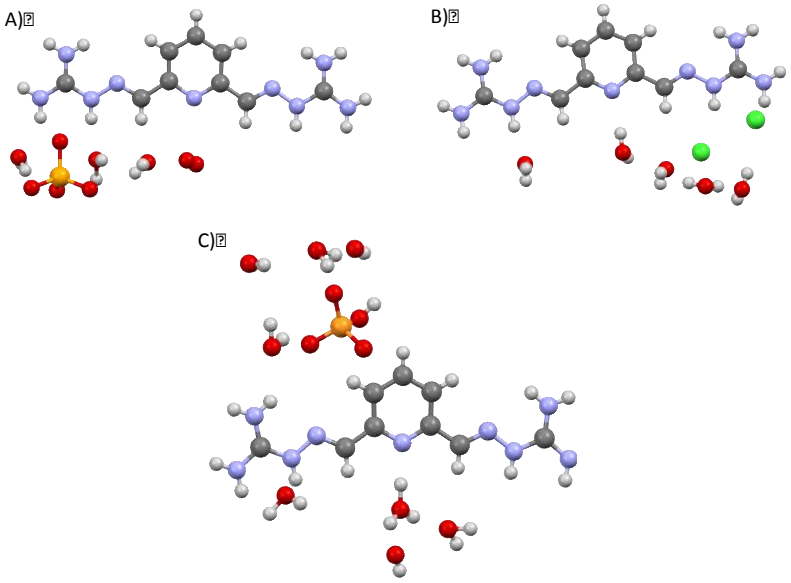

Figure 3.9: Crystal structures of PyBIG and sulfate (a), chloride (b), and phosphate (c). Chromate and selenite are omitted as they are isomorphic with sulfate.

The single-crystal X-ray structure of PyBIG-SO_4 (PyBIG-CrO_4 and PyBIG-SeO_4 are isomorphic with PyBIG- SO_4) revealed a nearly planar conformation of the guanidinium cation stacked in an antiparallel fashion with two-dimensional "tapes" of sulfate-water clusters running through the crystal structure. Each sulfate accepts seven N-H hydrogen bonds from the adjacent guanidiniums (average bond length: 2.864 angstroms) and five

H-O hydrogen bonds from the surrounding water molecules (average bond length: 1.88 angstroms). The stacked guanidiniums have a mean interplanar distance of 3.25 angstroms.

These structures are similar to what has been seen in the previously reported BBIG system. In both cases SO_4-H_2O clusters are found embedded within cation stacks of the guanidiniums. While the relative orientation of the cations (parallel or antiparallel) and how they are offset from one another vary, the cations are always closely associated and they are stacked so areas of electron density are proximal to areas of relative electron deficiency. One notable difference is that PyBIG- SO_4 contains two additional water molecules in the crystal structure and is bound by one additional H-O hydrogen bond but one fewer N-H hydrogen bond. The coordination number of the sulfate is 11 in both cases.

Out of the complexes analyzed, PyBIG-HPO_4 contains 8 waters in the unit cell, the most hydrated of the series. Two-dimensional channels of phosphate water clusters extend throughout the crystal lattice. PyBIG-Cl structure is markedly different than that of the PyBIG- SO_4 structure in that it has perpendicular layers of antiparallel stacked cations. These cations create channels of chlorine water clusters, with each crystal containing a total of five water molecules and two chlorides. In the free base of PyBIG, the guanidines take on a bent conformation, which is unique to this structure.

During crystallizations it was observed that the solubilities of both the PyBIG-SO_4 and PyBIG-CrO_4 seemed exceedingly low. The solubility of PyBIG-SO_4 was determined to be 2.60 x 10^{-5} M at 25 °C (K_{sp} = 6.8 x 10^{-10}). This solubility is actually slightly higher than that observed for BBIG-SO_4, yet still on par with that of Barium Sulfate (K_{sp} of $Ba(SO_4)$ = 1.08 x 10^{-10}). It is interesting that both PyBIG-SO_4 and PyBIG-CrO_4 share features seen in the other insoluble iminoguanidinium salts, GBAH-SO_4 and BBIG-SO_4 that we suspect are important driving forces of the insolubility. First, the cations show are planar and are pi-stacked. This makes for a densely packed and energetically favorable crystalline lattice. Second, the oxoanion is recognized an anion water cluster. While the exact significance of this is unknown, we suspect that there is less of an energy cost when the sulfate species does not need to be dehydrated. This eliminates any energy cost for the desolvation of the inner-shell hydration of the oxoanion.

It should be noted that crystallization of these compounds presents a unique challenge due to their inherent insolubility. After all, crystallization is based on a solution of an analyte reaching supersaturation. The rate of crystal formation in turn is increases with the degree of supersaturation. Growing X-ray quality crystals requires extremely slow crystal growth. Thus, in these cases where the compounds are extremely insoluble, instant precipitation of a polycrystalline mixture is common. Furthermore, even if the concentration can accurately be limited to the micromolar amount, there would need to be

liters of solution for there to be enough material for even a single crystal to form assuming the resultant slow kinetics of crystallization could be overcome.

Obtaining a crystal structure of PyBIG-SO_4 provides a perfect example of the difficulties faced. Methods of attempted crystallization are summarized in **(Table 3.4).**

Table 3.4: Crystallization methods attempted in order to obtain a single PyBIG-SO_4 crystal.

Trial:	**Method:**	**Trials**	**Number of usable crystals:**
1	Layering (miscible solvents)	>300	0
2	Layering (immiscible solvents)	>300	0
3	Slow evaporation	>500	0
4	Dissolution of insoluble salts	10	0
5	Convection	10	0
6	High temperature + pressure	20	0
7	Hanging drop	10	0
8	Membrane permeation	10	0
9	*In situ* synthesis	100	0
10	Autoxidation of Sulfite	20	2

Methods attempted ranged from conventional to rather uncommon approaches, but each revolved around severely limiting the amount of one, or both of the reagents that were together at any given time. Methods **1** and **2** used layering to take advantage of the rather slow kinetics of diffusion. In the first approach, two miscible solvents, one containing PyBIG-Cl and the other a sulfate salt, were carefully layered on each other. With time, the two solvents mix, introducing the two reagents. This yielded no crystals. Method **2** used a similar approach but with two immiscible solvents (e.g., water and dichloromethane) relying instead on the phase transfer of the two reagents. No crystals were yielded in this case either.

Method **3** was an attempt to use dilutions in order to keep the concentration of PyBIG-SO_4 low enough to have favorable crystallization kinetics. Unfortunately, in all cases there was either instant precipitation or not enough material to yield a single crystal. Dissolution of insoluble salts **(4)** was an attempt to suspend single crystals of barium, strontium, or calcium sulfate in a solution of PyBIG-Cl, the idea being that the insolubility of these salts would limit the amount of sulfate present to interact. After two months of sitting, only a fine precipitate at the bottom of the beaker was observed in all cases.

Method **5,** also resulting in failure, involved the construction of complex glassware setups to take advantage of the tendency of hot fluids to rise. In several other cases (**6)** a high-temperature pressure reactor was used in order to dissolve more of the PyBIG-SO_4 complex at high temperatures. This was allowed to slowly cool over several days in a temperature controlled oven. While single crystals were obtained, none were thick enough to properly diffract. Hanging-drop **(7)** and slow permeation through a membrane **(8)** are methods often used in protein crystallizations, but both resulted in failure. *In situ* synthesis (**9**) was hoping to utilize the formation of the guandinium as a rate-limiting step. Thus the dialdehyde, aminoguanidinium chloride, and sodium sulfate were all added to a single solution and allowed to settle. Only a fine dust was formed.

The method that finally worked, and developed by myself, was taking advantage of the slow autoxidation of aqueous sodium sulfite in the presence of air.[70] A solution of PyBIG-Cl and sodium sulfite upon sitting for several days, yielded beautiful single crystals of PyBIG-SO_4. While these crystals were still small and rather thin, they were of high enough quality to finally obtain the desired crystal structure. This sort of creativity had to be applied to nearly every solved structure. For PyBIG-CrO_4 and PyBIG-SeO_4, the choice method was adding a few drops of ammonium hydroxide to a solution of anion and PyBIG-Cl. The ammonia allowed for deprotonation of the ligand, thus preventing precipitation. As the solution sits open to air, the ammonia evaporated slowly protonating the ligand and forming the desired complex as single crystals. While these methods seem

very different, they all rely on a single unifying principle: keep the concentration of reagents and the formed complex at an absolute minimum. If that can be done, single crystals of even the most insoluble complexes can be formed.

While troublesome from a structural elucidation perspective, the insolubility of these complexes did come with a rather useful perk. The relative solubilities and differences in precipitation kinetics allowed PyBIG-Cl to separate oxoanions from aqueous mixtures of anions **(Table 3.5).**

Table 3.5: Distribution ratios and separation factors of anions precipitated by PyBIG

Equilibration (h)	D_{Cl}	$D_{Nitrate}$	$D_{Sulfate}$	$D_{Phosphate}$	$SF(SO_4/PO_4)$	$SF(PO_4/SO_4)$
24	0	0	4.09	0.11	36.80	0.03
48	0	0	4.31	0.10	43.80	0.02
72	0	0	4.46	0.10	45.60	0.02
96	0	0	4.84	0.09	52.73	0.02

Ion Chromatography (IC) was used to quantify the selectivity of the PyBIG species by analyzing the residual aqueous solution once the solid precipitate was filtered. Selectivity for sulfate was very high, with *D* values ranging from 4.09 to 4.84 for sulfate while no corresponding removal of chloride or nitrate was observed, and only a minimum amount of phosphate was removed. In fact, the separation factor for sulfate and phosphate ranged from 36.80 to 52.73 depending on the time equilibrated showing that PyBIG has a very

high selectivity for sulfate from this anionic mixture. Thus, PyBIG provides a competent method for the purification of sulfate from aqueous solutions.

To test the ligand on a real world complex mixture, the ability of PyBIG to remove sulfate from seawater was determined by beta-scintillation counting **(Table 3.6).**

Table 3.6: Removal of sulfate from seawater using PyBIG.

Equiv. PyBIG-Cl	[mmol]	% Sulfate Removed
0.5	15	48.29
1	30	94.79
1.1	33	99.95
1.5	45	99.99
2	60	99.99

Here, we see that PyBIG-Cl is capable of removing more than 99.95% of sulfate from seawater with just 1.1 equivalents added, while additional ligand makes the removal quantitative. Compared to the previously reported BBIG, this ligand performs much better and achieves sulfate removal > 99% with fewer equivalents of ligand added. This here does raise a question though, as the solubility of PyBIG-Cl is slightly greater than that of BBIG-Cl, yet this does not appear to affect the efficacy of the ligand in regards to

its performance in seawater. Whether this is a function of the ionic strength (the pyridine, being a hydrogen bond accepting functionality, may be more soluble in higher ionic strengths) or a kinetic effect is currently being investigated.

As the structures of PyBIG- SO_4, SeO_4, and CrO_4 are isomorphic, a considerable difference in selectivity would not be expected. Yet, we reasoned that the difference in size of the oxoanions may have more subtle effects to the structure and the kinetics of the precipitation that may be observed. IC was used in order to probe the system for any selectivity between these three similar oxoanions **(Table 3.7)**.

Table 3.7: Distribution ratios and separations factors for the $SO_4/SeO_4/ CrO_4$

$D_{Sulfate}$	$D_{Selenate}$	$D_{Chromate}$	$SF(SO_4/SeO_4)$	$SF(CrO_4/SO_4)$	$SF(CrO_4/SeO_4)$
0.35	0.15	1.09	2.32	3.32	7.23

Surprisingly, the system has a strong preference for the removal of sulfate from solution in preference to both selenate and sulfate, showing a separation factor of 3.32 and 7.23 for chromate over sulfate and selenate respectively. While we have not arrived at an explanation for this observed selectivity, the results are notable and intriguing. For water purification applications where these similar oxoanions are present, this molecule provides a means of not only differentiation between the anions but also a means of separation.

3.4: DIRECT AIR CAPTURE OF CO_2 USING PYBIG

During the previous experiments, it was observed that an aqueous solution of PyBIG standing in ambient air precipitated large crystalline prisms at the air-water interface. Given the current problem presented by climate change, we decided to pursue this observation further. Direct air capture of CO_2 provides a means of capturing dispersed emissions without limiting the location of the separations plant. Until recently, it had been thought that direct air capture was too cost-prohibitive to use as a viable method of CO_2 sequestration[71], yet with advancing technology and more accurate price modeling, air capture is quickly becoming seen as not only economically viable but also an important technology.[72] This uplifting view has spurred much research in the area, and many new and novel approaches to CO_2 are coming to the forefront. The ideal air capture system would have fast kinetics of capture, an exceedingly high CO_2 capacity, a minimal energy input requirement for release of the trapped gas, infinite regenerateness, and non-volatility. Aqueous sodium hydroxide can be used as an efficient scrubber that meets most of these criteria and reacts with carbon dioxide to yield sodium carbonate and sodium bicarbonate. These carbonates are then precipitated with calcium hydroxide to form calcium carbonate, which must then be heated at over 800 °C to release the carbon dioxide and revert back to the active hydroxide. The high-energy input required for release and regeneration limits the utility of this reagent for practical purposes. In fact,

many modern approaches suffer from high energy costs associated with the release of the gas and regeneration of the active species. It was proposed by the American Physical Society[73] that in order to lower the cost of air capture even further it is necessary to identify new materials to lower the temperature of carbon dioxide release. Here, we address this concern by demonstrating a new CO_2 capturing agent that allows for removal of CO_2 from ambient air, and subsequent release of the gas and regeneration of the ligand at mild temperatures.

Single crystal x-ray diffraction revealed a 1:1 PyBIG-CO_3 complex co-crystallized with four water molecules **(Figure 3.10)**.

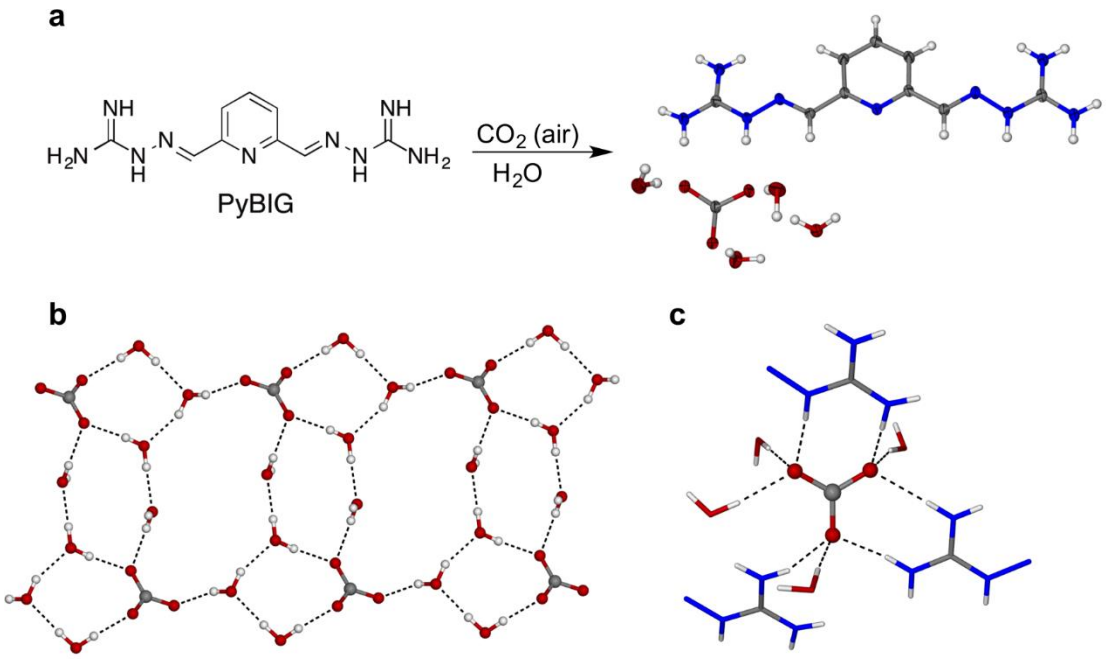

Figure 3.10: Net reaction of PyBIG and CO_2 (a), the carbonate water cluster formed (b), and the overall hydrogen bonded complex (c)). *Used with permission from John Wiley and Sons and Angwandte Chemie and is taken from: Seipp, C.A.; Williams, N.K.; Kidder, M.K.; Custelcean. R.; Angwandte.* DOI: 10.1002/anie.201610916

The PyBIG-CO_3 complex forms an extended network of symmetric-planar cation-π stacked molecules, with the carbonate partaking in a total of nine hydrogen bonds (the free ligand, while stacked, is asymmetric as shown in **Figure 3.11).** Five of the hydrogen bonds are donated from the guanidinium group (avg. 1.898 angstroms) and four from the included water molecules (avg. 1.941 angstroms). When left in a vial open to air for a week, a 0.11 mM solution of ligand in water yielded the carbonate complex in a 50.0 ±

0.4% yield. These carbonate crystals are extraordinarily insoluble, with a K_{sp} of 1.9×10^{-8} as determined by UV-Vis. The insolubility of this complex is comparable to calcium carbonate (K_{sp} of 3.4×10^{-9}), a commonly used carbonate precipitant in the Kraft-process.[74] While the yield and reaction rate is modest, no attempts at optimizing the air-liquid contacting were made; the rate of airflow of air into the vial and subsequent contact with the stagnant solution is feeble at best. It is likely that through optimization of reaction conditions, greater efficacy could be obtained.

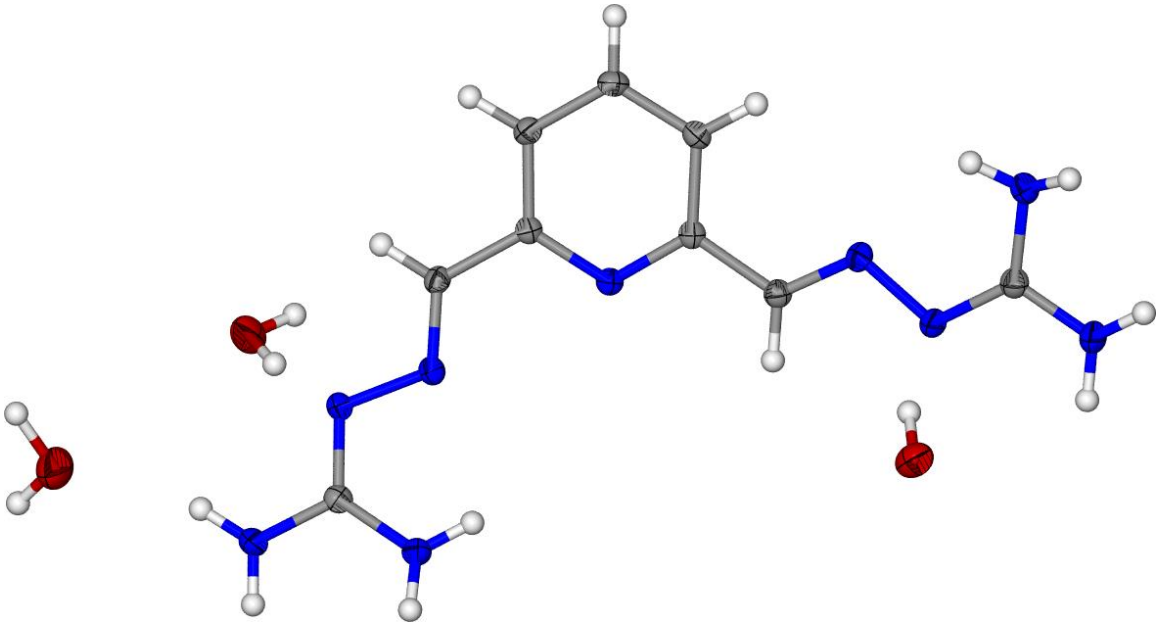

Figure 3.11: Single-crystal X-ray structure of PyBIG·2.5H_2O showing its asymmetric orientation which is not seen in the protonated versions.

Due to the close proximity of the guanidinium protons to the carbonate, we thought it possible that heating the complex gently could stimulate protonation of the carbonate and subsequent loss of water and carbon dioxide. TGA-MS confirmed loss of both CO_2 and water, and provided a detailed picture of the decomposition process. Slow heating of the PyBIG-CO_3 salt caused loss of CO_2 beginning at 65 °C and ending at 140 °C for a total mass loss of 35% **(Figure 3.12 and Figure 3.13)**.

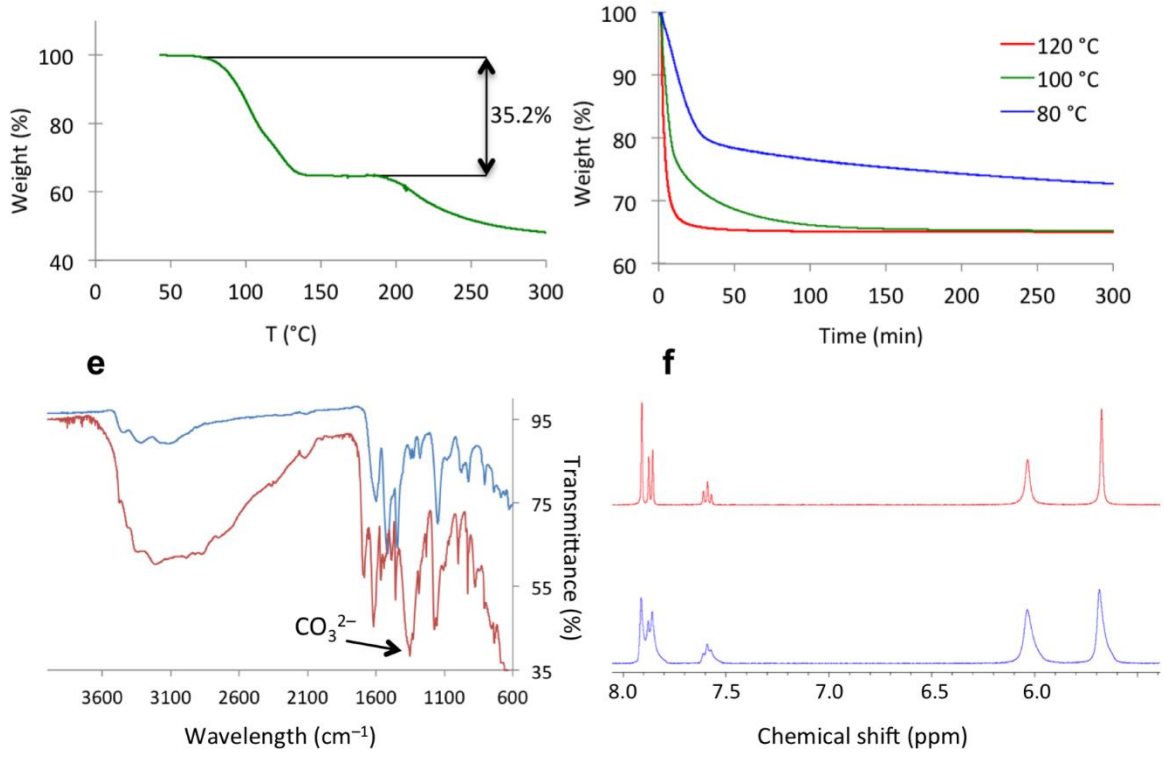

Figure 3.12: Variable temperature TGA of the PyBIG-CO_3 complex showing loss of CO_2 and H_2O (a) Comparison of three isothermal TGA runs (b), IR showing loss of CO_3^{2-} after heating (red) and presence of the anion before heating (blue) (c), NMR of the free complex as synthesized (red) and after baking PyBIG-CO_3 at 120 °C. *Used with permission from John Wiley and Sons and Angwandte Chemie and taken from: Seipp, C.A.; Williams, N.K.; Kidder, M.K.; Custelcean. R.; Angwandte.* DOI: 10.1002/anie.201610916

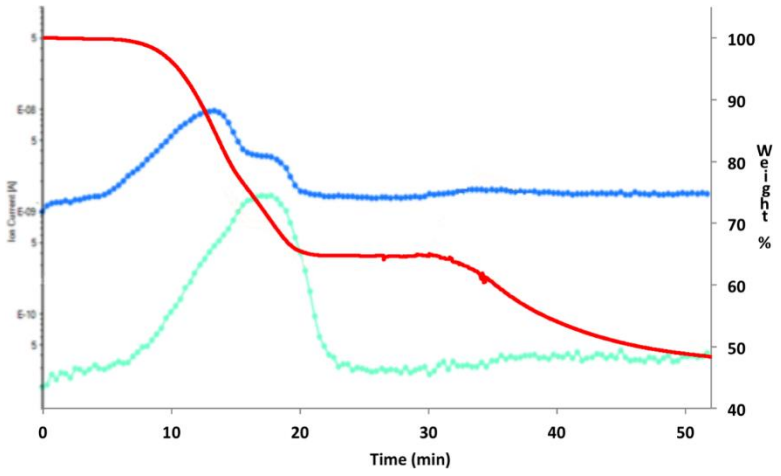

Figure 3.13 : TGA-MS of $PyBIGH_2(CO_3)(H_2O)_4$. Overlay of the molecular peaks in the MS, corresponding to CO_2 (m/z 44, teal) and H_2O (m/z 18, blue), and the weight loss from the TGA (red), as a function of time. Fragmentation peaks in the MS are omitted for clarity. *Used with permission from John Wiley and Sons and Angwandte Chemie and is taken from: Seipp, C.A.; Williams, N.K.; Kidder, M.K.; Custelcean. R.; Angwandte.*
DOI: 10.1002/anie.201610916

This corresponds well with the loss of one carbonate and two protons (as CO_2 and H_2O), and an additional four water molecules as observed in the obtained crystal structure. Peaks corresponding to the evolution of both carbon dioxide and water were seen by mass spectrometry. The loss of CO_3 and water is observed by IR. After heating, the CO_3 peak present at about 1350 is seen to vanish. Furthermore, the characteristic bends and stretches of water water (3500-2400, br and 1650, str) are also seen to vanish.

Another important feature of the TGA-MS is the observed stability of the compound post CO_2-release. There is no observed decomposition until 190 °C is reached, speaking to the thermal stability of this compound. Subsequent isothermal runs at 100 °C, and 120 °C showed complete loss of carbon dioxide and water at 150 and 60 minutes respectively. At 80 °C, the run reached 78% completion at 300 minutes, further highlighting the mild conditions at which CO_2 release occurs. To demonstrate the real world applicability of these results, a microscope slide of PyBIG-CO_3 was put in a drying oven at 120 °C for one hour **(Figure 3.14).**

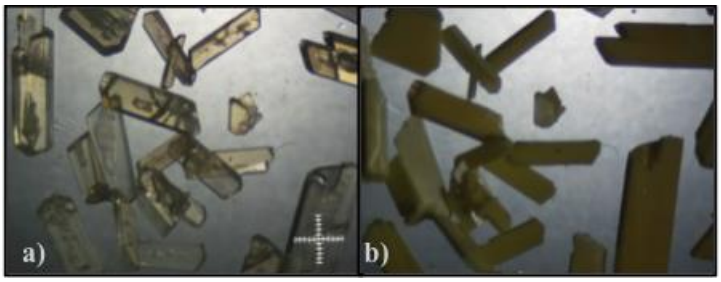

Figure 3.14: Crystals of PyBIG-CO_3 before heating (a), and the same crystals after heating (b).The change in opacity and color corresponds to the formation of the free ligand. *Used with permission from John Wiley and Sons and Angwandte Chemie and is taken from: Seipp, C.A.; Williams, N.K.; Kidder, M.K.; Custelcean. R.; Angwandte.* DOI: 10.1002/anie.201610916

The total weight loss was 35%, matching both theory and the TGA-MS results, proving that this transformation occurs readily in open air without decomposition. Further, one can visually observe the transformation occur. The PyBIG-CO_3 complex is composed of large, clear, and translucent crystals; however, upon heating, these crystals yellow and

become opaque. This observation corresponds to changes in the IR spectra of the compounds, with loss of a broad peak at 1350 occurring after heating of the compound. Not only does PyBIG-CO_3 release CO_2 and regenerate its active form at low temperatures, but it also removes the need to heat bulk aqueous solution. As the CO_2 containing solid is filtered away from the water, the only energy input needed is that of heating the residual crystals. As water's large heat capacity necessitates a large input of wasted energy, this ligand provides a much more economical alternative for CO_2 release.

The ability of PyBiG to form the carbonate salt from exposure to CO_2 made us wonder if the ligand could protonate in bicarbonate/carbonate solutions and form the CO_3 complex. There have been several studies proving the feasibility of a $NaHCO_3$ / Na_2CO_3 cycle for CO_2 capture,[75] and the ability to bind and precipitate carbonate could lend itself to these processes (**Figure 3.15)**.

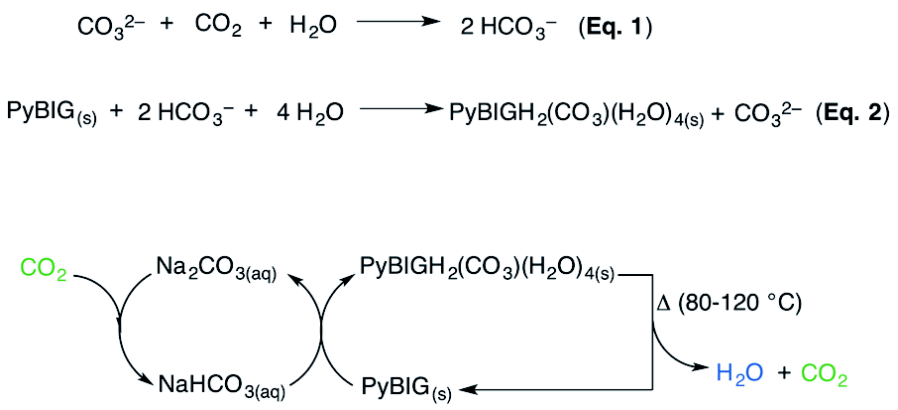

Figure 3.15: The proposed mechanism of the formation of the PyBIG-CO_3 salt (eq1 + eq2). This leads to the formation of carbonate which has been demonstrated as a viable agent for CO_2 capture. The incorporation of PyBIG into such a cycle is shown at the bottom of the figure. *Used with permission from John Wiley and Sons and Angwandte Chemie and is taken from: Seipp, C.A.; Williams, N.K.; Kidder, M.K.; Custelcean. R.; Angwandte.* DOI: 10.1002/anie.201610916

BiPyG (1 mol. Eq.) was suspended in a 1 M bicarbonate solution (5 mol. Eq.) and allowed to mix for one hour. The mixture was filtered, decomposed via heating for one hour at 120 °C, and re-subjected to the original bicarbonate mixture for a total of three cycles. The ligand is recyclable over multiple trials—in all cases regeneration of the ligand was essentially quantitative and the recovery of carbonate in subsequent uses falls only slightly. The overall recovery from the "slurry" is 98.9 ± 0.3% yield for the first trial, 99.2 ± 0.2% yield for the second trial, and 97.1 ± 0.5% yield for the third trial. For the first two trials, FT-IR showed quantitative formation of the PyBIG-CO_3 complex **(Figure 3.16)**. In the final trial, only the peaks representing the carbonate complex and a small amount of free ligand were present. Confirmation that this precipitated product is

equivalent to that of the obtained single crystals can be seen in comparing the powder pattern of the precipitate with the calculated power pattern from the single crystal **(Figure 3.17).** Given that the two are nearly identical, we know with certainty that these two phases are the same. As the pH of the solution is increasing in each subsequent trial (two protons are lost from the bicarbonate present for each unit of carbonate removed), it is expected that the efficacy of the ligand will slowly diminish, as protonation is a requirement for crystallization. Furthermore, in all cases the FT-IR of the regenerated ligand matches that of a known sample of PyBIG **(Figure 3.18).** The ease at which this ligand precipitates carbonate and the low temperature of CO_2 release, provides an economical alternative to calcium carbonate precipitation in carbonate-based direct air capture cycles.

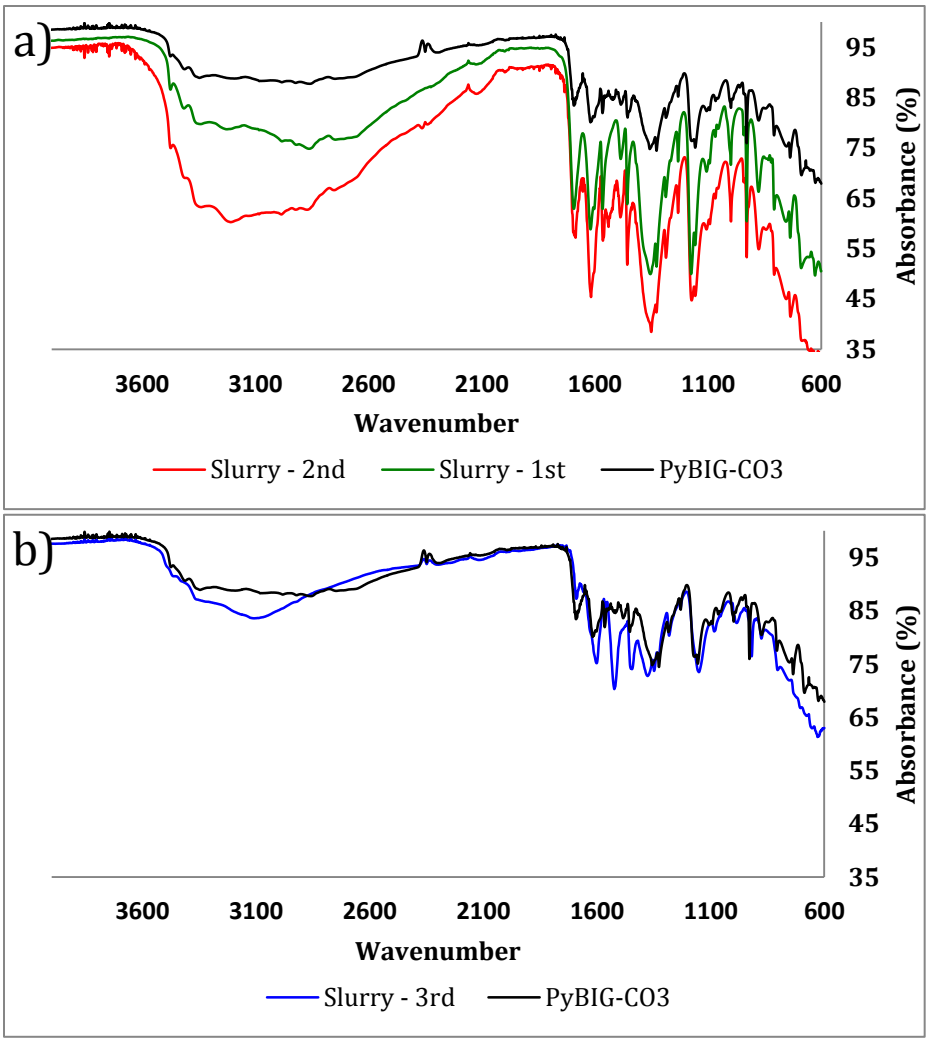

Figure 3.16: Comparative FTIR spectra of the solids isolated from the slurry reaction of PyBIG with aqueous sodium bicarbonate. a. Products from the first two cycles (green, red) overlaid over the reference spectrum of $PyBIGH_2(CO_3)(H_2O)_4$ (black); virtually no PyBIG ligand is observed. **b.** Product from the third cycle (blue), overlaid over the reference spectrum of $PyBIGH_2(CO_3)(H_2O)_4$ (black), indicating a mixture of carbonate and PyBIG. *Used with permission from John Wiley and Sons and Angwandte Chemie and is taken from: Seipp, C.A.; Williams, N.K.; Kidder, M.K.; Custelcean. R.; Angwandte.*
DOI: 10.1002/anie.201610916

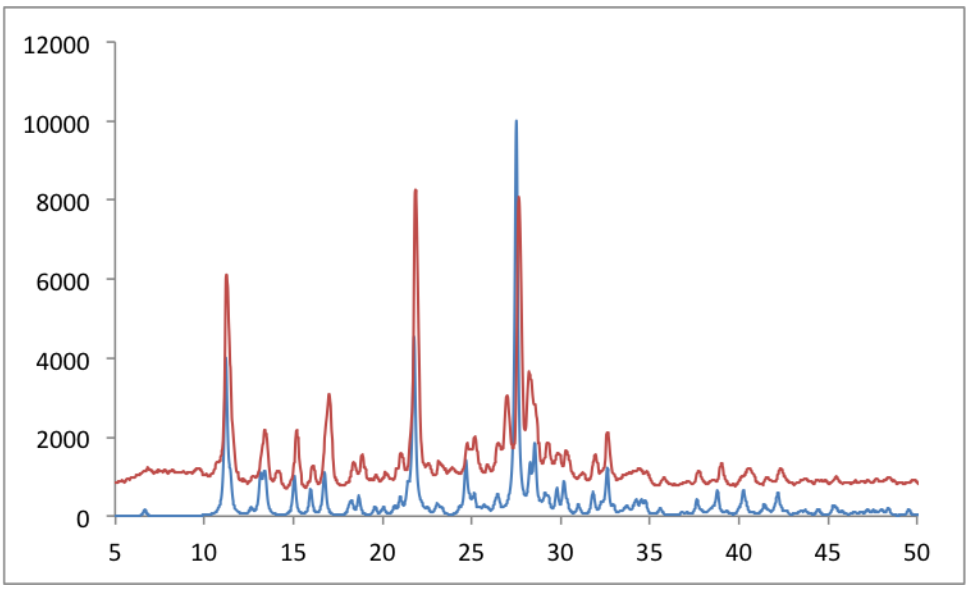

Figure 3.17 : PXRD pattern of crystalline solid isolated from the slurry reaction of PyBIG with aqueous sodium bicarbonate (red) overlaid over the simulated PXRD pattern from the single-crystal X-ray structure of $PyBIGH_2(CO_3)(H_2O)_4$ (blue). *Used with permission from John Wiley and Sons and Angwandte Chemie and is taken from: Seipp, C.A.; Williams, N.K.; Kidder, M.K.; Custelcean. R.; Angwandte.*
DOI: 10.1002/anie.201610916

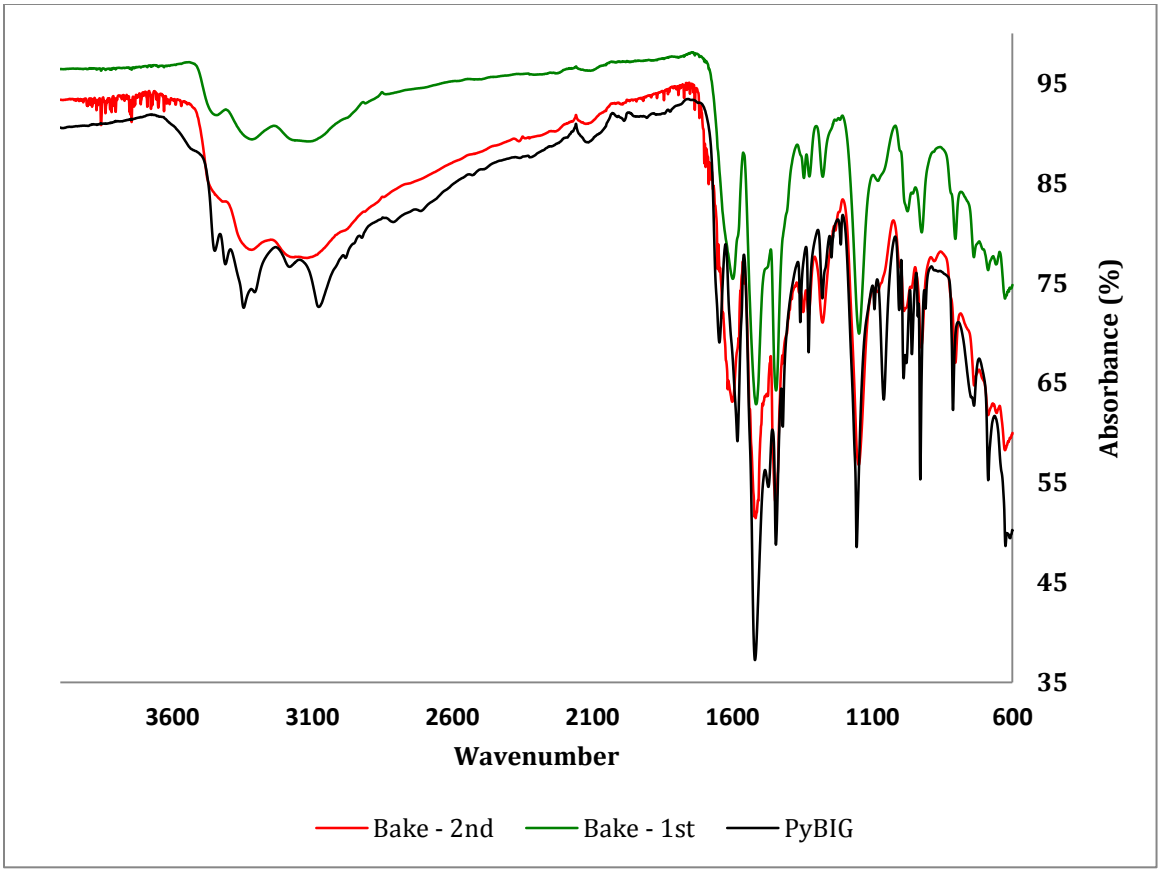

Figure 3.18: Comparative FTIR spectra of the recovered PyBIG ligand from the slurry reaction with aqueous sodium bicarbonate. The regenerated ligand matches the spectra of the as synthesized PyBIG. The only difference is the water peaks in the 3100-3600 region (O–H stretch) and at 1640 (H–O–H bend), present in the as synthesized PyBIG·2.5H_2O (black), and absent in the recovered anhydrous PyBIG (green, red). *Used with permission from John Wiley and Sons and Angwandte Chemie and is taken from: Seipp, C.A.; Williams, N.K.; Kidder, M.K.; Custelcean. R.; Angwandte.* DOI: 10.1002/anie.201610916

The utility of the PyBIG reagent cannot be understated. Here, we have a molecule that cannot only effectively separate sulfate and chromate from aqueous solution but can also be adapted to the recovery and controlled release of CO_2. We hope that further exploration of these bis(imino)guanidinium systems may yield even more useful and interesting separation technologies. There is much future work currently planned on this system. First and foremost, we have a library of bis(aldehydes) that we plan on synthesizing and turning into receptors. We hope to determine the solubility products of sulfate of each of these, obtain single crystal structures, and try to develop the knowledge needed to rationally design these insoluble complexes. Next, the mechanism of CO_2 capture and subsequent release is being explored. From a basic research standpoint, a firm understanding of the mechanism of capture and release would allow for the design of even better ligands. Finally, either a less expensive alternative to PyBIG or a cheaper route to the system is being devised. Economics is one of the most important factors in whether or not a system is adapted for industrial use. We aim to minimize cost by producing even more cost-efficient systems.

Chapter 4: Bis(Imino)Guanidiniums for Extraction – Present and Future Work

SUMMARY: *In Chapter 4, the theoretical bis(urea)guanidinium (BUG)will be briefly discussed. The possibility of adaptating our iminoguanidinium chemistry to making this kind of species will be discussed. The work underway, as well as future directions of this project are then outlined. For Supplementary Information, please see Appendix I.*

4.0: PROGRESS TOWARDS A BIS(UREA)GUANIDINIUM

Given that shape and charge complementarity are key factors in determining the affinity and selectivity of a receptor for a ligand, we wanted to expand upon our *N,N'*-bis(2-pyridyl)guanidinium scaffold discussed in Chapter 2 to include additional convergent groups. Initially, our goal was to create a **B**is(**U**rea)**G**uanidinium species around this motif so that a completely complementary receptor for sulfate could be formed **(Figure 4.1)**.

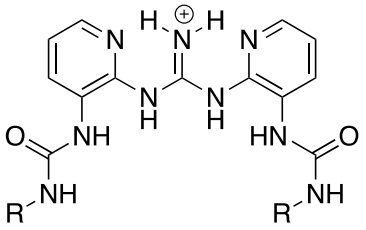

Figure 4.1: The ideal bis(urea)guanidinium (BUG) compound.

Given its positive charge, it was expected that the ligand would associate in a 2:1 complex, thereby completely coordinating to sulfate and saturating coordination sphere with 12 hydrogen bonds.

Retrosynthetically, the BUG could be realized starting from 2-amino-3-nitropyridine. **(Figure 4.2).**

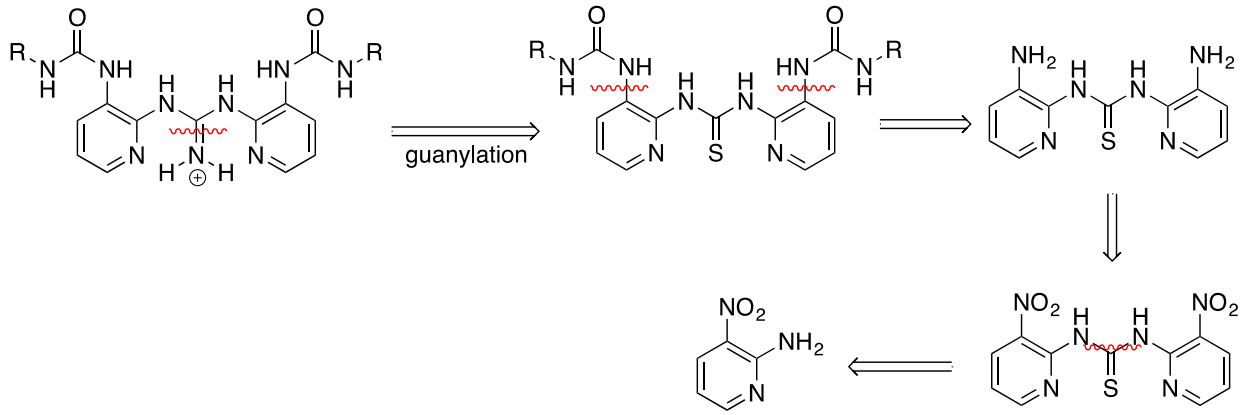

Figure 4.2: Retrosynthetic analysis of the BUG.

2-Amino-3-nitropyridine could be dimerized using thiophosgene or CS_2 to give the desired thiourea. Subsequent reduction of the nitro groups utilizing hydrazine hydrate and Pd/C, followed by reaction with an isocyanate of choice could give the bis(urea)thiourea intermediate. Finally, desulfurization and reaction with ammonia would give the desired compound. All of these reactions were used / developed previously for the BiPyG system, and it was expected that completion of the BUG would straightforward.

Unfortunately, the chemistry in this case was not cooperative. In all cases unexpected reactivity, un-reactivity, or degradation occurred. Just the first step, the synthesis of the thiourea, was met with considerable difficulty. In all, we envisioned two potential pathways, both involving the use of 2-amino-3-nitropyridine to reach the desired thiourea intermediate **(Figure 4.3, Table 4.1)**.

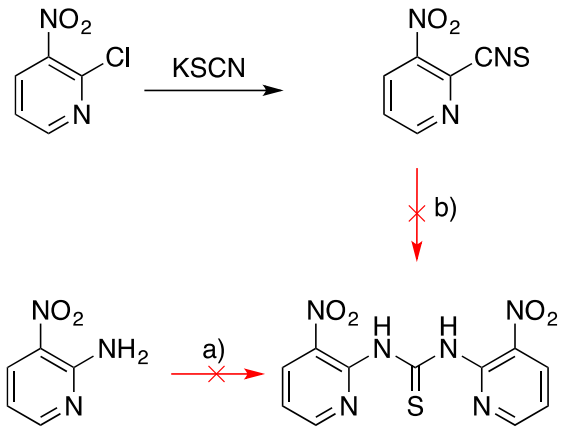

Figure 3.3: Two separate synthetic pathways to access the required thiourea derivative.

Table 4.1: Representative sample of attempted thiourea formations.

Trial:	**Reagents:**	**Conditions:**	**Result:**
1a-6a	Thiophosgene, K_sCO_3	DCM (0 °C, RT, reflux) **or** DCM/water (0 °C, RT, reflux)	No reaction
7a-10a	Thiophosgene, TEA	DCM (0 °C, RT, reflux)	No reaction
11a-12a	TCDI + base (KOtBu **or** K3PO$_4$)	THF, reflux	No reaction
13a-19a	CS_2 neat, base (pyridine **or** NaOH) **or** S_8	Reflux or in microwave (150 °C)	No reaction
1b	2-amino-3-nitropyridine	Reflux	No reaction
2b-3b	2-amino-3-nitropyridine, KOtBu	0 °C **or** reflux	No reaction
4b	2-aminopyridine	Reflux	No reaction

Despite our best of efforts, it proved impossible to form the thiourea of 2-amino-3-nitropyridine using either of the two proposed routes. In the first route (**a**)**,** we attempted to couple 2-amino-3-nitropyridine with a thiourea-forming reagent. We tried various coupling reagents (CS_2, thiocarbonyldiimidazole (TCDI), thiophosgene) of increasing reactivities with no success. The addition of bases, or catalysts did not affect the

transformation. Increasing temperatures were also used, even going so far as to reflux the compound in thiophosgene. Neither reaction nor decomposition occurred. This interested us, as in our past experience thiophosgene would typically elicit a low-yield and a large amount of decomposition yet here was a system in which neither was observed. In an attempt to circumvent this obstacle, the 2-isothiocyanato-3-nitropyridine was synthesized directly from 2-chloro-3-nitropyridine (**Figure 4.3)**. This compound gave us access to the thioisocyanate intermediate usually formed by reaction of thiophosgene with our aminopyridines, so we thought this would enable the facile formation of the thiourea. This reaction also failed to occur, even in the presence of strong bases (**2b-3b)**, and at reflux conditions.

The fact that the isothiocyanate would not react surprised us. After all, the isothiocyanate is an electrophilic site, being adjacent to both a nitrogroup and a pyridine should vastly increase this already reactive group's tendency towards nucleophilic attack. We strongly suspected that the nitro-group was deactivating the amine enough to where facile reaction was not possible, although evidence against this being the only factor was given when 2-isothiocyanato-3-nitropyridine was unreactive towards 2-aminopyridine. As we had complete characterization of the isothiocyanato-3-nitropyridine, we knew that there had to be something else contributing to the unreactivity of these species. At this time though, we were unsure of what that contributing factor was. Thus, we decided to change our approach towards the molecule.

2,3-Diaminopyridine was chosen as a new starting path, which underwent facile mono-urea formation with a variety of isocyanates (Figure **4.4**).

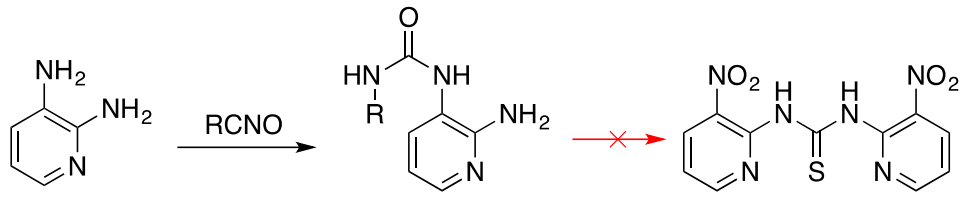

Figure 4.4: Synthesis of the thiourea did not proceed from 3-urea functionalized amino pyridines.

With our 2-amino-3-ureapyridine in hand, we were just a simple coupling away from forming our pre-functionalized thiourea. Unfortunately, the next step would not proceed, and no matter the strength of the electrophile used, the 2-amino group remained unreacted **(Table 4.2)**.

Table 4.2: Representative sample of attempted thiourea formations of the 3-urea-functionalized aminopyridines. (All reactions were attempted twice, once each with an alkyl and an aryl urea).

Trial:	**Reagents:**	**Conditions:**	**Result:**
1-12	CS_2 neat, base (pyridine **or** NaOH) **or** S_8	Reflux or in microwave (150 °C)	No reaction.
13-23	Thiophosgene **with and without** TEA.	DCM (0 °C, RT, reflux)	No reaction
24-29	TCDI + KOtBu	THF, RT **or** reflux	No reaction
25-37	2-isothiocyanate-3-nitropyridine, **with and without** TEA	THF (RT **or** reflux), dioxane (RT **or** reflux)	No reaction

Neither mild (CS_2), intermediate (TCDI), or harsh (thiophosgene) conditions gave any sort of reaction with the starting material. Increasing the temperature, the strength of base, or addition of a sulfur catalyst did not give any noticeable product or decomposition. Now, previously we had observed that the 2-amino-3-nitropyridines were inert to even forcing conditions, but we had hypothesized that there was an additional contributing factor to its observed un-reactivity after 2-isothiocyanato-3-nitropyridine did not reaction with 2-aminpyridine. In this case, the 3-urea group should actually *slightly* activate the 2-amino group of the pyridine ring towards nucleophilic substitution yet a reaction of *any* kind is not observed. In searching for an answer to these observations, a literature article was found demonstrating that the 2-aminogroup was nearly impossible

to react once a sterically hindering group was placed in the 3-position.[76] Between the deactivating effect of the pyridine, and the added bulk of either the nitro or the urea group, it was impossible for them, and for us, to achieve the desired transformation.

As the presence of the pyridine was providing an electron sink, thereby deactivating the starting material towards subsequent transformations, it was decided to attempt to synthesize derivatives based on the phenyl group. While the intramolecular hydrogen bonding we hoped to observe in the bis(2-pyridyl) case would surely not be observed, we could at least obtain a bis(phenyl)guanidinium. To this aim, two synthetic pathways were devised (**Figure 4.5**).

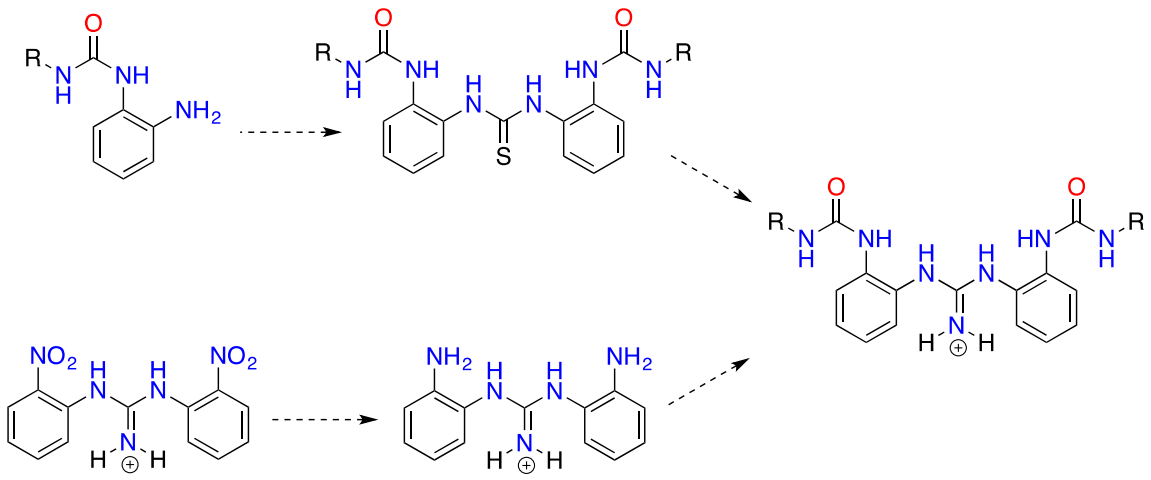

Figure 4.5: Two additional synthetic pathways to a BUG. R = lipophilic alkyl group (such as 2-ethyl-hexyl, dodecyl, or 3,7-dimethyloctyl).

The first pathway relies on the formation of the bis(2-nitrophenyl)guanidinium compound, followed by subsequent reduction and urea formation with an isocyanate. Synthesis of the guanidine was attempted starting from commercially available 2-nitrophenylisocyanate (**Figure 4.6**).

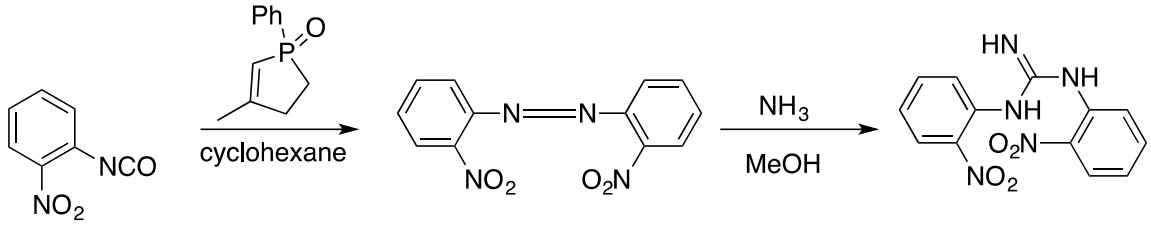

Figure 4.6: Carbodiimides could be easily obtained from a corresponding isocyanate and a phosphorous catalyst.

The carbodiimide was formed readily from 2-nitrophenylisocyanate and a phosphorous catalyst in a 93% yield. Unfortunately, subsequent reaction with ammonia did not appear to give the corresponding guanidinium which lead to some confusion. The ^{1}H-NMR appeared to be missing a relevant aromatic proton, while ^{13}C NMR, even after several thousand scans on a concentrated solution, showed both broad and missing carbon signals.

In an attempt to make sense of these observations, a sample was sent out for mass spectrometry in order to identify the dominant species. This lead to only more confusion,

as the results of the mass spec indicated that the product had a mass corresponding to that of *N,N'*-bis(2-nitrophenyl)guanidine (Observed m/z: 302.08930, Calculated m/z: 302.08840). Trying to rationalize these two observations proved difficult. While it is seen that due to attached strongly withdrawing groups and resonance effects that protons can sometimes broaden, this effect is not often seen with aromatic groups. We hoped that if the mystery product were subjected to the next set of reaction conditions, perhaps the obtained product could help us elucidate the structure. Unfortunately, this would not be the case as the reaction would give rise to *N,N'*-bis(phenyl)urea, an unsuspected product that only caused more confusion **(Figure 4.7).**

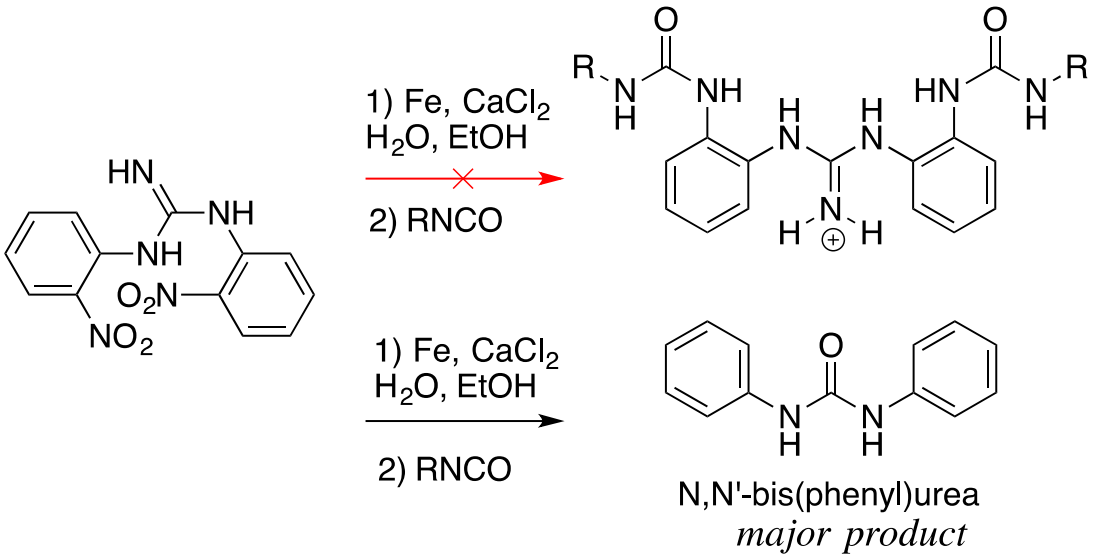

Figure 4.7: Reduction and reaction with phenylisocyanate of the N,N'-bis(2-nitrophenyl)guanidine formed an unexpected product.

This was a one pot, two step procedure where the reduction was allowed to take place first and the iron catalyst was filtered. An extractive workup was utilized in order to separate the intermediate from any residual catalyst and calcium chloride. Upon addition of the isocyanate in dichloromethane, a white precipitate formed as the major product which was later found to be *N,N'*-bis(phenyl)urea. The isolated product was intriguing as there is no obvious route to get to it. After all, the urea obviously comes from the phenylisocyanate yet requires addition of an aniline equivalent—of which there is none present in our system that we were aware of. While the high-res mass spec did confirm the presence of *some* amount of a species isomeric with the desired dinitrophenylguanidinium, the proton spectra made us question the identity of the starting material. Often, when unexpected and unexplained reactions occur, it can be easily tracked due to a misidentified intermediate. Additional attempts towards further characterizing our dinitrophenylguanidinium were taken, but 2-D NMR experiments were inconclusive and a single crystal was unable to be grown. Thus, work on this synthetic pathway ceased.

Our next attempted pathway utilized 1,2-phenyldiamine as a starting material to remove the deactivating effect of the pyridine. While the monourea could be obtained in high-yield, it was found impossible to form the thiourea from an isothiocyanate, or similarly reactive intermediate (such as *S*-methylthiouroniums). In all cases, either pure starting

material or a mixture of products were obtained. We suspected that intramolecular cyclization was occurring on the urea nitrogen, affording the cyclic *N*-ureathiourea (**Figure 4.8**). This is lent further credence by an analogous reaction reported by Martin *et. al.* in which cyclization to this very compound is reported in the presence of thiophosgene.[77]

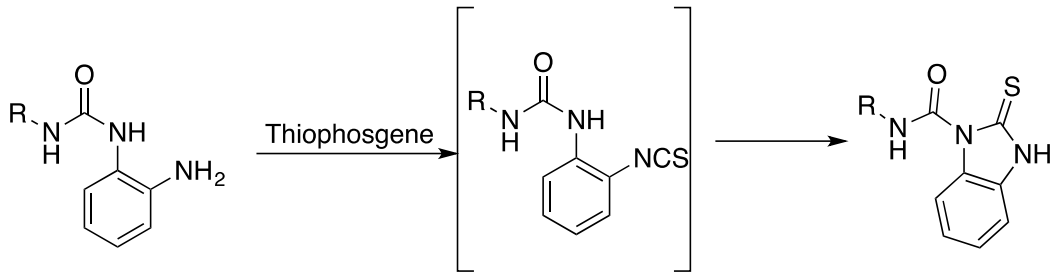

Figure 4.8: The cyclization of the ortho-phenylaminourea in the presence of an activating reagent.

Ultimately, the BUG was never realized but as its structure has the potential to be a perfect sulfate binding agent, we sought structural modifications that could both ease the synthetic liability and still provide a competent anion binding motif. We had seen the success of the BIG series (Chapter 3), and wondered if there would be a way to adapt the iminoguanidinium chemistry to the idea of the BUG. Given the ease of the formation of the iminoguanidinium bond and its apparent stability, it seemed to be a natural progression of thought **(Figure 4.9)**.

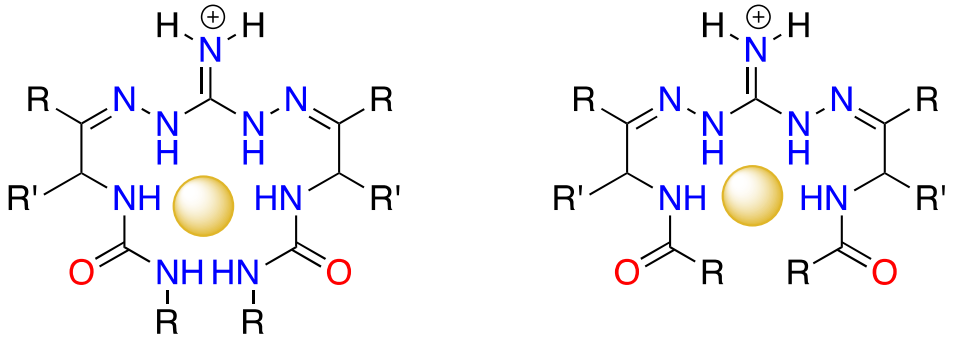

Figure 4.9: Adapting the imino(guanidinium) chemistry to the BUG allows for easier formation of the guanidinium core.

The bis(amide)iminoguanidinium (BAG) would still have a positively charged guanidinium core. As the installation of the central guanidinium would proceed under mild conditions in the presence of an aldehyde and 1,3-bis(amino)guanidinium, we hoped that we could prevent unwanted side reactions of the amide/urea side-chains and develop a new class of convergent anion receptors.

4.1: Present and Future Work – The "Bis(amide)guanidinium":

Initial plans were set out to make the bis(urea) version of the molecule, but upon discovering in the literature search that alpha-urea aldehydes are prone to undergo intramolecular cyclization even at low temperatures, as well as our previous experience in synthesizing the BUG, we abandoned this approach.[78] Attention was thus turned towards making bis(amide)guanidiniums, or BAGs, as the amide nitrogen is less activated than the urea nitrogens. This proposed molecule removes the favorable pathway

towards formation of the ring, and enables the central guanidinium to be formed under extraordinarily mild conditions. While this proposed molecule has a distorted geometry when compared to the original BUG, we wanted to see if it would still create a viable complexant.

To this aim, a synthetic path was devised using natural amino acids. Amino acids are common, abundant, and cheap. Furthermore, there exists a plethora of side chains of interesting and potentially useful functionality. Designing receptors that can be synthesized easily from these species gives access to a myriad of potential receptors. Most importantly, aminoacids are capable of undergoing a Dakin-West reaction in the presence of pyridine and acetic anhydride, affording alpha amide ketones in high yield and a single step.[79] This reaction provides an easy, one pot method to convert an amino acid directly to the precursor of the receptor. Subsequent reaction with bis(amino)guanidinium chloride affords the desired BAG **(Figure 4.10).**

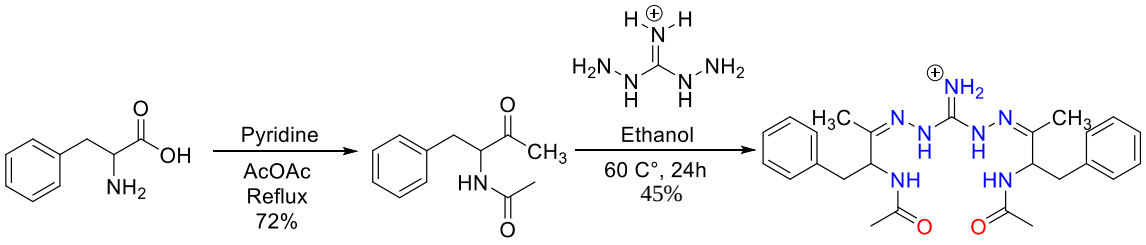

Figure 4.10: Synthetic route to get to the first generation BAG. The synthesis requires just two steps to get to the final structure.

The first generation of BAG based off of phenylalanine was very water soluble and only sparingly soluble in organic solvents such as dichloromethane, making it a poor candidate for both extractions and crystallizations. NMR titration studies were performed and sadly no affinity for sulfate was observed in either methanol or DMSO. In order to troubleshoot this observation, we attempted to grow single crystals in order to gain additional insight on its conformation. No single crystals could be obtained despite trying many of the methods outlined in **Table 3.2.** In this case however, the complex itself is rather soluble in a variety of organic and aqueous solvent systems. Thus, we hypothesize that the observed reluctance to crystalize likely comes from the stereocenters present in the molecule as the presence of stereoisomers often leads to difficulty in crystal growing.

We anticipated that due to the convergent nature of the hydrogen bonds, as well as the positive charge, the ligand was likely to bind oxoanions, but the determination of its preferred partner would be difficult due to the sheer number of available oxoanions. NMR titration studies are very time intensive, and in order to broadly screen for anion binding a competitive extraction experiment was devised. First, a lipophilic derivative of the BAG (LipBAG) would be synthesized. Next, a mixture of anions in aqueous solution would be contacted with a known concentration LipBAG on a centrifugal wheel for 24 hours. The aqueous solution would then be analyzed by ion chromatography and the relative concentration of anions would be determined. Any decrease in anion

concentration would be attributed to extraction via LipBAG and those specific anions would be examined by NMR titration studies.

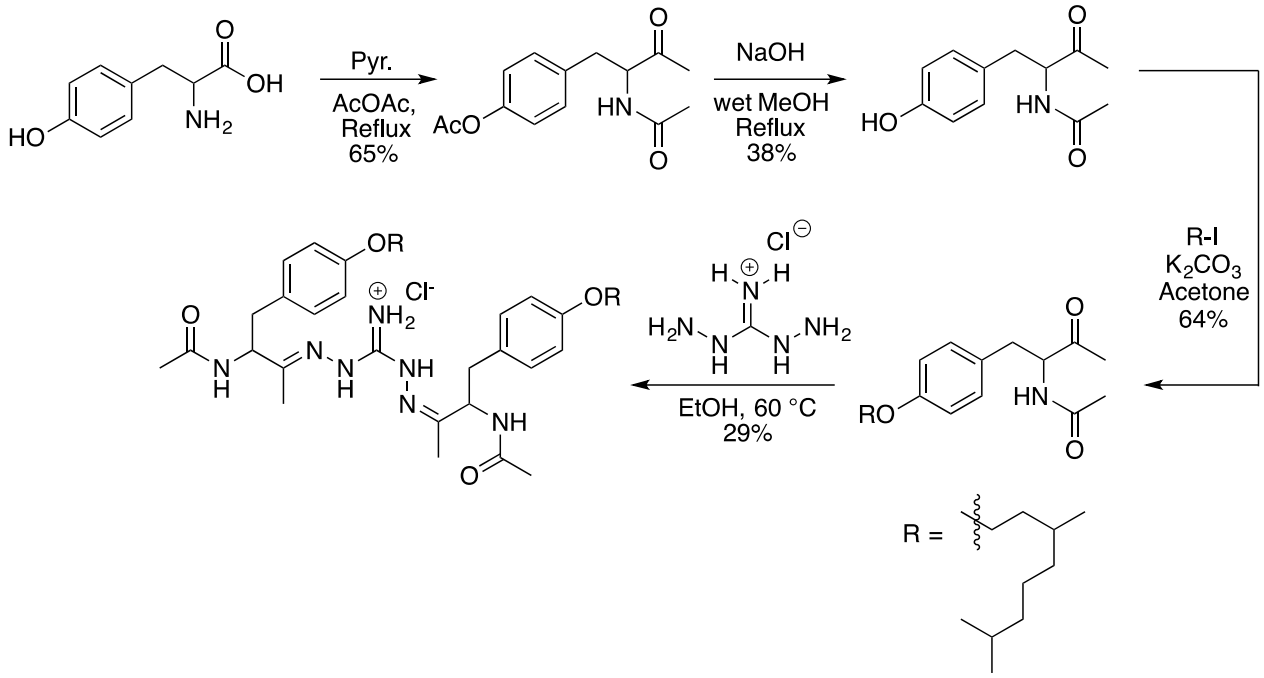

Figure 4.11: Synthetic route to get to the lipophilic BAG.

The synthesis of this lipophilic BAG is outlined in **Figure 4.11**. To this aim, we envisioned the creation of the LipBAG from tyrosine as the presence of the phenol gives us access to a functional handle with which we can subsequently alkylate. Tyrosine when subjected to Dakin-West conditions give the desired keto-amide, but additionally protects the phenol of tyrosine. This compound is obtained pure by trituration with ethyl acetate, and the acetyl group is selectively removed by sodium bicarbonate in wet methanol. It

should be noted that in the original procedure, the acetyl group was removed via the blowing of steam over the remaining solution, in the presence of sodium bicarbonate, after the pyridine and acetic anhydride had been removed via distillation. Attempts to replicate this in a modern lab setting (namely, without access to a steamline) failed. The concentrated reaction mixture was boiled in water for three days, yet little deprotection was seen. Furthermore, reaction with sodium bicarbonate in the 10% water / MeOH also did not give an appreciable yield. Best results were seen with bottles of old (> 3 months) of anhydrous methanol, and were reproducible across several bottles that fit this description. Next, alkylation with 3,7-dimethyloctyliodide affords a highly lipophilic ketoamide that undergoes facile coupling in the presence of N,N'-bis(amino)guanidine hydrochloride to give the final receptor. While a small amount of this compound has been made, the reaction has yet to be fully optimized. Further, analytical testing including selectivity and binding affinity experiments have not been performed as of this time.

This project has the potential to be rather important in the field anion receptors. As discussed in Chapter 1, Yang *et. al.* made a trisurea receptor that was perfectly complementary to sulfate and showed large binding affinities in competitive solvent.[24] The BAG shows a similar level of complementarity, allows for six hydrogen bonds per molecule to sulfate, and has the addition of a positive charge. This positive charge not only should have an attractive interaction on the target anion, but will also cause the hydrogen bonds donated by the guanidiniums to be extremely strong due to both

inductive and resonance effects. This should drastically enhance the binding affinity for whatever oxoanion fits in its cleft. This sort of system with its convergent and strong hydrogen bonds, complementary charge, and easy self-assembled guanidinium core would be unprecedented in the literature and may have substantial commercial applications.

Appendices:

Appendix A: Statement of Performed Work

Given the highly collaborative nature of the work I performed, it is necessary to list what work was performed by me, what work was performed by my colleagues, and which work was done as a collaborative effort. The following paragraphs will attempt to clarify that by chapter.

Chapter 2: The idea for making a pseudo-bicyclic guanidinium species using bis(2-pyridyl)guanidiniums was developed jointly by Dr. Bruce Moyer and myself. All synthetic planning, synthesis, and compound characterization was performed entirely by myself. All single crystals were also grown by myself. X-ray crystallography, as well as solving the structures, was performed by Dr. Radu Custelcean. I performed all binding constant titrations by NMR, fitted the binding models, and had responsibility for all experimental design for these binding-constant experiments. Solubility of the BiPyG-SO_4 complex was determined gravimetrically by me. Extraction studies were performed in tandem by both myself and Neil J. Williams. Computational studies were performed entirely by Dr. Bryantsev. Powder diffraction patterns were obtained by Dr. Radu Custelcean.

Chapter 3:

-GBAH: Dr. Radu Custelcean initially thought of and discovered the GBAH ligand. I performed gravimetric solubility measurements, as well as synthesized large quantities of the ligand for testing. Neil J. Williams performed all solubility measurements utilizing UV/Vis. Radu Custelcean performed the crystal growth as well as the X-ray diffraction. Powder diffraction patterns were obtained by Dr. Radu Custelcean.

-BBIG: Dr. Radu Custelcean initially thought of and discovered the BBIG ligand. I performed gravimetric solubility measurements, as well as synthesized large quantities of the ligand for testing. Neil J. Williams performed all solubility measurements that required UV/Vis or $^{35}SO_4^{2-}$. Neil J. Williams performed a majority of the sulfate removal from seawater experiment, although I assisted with the set-up of the experiment as well as the data analysis. I determined the degree of ligand recyclability and demonstrated a complete cycle. Radu Custelcean performed the crystal growth as well as the X-ray diffraction. Powder diffraction patterns were obtained by Dr. Radu Custelcean.

-PyBIG (non-CO_2 work): The idea for using a pyridine-based linker for its electron withdrawing nature as a way of increasing the insolubility of a salt was developed by myself. I grew all single crystals and performed many of the X-ray diffraction experiments (working closely with Dr. Radu Custelcean). I developed the synthetic route and carried out the large-scale synthesis of the PyBIG ligand. Neil J. Williams and myself worked on the solubility measurements and competition experiments by ion chromatography. Neil Williams did a majority of the $^{35}SO_4^{2-}$ work, although I assisted with experimental setup as well as the data analysis. I developed new methodology for the growth of insoluble PYBIG sulfate, chromate, and phosphate single crystals. Powder diffraction patterns were obtained by Dr. Radu Custelcean.

-PyBIG (CO_2 work): I initially discovered the fact that the ligand was pulling CO_2 from air and proposed it could be used for CO_2 capture. Radu Custelcean and myself jointly thought of using external stimuli to release the CO_3 as gaseous CO_2. Crystal growth and determination of the initial structure was performed by me. Synthesis of the free ligand was also performed by myself. The methodology and demonstration of the recyclable nature of the ligand was performed by myself. Before and after pictures, as

well as the open-to-air thermal decomposition of the ligand, was performed by me. Single crystals for neutron diffraction were obtained by me. TGA-MS was run by Dr. Michele kidder while data analysis was performed by both of us. FT-IR and NMR experiments demonstrating the loss of CO_2 was performed by myself. Solubility of the carbonate complex was measured by Neil Williams. Powder diffraction patterns were obtained by Dr. Radu Custelcean.

Chapter 4: The original concept of the BAG was developed by myself, and fine-tuned through discussion with Dr. Bruce Moyer. All synthetic planning, synthesis, and compound characterization was performed entirely by myself. The realization that these anion receptors could be developed using amino-acids was my own.

Appendix B: General Information on Experimental Procedures

NMR spectra were collected on a Bruker Avance III 400 using either a 5mm PABBI or PABBI probe in $CDCl_3$ as solvent unless otherwise noted. Chemical shifts (δ) are given in ppm and are referenced to residual solvent in the sample tube. Coupling constants (*J*) are reported in Hz and are classified as singlet (s), doublet (d), triplet (t), broad (br), or multiplet (m).

All FT-IR spectra were collected neat on a diamond-ATR equipped Digilab FTS 7000 spectrometer using a diamond ATR setup. HR-MS were obtained from an Agilent 6530 qToF using electrospray ionization and the detector set to positive mode.

UV-Vis spectra were measured in 10 mm path length quartz glass cuvettes using a Cary Varian 5000 spectrometer.

Powder X-ray diffraction (PXRD) measurements were done with a Panalytical Empyrean diffractometer using Cu Kα radiation (λ = 1.5418 Å). Single-crystal X-ray data were collected on a Bruker SMART APEX CCD diffractometer with fine-focus Mo Kα radiation (λ = 0.71073 Å), operated at 50 kV and 30 mA. The structures were refined on F^2 using the SHELXTL 6.12 software package (Bruker AXS, Inc., Madison, WI, 1997). Absorption corrections were applied using SADABS.

Thermogravimetric analysis (TGA) was conducted on a TA Instruments Q5000 IR equipped via inline with a heated capillary to a Pfeiffer OminStar GSD 320 Mass spectrometer to analyze evolved gases.

pH measurements were conducted with a Thermoscientific Orion Star A211 pH meter (using a five point calibration curve) and with Millipore MColorphast pH 7.5 - 14 strips.

All reagents and solvents were used as received unless otherwise noted; exceptions to this statement are listed where applicable.

Appendix C: Chapter 2 – Receptors and Extractants Based on the Pseudobicyclic N,N'-bis(2-pyridyl) Guanidinium Motif (Paper)

*Reproduced from C. A. Seipp, N. J. Williams, V. S. Bryantsev, R. Custelcean and B. A. Moyer, RSC Adv., 2015, **5**, 107266* with permission from The Royal Society of Chemistry.

Conformationally Persistent Pseudo-bicyclic Guanidinium for Anion Coordination As Stabilized by Dual Intramolecular Hydrogen Bonds

Charles A. Seipp,[a,b] Neil J. Williams,[a,c] Vyacheslav S. Bryantsev,[a] Radu Custelcean,[a] and Bruce A. Moyer [*a]

The first example of a pseudo-bicyclic guanidinium ligand is reported. When bound to an anion, the *N,N'*-bis(2-pyridyl)guanidinium cation persistently adopts the planar *α,α* conformation featuring intramolecular N···H–N–H···N hydrogen bonds in the solid state, which facilitates crystallization of sulphate from aqueous mixtures of anions.

Guanidiniums are excellent oxoanion receptors owing to their ability, like the related urea family of receptors,[1] to direct two hydrogen bonds in bidentate fashion along an oxoanion O–X–O edge.[2,3] In the case of guanidiniums, the presence of the cationic charge further provides for coulombic strengthening of the binding interaction as well as gives the ligand designer the means to build in charge-complementarity as an additional selectivity principle. One problematic issue with simple substituted guanidinium-based receptors is their innate conformational flexibility, which enables them to exist in several different conformations.[4] Reflecting a generic challenge in ligand design,[5,6,7] restricting such conformational freedom is thus necessary to control the directionality and cooperativity of their N–H donor groups (**Figure C.1**). This has been accomplished very effectively by employing a bicyclic

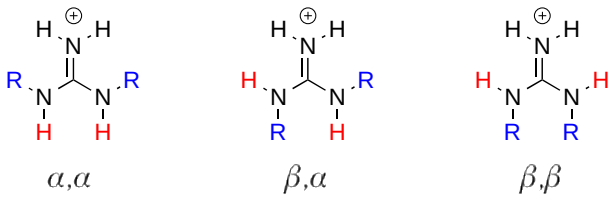

Figure C.1: The three major conformations of *N,N'*-disubstituted guanidinium cations. α and β refer to the orientation of the R group relative to the NH_2^+ group.

framework, which has since often been used in guanidinium based anion-receptor design.[8,9,10,11] By analogy, it occurred to us to ask whether intramolecular hydrogen bonding could be employed to achieve a pseudo bicyclic guanidinium frame and how such an arrangement would be reflected in the structure of the resulting anion complexes.

A current research direction in our group is to employ simple guanidinium ligands for selective separation of oxoanions, such as sulphate, via crystallization.[12] A major challenge with this approach is to identify guanidinium cations that form relatively insoluble sulphate salts for effective separation from water. This is a difficult proposition, as most guanidinium salts have high aqueous solubilities. For example, the solubility of guanidinium sulphate in water is about 10 M.[12]

Nevertheless, some isolated examples of highly insoluble guanidinium sulphate salts are known, such as 2-aminoperimidine sulphate, or more recently, glyoxal bis(amidiniumhydrazone) sulfate.[12,13] One common structural feature in these guanidinium salts is the presence of a rigid and planar extended π cation that can stack favourably in the crystalline state.

Herein we describe the simple *N*,*N*'-bis(2-pyridyl)guanidinium ligand (**1**) that is designed to achieve a planar *α,α* conformation through the formation of a pseudo-bicyclic motif via intramolecular N···H–N–H···N hydrogen bonding (**Figure C.2**). This pseudo-bicyclic motif is found to persist across a series of crystalline guanidinium salts and facilitates the selective crystallization of sulfate from aqueous anion mixtures. The *N*,*N*'-bis(phenyl)guanidine (**2**), which cannot

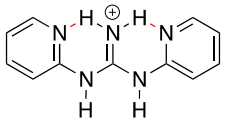

1

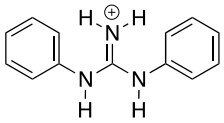

2

Figure C.2: The *N,N'*-bis(2-pyridyl)guanidinium (**1**) can have two intramolecular hydrogen bonds that enhance conformational rigidity compared to bis(phenyl)guanidinium (**2**), which can undergo free rotation about the guanidinium C–N bonds.

attain planarity due to the steric clashing of the aromatic-C2 and NH_2^+ protons, serves as a control for comparison with **1**.

Synthesis of **1** is achieved in two steps from 2-aminopyridine to give the free guanidine ligand (see ESI). Addition of a stoichiometric amount of the corresponding acid, followed by vapor diffusion of ether into methanol, yielded the sulfate, chloride, and nitrate salts of **1**. The single-crystal X-ray structures of these salts (**Figure C.3**) show that **1** persistently adopts the planar, pseudo-bicyclic α,α conformation throughout the series via the formation of two intramolecular N–H···N hydrogen bonds between the guanidinium NH_2 and the pyridine groups. [14] The remaining two N–H hydrogen bond donors chelate the anion in either a 1:1 (Cl^- and NO_3^-), or a 2:1 (SO_4^{2-}) fashion. The sulphate anion also has four water molecules bound in the equatorial plane, which complete the 12 hydrogen bonds of the coordination sphere of sulphate. From the chloride structure, the preference of **1** for anion binding via the α,α conformation may be seen to extend beyond oxoanions, raising the question of the origin of the stability and generality of this conformer.

In direct contrast, the previously reported crystal structures of **2** with a variety of anions showed this guanidinium cation is generally non-planar and lacks any conformational preference. [15,16] Accordingly, in the case of **2**-NO_3^-, the

guanidinium binds nominally in an α,α conformation but is twisted largely out of plane. The sulfate salt of **2** has the guanidinium existing as a mixture of conformers with no clear conformational preference. A Cambridge Structural Database (CSD Ver. 1.17) search for **2** yielded 24 hits (excluding disorder and errors); the salts show no preference for any particular orientation, and both types of N–H groups function as hydrogen-bond donors to anions. Our ligand also compares well with previously reported structures of true bicyclic guanidiniums bound to various anions. [17,18,19] These bicyclic systems, like our **1**-complexes, maintain the planar

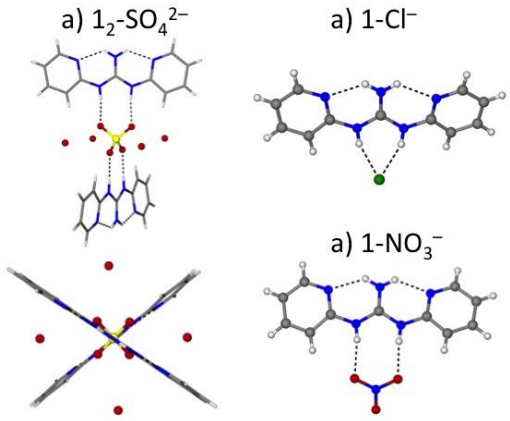

Figure C.3: Crystal structures of **1** bound to various anions. a) Side view and top view of **1** bound to sulphate, which is additionally hydrogen bonding to four water molecules (water protons could not be located). b) **1** bound to chloride. c) **1** bound to nitrate.

guanidinium group observed only in the α,α conformation. One distinct characteristic of the pseudo bicyclic structure seen in the **1**-complexes is the planarity of the entire guanidinium molecule, while the aliphatic backbones of the true bicyclic systems are often twisted out of plane.

In order to gain a better understanding of the observed structures, we employed electronic-structure calculations and Natural Bond Orbital (NBO) analysis[20] to assess the relative stabilities of the major conformations of **1** and **2** and their anion-binding preferences using the 1:1 complexes with nitrate as representative models.

Binding energies for 1:1 **1**–NO_3^- complexes and the relative stabilities of the three major conformations of free **1** and **2** calculated at the ωB97X-D/6-311++G(3df,3pd) level of theory are given in (**Figure C.4** and **Table C.1**, respectively. [21] The calculations are in accord with the structural evidence showing that **1** prefers to bind anions in the α,α conformation, while **2** has no preference. In this regard, the calculated 3.7 kcal/mol stabilization of **1**-α,α-NO_3^- vs **1**-α,β-NO_3^- appears to be significant, especially in view of the R*T*ln(2) statistical (entropic) advantage enjoyed by the α,β conformation.

Table C.1. Relative stabilities of the three major conformations of free cationic ligands **1** and **2** (kcal/mol).[a]

Ligand	α,α	α,β	β,β
1	2.20	0	15.7
2	0.34	0	4.50

[a] Conformations are defined in Figure 1. Relative energies are obtained at the ωB97X-D/6-311++G(3df,3pd) level. Zero-point energies and thermal corrections to enthalpy are included at the B3LYP/6-311++G(d,p) level. [22]

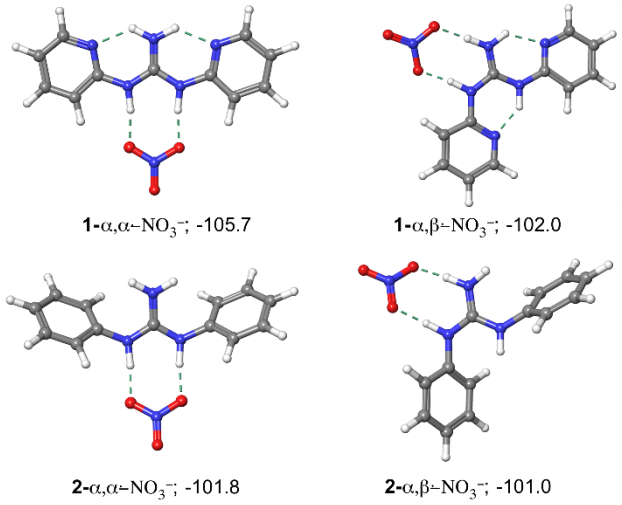

Figure C.4: Structures and binding energies (kcal/mol) for 1:1 nitrate anion–ligand complexes in the α,α and α,β binding conformations obtained after geometry optimization at the ωB97X-D/6-311++G(3df,3pd) level of theory. Binding energies are obtained with respect to a free ligand in the most stable α,β conformation.

The persistence of the α,α form of **1** in its anion complexes may be explained in that the α,α form delivers the strongest pair of hydrogen bond donor groups and thus the most stable complexes. Stronger hydrogen bonding occurs via the PyrN–H group vs the NH_2 group due to the electron- withdrawing ability of the pyridyl substituent, making the NH proton ostensibly more acidic. This argument is supported by the NBO analysis,[21] which quantifies hydrogen bonding strength by a leading two-electron intermolecular donor-acceptor interaction ($n_B \rightarrow \sigma_{HA}^*$) between the lone pair n_B of the Lewis base B and the unfilled hydrogen antibonding orbital σ_{HA}^* of the Lewis acid AH.[23] We find (Table S3 of ESI) that the leading donor-acceptor interaction for the PyrN−H···N hydrogen bond in **1**-α,β (26.2 kcal/mol) is much stronger than that for the HN−H···N hydrogen bond (19.7 kcal/mol). Moreover, when the NH_2 group forms two hydrogen bonds in **1**-α,α the leading $n_N \rightarrow \sigma_{HNH}^*$donor-acceptor interaction (per bond) becomes even weaker (16.9 kcal/mol). Thus, in the absence of an external hydrogen bond acceptor, the stronger PyrN–H donors will favor a stronger interaction with the other pyridine N atom, stabilizing the α,β conformer. By contrast, in the presence of strongly coordinating anions, the stronger PyrN–H donors will favor a symmetric planar α,α conformation. Consistent with this notion, the HN−H···O hydrogen bond (1.660 Å) in **1**-α,β□NO_3^- is substantially longer than the PyrN−H···O hydrogen bond (1.600 Å) in **1**-α,β-NO_3^- and the HN−H···O (1.632 Å) hydrogen bond in 2-α,β□NO_3^-.

Similarly, in the free guanidinium **1**, the two H−N−H donor hydrogen bond distances are calculated to be 1.882 Å for the α,α conformation and 1.847 Å (HN–H) and 1.794 Å (pyN–H) for the α,β conformation.

Unlike the conformational preferences upon anion coordination, the non-symmetric α,β conformer is the global minimum for both ligands in their unbound free state (**Table C.1**). We note that the **2**-α,α form is only marginally less stable than the global minimum, while **1**-α,α is considerably less stable. Due to lack of any intramolecular hydrogen bonding, the π−π stacked β,β conformation of **1** (see ESI) is greatly destabilized compared to the other forms, while the β,β conformation of **2** is only 4.5 kcal/mol above the global minimum (**Table C.1**) and can still be accessible under standard conditions, as evident from several crystal structures containing this conformation (such as $\mathbf{2}_2$-SO_4^{2-}). While the symmetrical α,α form of **1** is thus not the energetically stable form of the free ligand, the theoretical study shows that the pseudo-bicyclic scaffold of **1**, unlike **2**, confers strong directionality upon coordination to an anion and restricts the number of conformations accessible at room temperature. Similar results are seen for the $\mathbf{1}_2$-SO_4^{2-} complex (See ESI). The results thus elucidate the persistence of the α,α form of **1** on anion binding but naturally raise questions regarding the conformations that exist in the solution state and the attendant issue of preorganization in binding reactions. Such new questions entail aspects of solvation and entropy that are the

subject of our ongoing investigations. What we can already see at this point, though, is that by comparison to the fused-ring bicyclic systems[24] a pseudo-bicyclic approach allows additional conformational freedom that must be taken into account.

The preference of **1** for a planar, conformationally locked structure, as observed in other guanidinium sulfate salts of low aqueous solubility, prompted us to evaluate the potential of **1** for sulfate separation by crystallization from water. Mixing equimolar aqueous solutions of **1**-Cl^- and sodium sulphate resulted in the immediate formation of a white precipitate, which was identified as $\mathbf{1}_2$-SO_4^{2-} $(H_2O)_7$ by single-crystal and powder X-ray diffraction. No precipitate formed with other anions, including I^-, Cl^-, and NO_3^- (**Figure C.5**). The gravimetrically measured solubility of $\mathbf{1}_2$-$SO_4^{2-}(H_2O)_7$ at 20 °C is 2.5 mg/mL (10 mM). On the other hand, no precipitate formed with sulphate or other anions when **2** was used instead. As well as the rigid and planar extended π stacks, intramolecular hydrogen bonding has been shown to increase the lipophilicity of a molecule, which may contribute in part to the observed insolubility of the $\mathbf{1}_2$-$SO_4^{2-}(H_2O)_7$ complex.[25]

To examine any structural impact due to crystallization from water vs the methanol/diethylether system used initially, a single crystal of $\mathbf{1}_2$-$SO_4^{2-}(H_2O)_7$ was

obtained via slow evaporation of a saturated solution from water. The X-ray structure showed the expected 2:1 sulphate binding, though

with slightly different packing than that obtained from methanol/diethylether (Figure 6). Notably, the guanidinium cation adopts, once again, a perfectly planar pseudo-bicyclic conformation, with the cations stacking along the crystallographic b axis with the shortest interplanar distance of 3.3 Å measured between the central C atom of guanidinium and the C2 carbon of the pyridine ring. The overall crystal is composed of alternating hydrophobic layers of stacked guanidinium cations and hydrophilic sulphate-water layers (Figure 6). Powder X-ray diffraction of the precipitate from water matched well the simulated powder pattern from the single crystal, confirming that the bulk precipitate was indeed the 2:1 complex with sulphate, as determined by single-crystal diffraction.

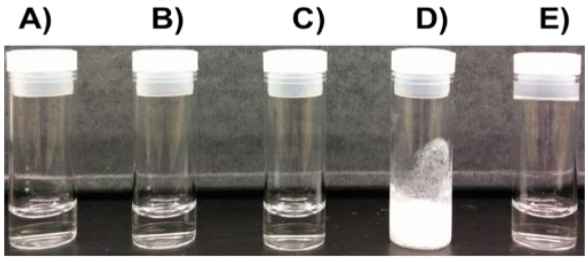

Figure C.5: A) **1** + NaI, B) **1** + NaCl, C) **1** + $NaNO_3$, D) **1** + Na_2SO_4, E) **2** + Na_2SO_4.

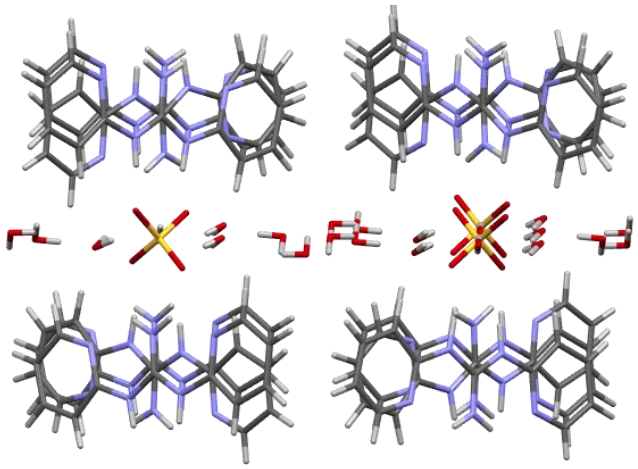

Figure C.6: X-ray crystal structure of $\mathbf{1}_2$-$SO_4^{2-}(H_2O)_7$, obtained by crystallization from water, showing alternating guanidinium stacks and sulphate-water layers.

This study demonstrates a persistent pseudo-bicyclic structure for the novel guanidinium receptor **1** in anion binding. Both X-ray crystallography and DFT calculations show that the guanidinium **1** prefers to bind anions in its planar □□□ conformation as rigidified by N···H–N–H···N intramolecular hydrogen bonds. In direct contrast, guanidinium **2** cannot form such intramolecular hydrogen bonds and exhibits no consistent structural preference. The ability of **1** to selectively crystallize with sulphate suggests an immediate use in anion separation. Moreover, with its strong inherent binding, positive charge, and hydrogen-bond induced

planarity, **1** represents a unique and promising scaffold for the design of selective oxoanion receptors. Current efforts in our research group are directed towards fully characterizing this receptor's ability to bind sulphate in solution, the nature of the intramolecular hydrogen bond in solution, potential alternatives to pyridine N-donors as intramolecular hydrogen bond receptors, as well as the synthesis and application of lipophilic derivatives for extraction.

Acknowledgements

This research was sponsored by the U.S. Department of Energy, Office of Science, Basic Energy Sciences, Chemical Sciences, Geosciences, and Biosciences Division. This research used resources of the National Energy Research Scientific Computing Center, a DOE Office of Science User Facility supported by the Office of Science of the U.S. Department of Energy under Contract No. DE-AC02-05CH11231.

1 F. P. Schmidtchen and M. Berger, *Chem. Rev.,* **1997**, 97**,** 1609–46.

2 B. A. Moyer, R. Custelcean, B. P. Hay, J. L. Sessler, K. Bowman-James, V. W. Day, S. Kang, *Inorg. Chem.,* **2013**, 52**,** 3473–90.

3 P. Blondeau, M. Segura, R. Pérez-Fernández, J. de Mendoza, *Chem. Soc. Rev.*, **2007**, **36**, 198–210.

[4] C. Schmuck, H. Y. Kuchelmeister in *Artificial Receptors for Chemical Sensors*, ed. V. M. Mirsky, A. K. Yatsimirsky, Wiley-VCH, 2010, pp. 270–313.

[5] D. J. Cram, *J. Inclusion Phenom.*, **1988**, 6, 397–413.

[6] F. P. Schmidtchen, *Coord. Chem. Rev.*, **2006**, 2918–28.

[7] P. A. Gale, N. Busschaert, C. J. E. Haynes, L. E. Karagiannidis, I. L. Kirby, *Chem. Soc. Rev.*, **2014**, 43, 205–41.

[8] H. Kurzmeier, F. Schmidtchen, *J. Org. Chem.*, **1990**, 749–3755.

[9] J. Sa ´nchez-Quesada, C. Seel, P. Prados, J. de Mendoza, *J. Am. Chem. Soc.*, **1996,** 118, 277–278.

[10] K. Kazuya, Y. Inoue, *Jour. Am. Chem. Soc.*, **2003**, 125, 421.

[11] D. Kneeland, K. Ariga, V. Lynch, C. Huang, E. Anslyn, *J. Am. Chem. Soc.*, **1993**, 115, 10042.

[12] R. Custelcean, N. J. Williams, C. A. Seipp, *Angew. Chemie Int. Ed.* **2015**, 10525–9.

[13] W. I. Stephen, *Anal. Chim. Acta.*, **1970**, 50, 413.

[14] C. Lee, W. Yang, R. G. Parr, *Phys. Rev. B,* **1988**, 37, 785–789.

[15] J. A. Paixao, P. S. P. Silva, A. M. Beja, M. R. Silva, L. A. Vega, *Acta Cryst. Section C.*, **1998,** *54*, 805.

[16] A. M. Beja, J. A. Paixao, P. S. P. Silva, L. A. Vega, E. M. Gomes, J. Z. Martin-Gil, *Kristallografiya*, **1998,** 213, 655

[17] P. Leibnitz, G. Reck, H. J. Pietzsch, H. Spies, *Forschungszent Rossendorf(Ber).*, **2001**, 311, 34

[18] A. Gleich, F. P. Schmidtchen, P. Mikulcik, G. Muller, *Chem. Commun.*, 1990, 55

[19] U. Wild, P. Roquette, E. Kaifer, J. Mautz, O. Hubner, H.Wadepohl, H. J. Himme, *Eur. J. Inorg. Chem.,* **2008,** 1248

[20] A. E. Reed, L. A. Curtiss, F. Weinhold, *Chem. Rev.*, **1988,** 88**,** 899-926.

[21] J. D. Chai, M. Head-Gordon, *Phys. Chem. Chem. Phys.*, **2008,** 10, 6615–6620.

[22] A. D. Becke, *Chem. Phys*., **1993,** 98, 5648–5652.

[23] Weinhold and C. Landis, Valency and Bonding, Cambridge University Press, Cambridge, **2005.**

[24] V. D. Jadhav, E. Herdtweck, F. P. Schmidtchen, *Chemistry* **2008**, 14, 6098–107..

B. Kuhn, P. Mohr, M. Stahl, *J. Med. Chem.,* **2010,** 53, 2601.

Appendix D: Chapter 2 – Receptors and Extractants Based on the Pseudobicyclic N,N'-bis(2-pyridyl) Guanidinium Motif (Supporting Information)

1. Synthetic Procedures:

Preparation of *N,N'*-bis(2-pyridyl)thiourea:

2-aminopyridine (20 g, 0.21 mol) was added to 40 mL of carbon disulfide. To this suspension was added a catalytic amount (0.25 g) of precipitated sulfur. The reaction was heated to reflux for 48 hours. The carbon disulfide was removed *in vacuo,* and the mixture was recrystallized from 50 mL of a 1:1 water / EtOH mixture to afford 13.3 g (52% yield). **^{1}H NMR** (400 MHz, $CDCl_3$) δ14.35 (bs, 1H), 9.54 (bs, 1H), 8.85 (bs, 1H), 8.39 (bs, 2H), 7.717 (bs, 2H), 7.062 (bs, 3H). NMR appears complex and broad due to likely thioenol equilibrium. Spectra taken at reduced temperatures show coalescence of peaks.

Preparation of *N,N'*-bis(2-pyridyl)guanidine (1):

1 was prepared via the method of Toptschiew.[80]

N,N'-Bis(2-pyridyl)thiourea (2 g, 8.7 mmol), basic lead carbonate (15.0 g, 19.3 mmol), and 7 M ammonia in methanol (7.6 mL, 53 mmol) were added to a sealed tube in 15 mL of ethanol and heated to 45 °C overnight. The flask was cooled, and the black lead salt was filtered off through celite. The solvent was removed *in vacuo* and recrystallized from 10 mL of ethanol to give the crude free ligand in 43% yield which was purified via formation of either the HCl or hemisulfate salt (see next two procedures).

Preparation of *N,N'*-bis(2-pyridyl)guanidine HCl:

Upon isolation, (**1**) was dissolved into the minimal amount of diethyl ether required to completely solubilize it. At this point, 0.95 equivalents of 1 M HCl in diethyl ether were added while stirring, and the solution allowed to sit for two hours. The precipitate was filtered, rinsed with excess diethyl ether, and isolated as pure **2.** **^{1}H NMR** (400 MHz, DMSO-*d6*) δ 10.21 (N-H, 1H, br), 10.20 (N-H, 1H, br), 8.43 (C-H, 1H, d, *J* = 4.8 Hz), 7.97 (C-H, 1H, t, *J* = 7.6), 7.29 (C-H, 1H, t, *J* = 6), 7.21 (C-H, 1H, d, *J* = 8.4) **^{13}C NMR** (100 MHz, DMSO-*d6*) δ 152.97, 151.95, 147.27, 120.53, 114.35. **HRMS:** $C_{11}H_{12}ClN_5$ (Calculated: 214.101, Observed: 214.10550), $C_{22}H_{24}ClN_{10}$ (Calculated: 463.186 Observed: 463.18520) **Melting Point:** 195-197 °C. **IR (Diamond ATR):** 3426 br. w., 3181 br. w., 1690 sh. med., 1497 sh. str., 1468 sh. str., 1359 br. med., 1237 sh. med. 1150 sh. med., 769 sh. str., 697 sh. med., 671 sh. med.

Preparation of *N,N'*-bis(2-pyridyl)guanidine hemisulfate:

2 was dissolved in the minimal amount of water required to effect complete dissolution. 0.50 equivalents of sodium sulfate dissolved in water (33 mM) were added. The solution was allowed to sit for 60 minutes and then sonicated for 30 minutes. The precipitate was filtered, washed with a small amount of cold water, and dried under vacuum. **^{1}H NMR** (400 MHz, DMSO-*d6*) δ 10.49 (N-H, 1H, br), 10.51 (N-H, 1H, br), 8.10 (C-H, 1H, dd),

7.80 (C-H, 1H, dt), 7.19 (C-H, 1H, d, J = 8.4), 7.13 (C-H, 1H, dt). **^{13}C NMR** (100 MHz, DMSO-*d6*) δ 154.42, 152.97, 146.89, 139.69, 119.43, 114.93. **HRMS:** $C_{11}H_{12}ClN_5$ (Calculated: 214.101, Observed: 214.10520), $C_{22}H_{24}N_{10}SO_4$ (Calculated: 525.17750, Observed: 525.17560) **Melting Point:** 239-241 °C. **IR (Diamond ATR):** 3312 br. med., 3162 sh. m., 2815 br. w., 1657 sh. str., 1568 sh. med., 1067 sh. str., 742 sh. w., 679 br. med.

2. Other Experimental Details

Determination of the Solubility of *N,N'*-bis(2-pyridyl)guanidine hemisulfate complex:

19.0 mg of **3** was dissolved in 4 mL of millipore-filtered water and allowed to stir for three days at 20 °C as measured by thermometer to fully equilibrate. The residual solid was filtered, and the residual solution was allowed to fully dry in a tared vial to give 10 mg of residual solid. Solubility was thus calculated at 2.5 mg/mL of water.

Carbonate (Na_2CO_3) and phosphate (K_2PO_4) were also checked for complex insolubility. Both anions induced the deprotonation of **1-Cl**, followed by precipitation of the free guanidine.

4. X-ray Crystallography

Hydrogen atoms were placed in idealized positions, except for the protons of the water molecules in 1-SO_4 water, which were located from the difference Fourier maps and refined isotropically. CCDC 1404793-1404796 contains the supplementary crystallographic data for this paper. These data can be obtained free of charge from The Cambridge Crystallographic Data Centre via www.ccdc.cam.ac.uk/data_request/cif.

Appendix E: Receptors and Extractants Based on the Pseudobicyclic N,N'-bis(2-pyridyl) Guanidinium Motif. Supporting Information for the Lipophilic Extractant and Binding Studies

1. Synthetic Procedures

Synthesis of 4-dodecyl-2-nitro-pyridine:

To a 180 mL of dioxane under argon was added 6.54 g (32 mmol) of 2-nitro-4-bromo-pyridine and 9.0 g (42 mmol) of 1-dodecylboronic acid and allowed to stir for two minutes. 0.369 g (1.6 mmol) of $Pd(OAc)_2$ and 1.26 g (4.8 mmol) triphenylphosphine were added, followed by 17.24 g (81 mmol) tribasic potassium phosphate and 6 mL of water. The reaction was heated at reflux for 72 hours before being filtered through a celite pad. The solvent was removed *in vacuo*. Water was added to the crude reaction mixture to dissolve the residual base and palladium acetate, and the mixture was extracted with ethyl acetate three times. The solvent was removed *in vacuo*, and the compound was subsequently purified by column chromatography (0 - 30% Ethyl Acetate / Hexanes) to yield 6.5 g of a pale yellow solid (32-81% Yield, Average: 53%). **^{1}H NMR (400 MHz, $CDCl_3$):** δ8.48 (d, 1H), 8.22 (d, 1H), 7.85 (d, 1H), 2.80 (t, 2H), 1.71 (t, 2H), 1.35-1.28 (br, 18H) 0.90 (t, 3H). **^{13}C NMR (100 MHz, $CDCl_3$):** δ148.84, 145.12, 139.21, 117.76, 32.83, 31.92, 30.83, 29.62, 29.49, 29.35, 29.32, 29.09, 22.70, 14.139 **HR-MS:** *Calculated m/z (M + Na):* 315.20420 *Observed m/z (M + Na):* 315.20430

Synthesis of 4-dodecyl-2-aminopyridine:

1.0 g of 10% Pd/C was added to an argon flushed 500 mL flask. 6.0 g (19.6 mmol) of 4- dodecyl-2-nitropyridine was then added, followed by 250 mL of ethanol through the septum. The reflux condenser was attached, and 25 mL of hydrazine monohydrate was added slowly through the top of the condenser. The mixture was heated to reflux until disappearance of the starting material was observed by TLC. The solution was thoroughly degassed with argon, and filtered through celite. A few mL of water was added to the reaction mixture, and it was concentrated *in vacuo*. The solution was diluted with 100 mL of water and extracted three times with ethyl acetate and three times with dichloromethane. The solvent was removed *in vacuo*, while never allowing the water bath temperature to reach over 30 ^{O}C. The compound was purified by column chromatography (0 - 50% Ethyl Acetate / Hexanes) to yield the title compound in 98% yield. **^{1}H NMR (400 MHz, $CDCl_3$):** δ7.90 (s, 1H), 7.28 (d, 2H), 6.48 (d, 2H), 4.30 (s, 2H), 2.473 (t, 2H), 1.55 (t, 2H), 1.29 (m, 18H), 0.893 (t, 3H) **^{13}C NMR (100 MHz, $CDCl_3$):** δ156.5, 147.2, 138.1, 128.1, 108.4, 33.1, 31.9, 31.5, 29.7, 29.7, 29.7, 29.6, 29.5, 29.4, 29.1, 22.7, 14.1. **HR-MS:** *Calculated m/z (M + H):* 263.24790 *Observed m/z (M + H): 263.24820*

Synthesis of N,N'-bis(4-dodecyl-2-pyridyl)thiourea:

To 1.0 g of 4-dodecy-2-aminopyridine in a 10 mL microwave tube equipped with a stirbar was added 3 mL of carbon disulfide. The tube was sealed and heated at 160 °C for six hours. The solvent was removed *in vacuo*, and the compound was purified by flash chromatography (0 - 30% Ethyl Acetate / Hexanes) to afford 730 mg (70 %) of a yellow oil that solidified on standing. *NMR analysis was complicated likely due to slow rotation around the bond, giving complex spectra. Spectra had to be obtained at 260K to resolve the broad peaks, HR-MS, purity by TLC, and successful conversion to the guanidinium in the next step confirmed the presence of the desired species.* **^{1}H NMR (400 MHz, $CDCl_3$):** δ14.43 (s, 1H), 9.71 (s, 1H), 8.72 (d, 1H), 8.26 (s, 1H), 8.14 (s, 1H), 7.49 (d, 1h), 7.29 (d, 1H), 6.96 (d, 1H), 2.58 (m, 5H), 1.59-0.964 (m, 60H). **^{13}C NMR (100 MHz, $CDCl_3$):** δ153.4, 150.2, 139.2, 134.1, 114.0, 32.3, 31.9, 31.03, 29.63, 29.6, 29.5, 29.4, 29.3, 29.1, 22.7, 14.1.**HR-MS:** *Calculated m/z (M + H):* 567.44420 *Observed m/z (M + H): 567.44550*

Synthesis of N,N'-bis(4-dodecyl-2-pyridyl)guanidinium chloride:

In a 150 mL bomb flask was added 550 mg of N,N'-bis(4-dodecyl-2-pyridyl)thiourea and 20 mL of EtOH. 1.65 g of basic lead carbonate and 1.0 mL of 7 N ammonia in methanol was added. The reaction was heated at 55 celcius for 48 hours. The product crude reaction mixture was washed with aqueous 1M NaOH and then 1M HCl. The reaction was extracted three times into chloroform, and purified via column chromatography (0 to 100% ethyl acetate / hexanes) to yield 60 mg of an off-white solid

(10.5% yield). **^{1}H NMR (400 MHz, $CDCl_3$):** δ11.0 (Br, 2H), 8.06 (s, 2H), 7.55 (d, 2H), 7.14 (d, 2H), 2.58 (d, 2H), 1.60 (t, 4H), 1.29 (m, 36H), 0.86 (t, 6H). **^{13}C NMR (100 MHz, $CDCl_3$):** δ153.4, 150.2, 139.2, 134.1, 114.0, 32.3, 31.9, 31.03, 29.63, 29.6, 29.5, 29.4, 29.3, 29.1, 22.7, 14.1. *Calculated m/z (M +):* 550.48470 *Observed m/z (M +): 550.48430*

Synthesis of 6-tridecyl-2-bromopyridine

Diisopropylamine (9.2 mL, 6.6 g, 66 mmol) was dissolved in anhydrous THF and cooled to -78 °C. nBu Li (2.5 M in hexanes, 26.4 mL, 66 mmol) was added dropwise and allowed to stir for 30 minutes to form LDA. 2-methyl-6-bromopyridine (6.8 mL, 4.5 g, 26 mmol)) was dissolved in 120 mL of dry THF. The LDA solution was cannulated into the bromopyridine solution, and allowed to warm to RT and stirred over night. The solution cooled, quenched *slowly* with water, and extracted into ethyl acetate. The solvent was removed *in vacuo*, and the product was purified using column chromatography (100% hexanes > 50% ethyl acetate) to afford 7.3 grams of product (81 %). **^{1}H NMR (400 MHz, $CDCl_3$):** δ7.429 (t, 1H), 7.290 (d, 1H), 7.110 (d, 1H), 2.759 (t, 2H), 1.706 (m, 2H), 1.313 (m, 22H), 0.892 (t, 3H) **^{13}C NMR (100 MHz, $CDCl_3$):** δ164.6, 141.4, 138.5, 125.4, 121.4, 38.0, 31.9, 29.6, 29.6, 29.6, 29.6, 29.4, 29.3, 29.3, 22.7, 14.1. **HR-MS:** *Calculated m/z (M + H)+:* 340.16340 *Observed m/z (M+H)+:* 340.16390.

2. Determination of Binding Constants

General Procedure for the Determination of Binding Constants:

A sample of **1** was dissolved in a known volume of a mixture of 10% Water / 90% MeOD-*d*4. A standardized solution (guest solution) of tetrabutylammonium sulfate in 10% Water / 90% MeOD-*d*4 was made. An NMR spectrum was obtained, and a quantity of guest solution was added to the NMR tube. The tube was given five shakes and then put on a vortex mixer for 15 seconds to ensure adequate mixing and another spectrum obtained. This addition – mixing – spectra was repeated until the shifts of the compound were stabilized. All measurements were done with volumetric glassware and recently calibrated pipetteman to ensure accurate measurements. The binding constant for sulfate was determined using HypNMR2008. Binding constants for chloride and nitrate were determined using software provided on supramolecular.org.[81] All protons are labeled on the spectra in section 6.

Extraction Study:[82]

For the two-phased extraction studies used equal volumes (600 uL) of the 1,2-dichloroethane and aqueous phases. The concentrations of the extractant was varied (0, 1,

3, 10, and 30 mmol) while the aqueous solutions composition remained constant (10 mmol NaCl and 0.1 mmol Na_2SO_4). The samples were contacted on a rotating wheel in a temperature controlled incubator at 25 ± 0.2 °C and then subsampled in a similar manner as previously described. (Ref. 1) After contacting and centrifugation of the two phases, 300 μL of each phase was removed and pipetted into 20 mL polypropylene vials containing 20 mL of ultima gold scintillation cocktail for scintillation counting. Organic and aqueous samples were counted for 30 minutes after dark adapting for 30 minutes. The solutions were counted using a Parkard Tri-Carb 2500TR Liquid Scintillation Analyzer.

To ensure the counts from the samples were not being quenched, tests were conducted where four vials containing 20 mL of ultima gold were spiked with each individual component (e.g. receptors, synergistic mixtures and aqueous solution). 10 μL of the sulfur-35 radiotracer was then spiked into each of the aforementioned solutions and then all of the solutions were counted for 30 minutes. The counts were compared to see if quenching (decrease in total counts) was observed. None of the components used in the extraction studies exhibited quenching. Therefore, it was not necessary to do a correction on the collected data.

All experiments were run in duplicate to reduce the chance of error affecting the results of the experiments. The numbers presented above are an average of the duplicates for the extraction experiments.

Binding Constant Data:

Graphs for Sulfate K_a:

For the sulfate titration, the shift of the **N-H** Proton was observed. The binding model was fit globally across both of these protons to give a K_1 and a K_2 of $3.78 \pm 0.12\ M^{-1}$ and $2.10 \pm 0.23\ M^{-1}$ respectively.

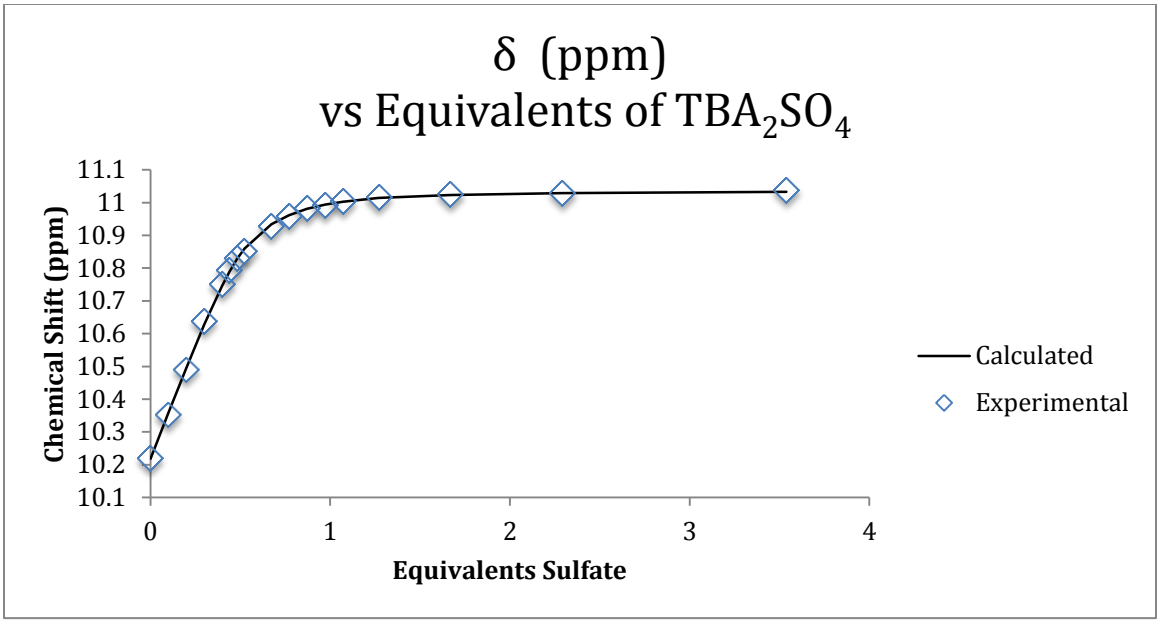

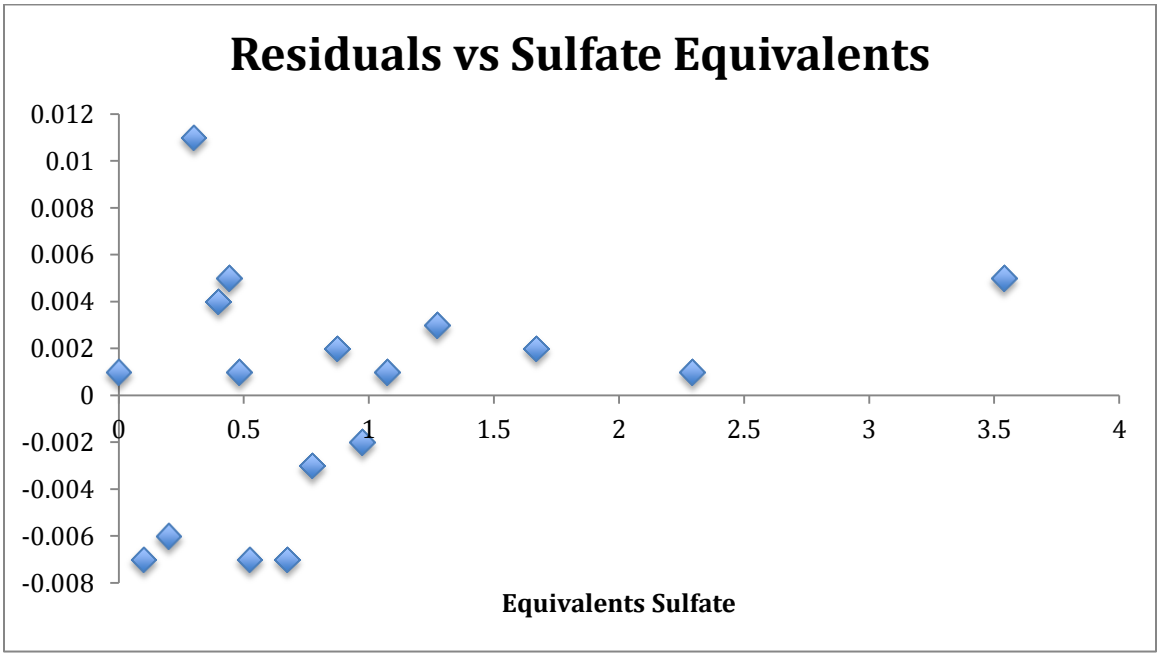

Figure E.1: Shifts of the N-H protons of BiPyG with increasing amounts of sulfate. The residuals of the graph show a suitably random orientation.

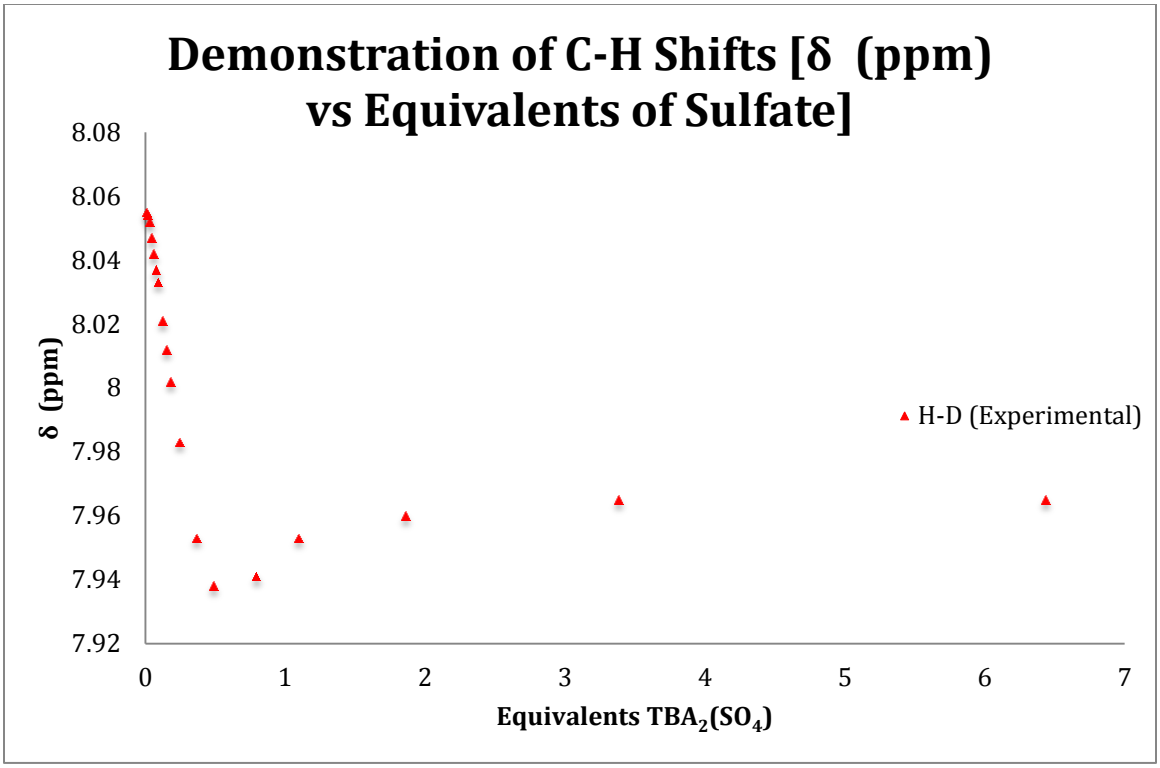

Figure E.2: Shifts of the C-H protons of BiPyG with increasing amounts of sulfate. Evidence of a 2:1 binding model can be clearly seen due to the maximum shift observed at 0.5 equivalents of added sulfate.

Graph for Nitrate K_a:

For the nitrate titration, the shift of the N-H proton was observed (See SI **6.1** and **6.2** for the relevant proton). The binding model was fit to these data points to give an estimate of the $\log K_a$ of < 1.

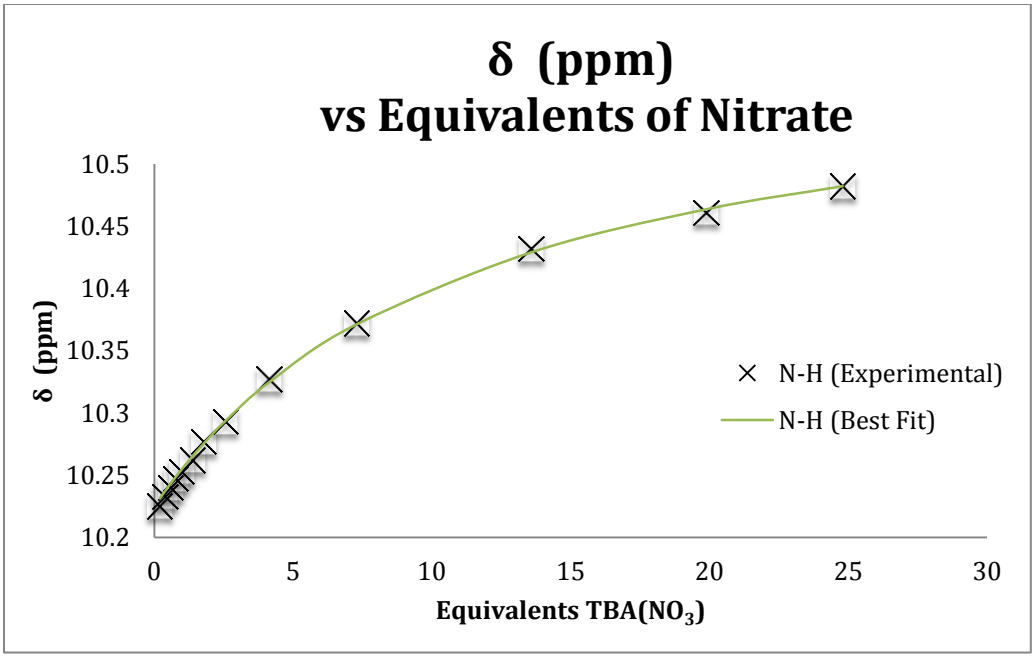

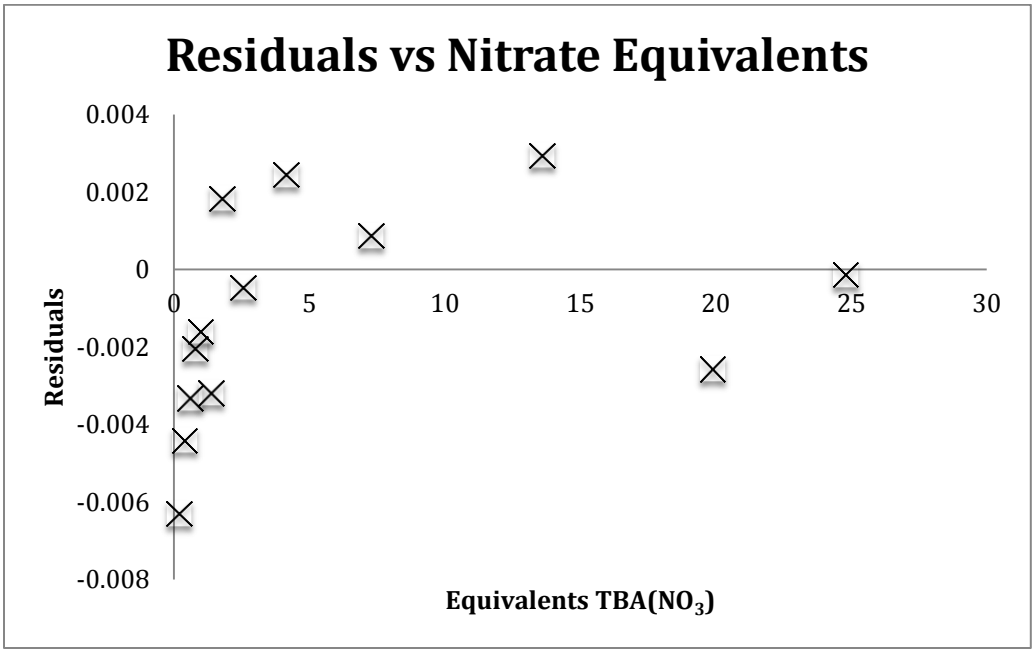

Figure E.3: Shifts of the N-H protons of BiPyG with increasing amounts of nitrate. A residual plot is also shown.

Graph for Chloride K_a:

For the chloride titration, the shift of the N-H was observed (See SI **6.1** for the relevant proton). The binding model was fit to this data point to estimate a logK of < -0.5.

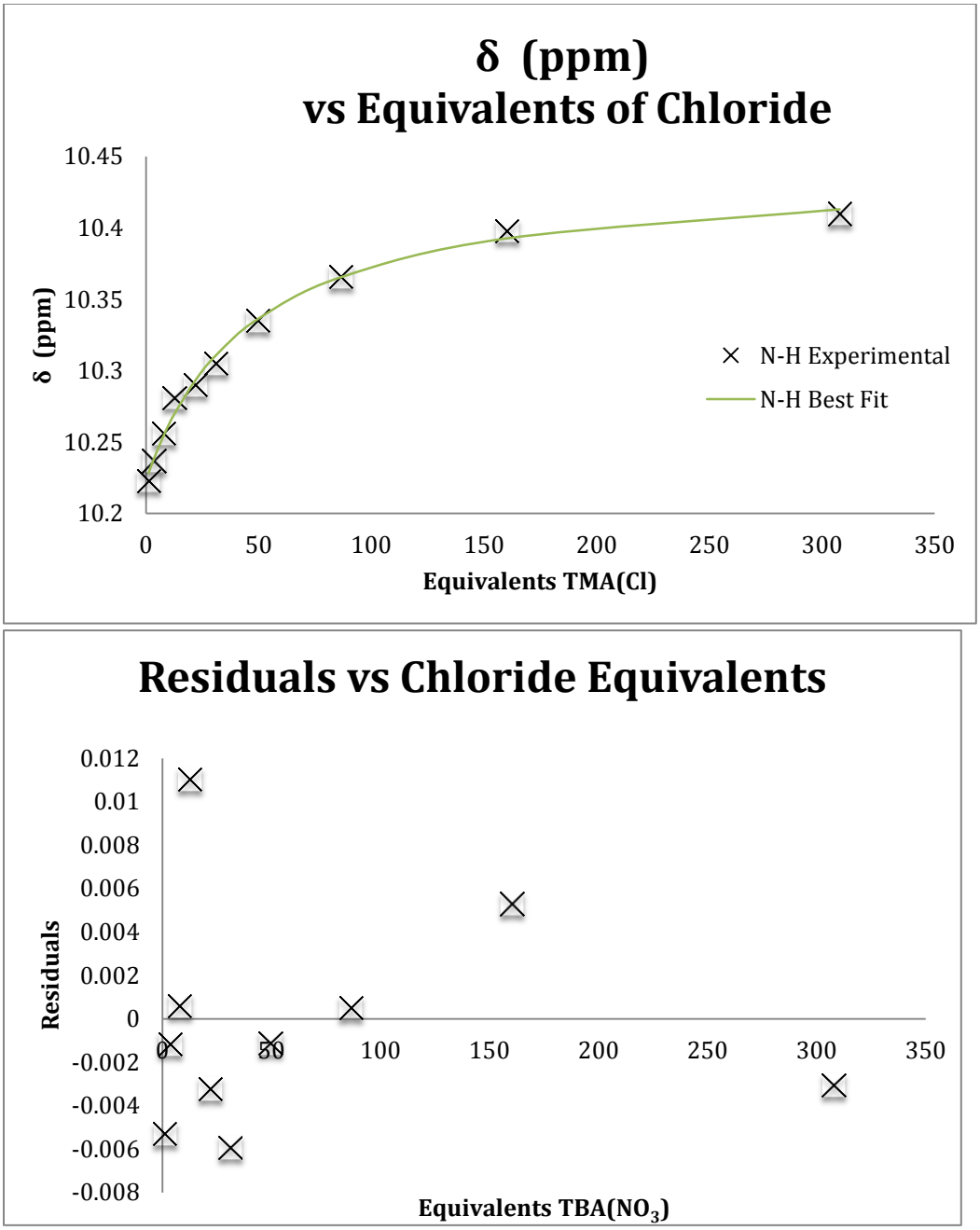

Figure E.4: Shifts of the N-H protons of BiPyG with increasing amounts of chloride. A residual plot is also shown.

Appendix F: Chapter 3 - Crystallization Agents Based on Bis(Imino)Guanidiniums (Paper)

Paper discussing PyBIG and its use in CO_3 capture used with permission from John Wiley and Sons and Angewandte Chemie and is taken from: Seipp, C.A.; Williams, N.K.; Kidder, M.K.; Custelcean. R.; Angwandte. **2017,** 1042.

DOI: 10.1002/anie.201610916

CO_2 Capture from Ambient Air via Crystallization with a Guanidine Sorbent

Charles A. Seipp, Neil J. Williams, Michelle K. Kidder, and Radu Custelcean[1]

Abstract: *Carbon capture and storage (CCS) is an important strategy aimed at stabilizing the atmospheric CO_2 concentration and thereby the global temperature. However, with our current rate of increase in the atmospheric CO_2 concentration, we may soon commit ourselves to significant global temperature increases. A possible approach toward reversing this trend is to pursue a 'negative emissions' strategy, whereby the CO_2 is removed directly from ambient air (direct air capture). Herein we report a simple aqueous guanidine sorbent that captures CO_2 from air and binds it as a crystalline carbonate salt via guanidinium hydrogen bonding. The resulting solid has very low aqueous solubility (K_{sp} = 1.0(4) × 10^{-8}), which facilitates its separation from solution by filtration. The bound CO_2 can be released by relatively mild heating of the crystals at 80-120 °C, which regenerates the guanidine sorbent quantitatively. Thus, this crystallization-based approach to CO_2 separation from air requires minimal energy and chemical input, and offers the prospect for low-cost direct air capture technologies that could stabilize or even reduce the atmospheric CO_2 concentration.*

[1] C. A. Seipp, N. J. Williams, Dr. M. K. Kidder, Dr. R. Custelcean
Chemical Sciences Division, Oak Ridge National Laboratory, Oak Ridge, TN 37831-6119 (USA)
E-mail: custelceanr@ornl.gov

C. A. Seipp
Department of Chemistry, The University of Texas at Austin, 1 University Station-A5300, Austin, TX 78712-0165 (USA)

N. J. Williams
Department of Chemistry, The University of Tennessee, Buehler Hall 1420 Circle Dr., Knoxville, TN 37996-1600 (USA)

Removal of greenhouse gases from dilute emissions has recently been identified as one of seven chemical separations to change the world.[1] Along this line, carbon capture and storage (CCS)[2,3] has been proposed as a strategy to stabilize the increasing concentration of CO_2 in the atmosphere, and thereby the global temperature. However, point-source CCS, which captures the CO_2 emitted by power plants, does not address the dispersed CO_2 emissions, such as those originating from automobiles and airplanes, which account for about 50% of total greenhouse emissions. Furthermore, given our society's inertia in dealing with the climate change, we may soon reach a point when merely implementing the point-source CCS will not be sufficient to stabilize the atmospheric CO_2 concentration at the desirable level, and will require us to achieve 'negative emissions', that is to reduce the amount of CO_2 in the atmosphere by extracting it directly from air (direct air capture).[4-7]

Due to the very low concentration of CO_2 in the atmosphere (~400 ppm), effective and economical direct air capture (DAC) requires a sorbent that optimally combines a number of attributes such as strong CO_2-binding affinity, fast sorption kinetics, high capacity, good selectivity against other components in the air (especially water), easy regeneration with minimal energy input, long-term stability, and low cost. While a material with all these characteristics has yet to be identified, sustained efforts in the last two decades[6] led to the development of different classes of sorbents with promising DAC performance, such as alkali and alkaline earth bases (e.g., NaOH, KOH, $Ca(OH)_2$),[8-11] solid-supported amine-based sorbents,[12-16] and metal-organic frameworks (MOFs).[17-19]

Most systems used to date in DAC involve chemisorbents, taking advantage of their strong and selective binding of CO_2 in the form of carbonate or carbamate anions.[6] Unfortunately, an undesirable consequence associated with strong CO_2 binding is the typically high temperatures required to release the gas and regenerate the sorbent. Furthermore, if the sorbent is in the aqueous state, a substantial amount of energy is required to heat the solutions due to the high heat capacity of water. For instance, aqueous NaOH, a benchmark chemisorbent for DAC, has very high capacity and fast kinetics of CO_2 absorption. However, the resulting sodium carbonate is too soluble in water, requiring a substantial amount of energy to concentrate the solution and isolate the solid Na_2CO_3, which then needs to be calcined at temperatures above 800 °C to decompose it into CO_2 and Na_2O. Alternatively, the aqueous Na_2CO_3 solution can be reacted with $Ca(OH)_2$ to precipitate $CaCO_3$ and regenerate the NaOH solution, but the thermal decomposition of calcium carbonate to release the CO_2 requires very high temperatures of about 900 °C.[6,7] Thus, the sorbent regeneration step is by far the most energetically demanding and expensive component of the overall DAC process, prompting the development of new sorbent materials with lower regeneration temperatures.[7] Here we report a simple aqueous guanidine sorbent that captures CO_2 from air and binds it as a crystalline carbonate salt of low aqueous solubility, which can be effectively removed from solution by filtration. The CO_2 can then be released under relatively mild conditions by heating the carbonate crystals at 80-120 °C, which regenerates the guanidine sorbent quantitatively.

2,6-Pyridine-bis(iminoguanidine) (PyBIG) was readily obtained by imine condensation of 2,6-pyridinedialdehyde with aminoguanidinium chloride, followed by neutralization with aqueous NaOH, which led to precipitation of the pure ligand (Supporting Information Fig. S1,2) as a crystalline hydrate ($PyBIG \cdot 2.5H_2O$) (Supporting Information Fig. S3). PyBIG belongs to the general class of bis(imino)guanidine ligands (BIGs) that have recently been found to form with oxoanions. They form crystalline hydrogen-bonded salts with very low aqueous solubilities, which facilitate the separation of this class of anions by crystallization.[20,21] We had reasoned that the electron withdrawing pyridine ring in PyBIG would impart enhanced acidity to the guanidinium groups, thereby leading to stronger binding and more effective separation of oxoanions.

An aqueous solution of PyBIG that was left open to ambient air for a few days led to the formation of large prism-shaped single crystals with an elemental composition consistent with the tetrahydrated carbonate salt of PyBIG ($PyBIGH_2(CO_3)(H_2O)_4$). Single crystal X-ray diffraction analysis confirmed this composition (Fig. 1a), and revealed the presence of extended one-dimensional $[CO_3(H_2O)_4^{2-}]_n$ clusters in the crystals (Fig. 1b). Each carbonate anion in the cluster accepts four water hydrogen bonds, with O–H···O contact distances ranging between 1.89 and 2.06 Å. The quasi-planar $PyBIGH_2^{2+}$ cations form extended stacks that flank the anionic $[CO_3(H_2O)_4^{2-}]_n$ clusters and bind them via multiple hydrogen bonds between the guanidinium groups and the carbonate anion and water, as well as between the pyridine N atom and water (Fig. 1d). Each carbonate anion

accepts five guanidinium hydrogen bonds with N–H···O contact distances ranging between 1.84 and 2.00 Å (Fig. 1c).

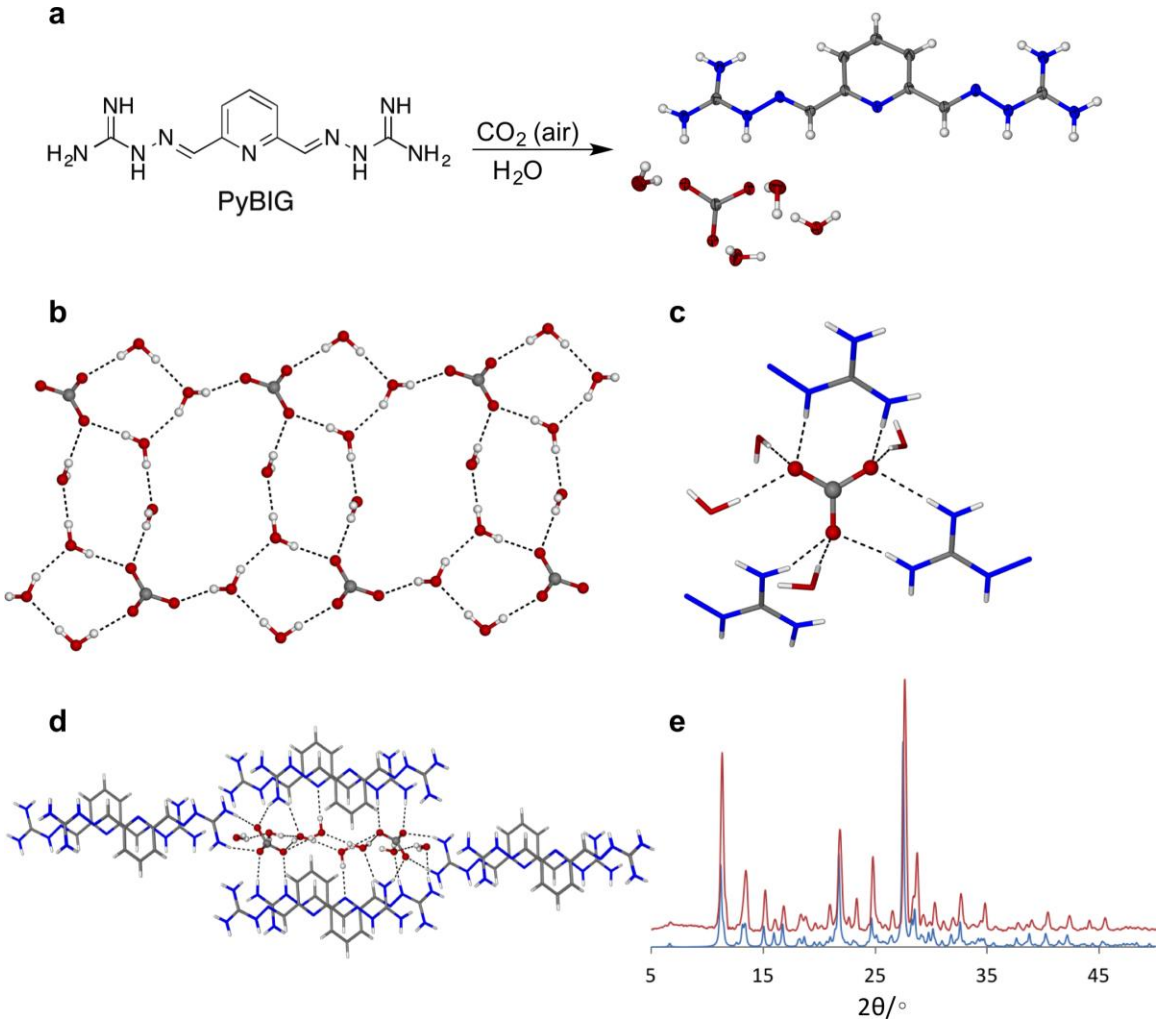

Figure F.1: Atmospheric CO_2 capture via crystalline $PyBIGH_2(CO_3)(H_2O)_4$. a) Reaction of aqueous PyBIG (ChemDraw structure on the left) with CO_2 to form $PyBIGH_2(CO_3)(H_2O)_4$ (X-ray crystal structure on the right). b) Hydrogen-bonded $[CO_3(H_2O)_4^{2-}]_n$ cluster formed in the crystal. c) CO_3^{2-} binding site, with the anion accepting 4 water and 5 guanidinium hydrogen bonds. d) Hydrogen bonding of the $[CO_3(H_2O)_4^{2-}]_n$ cluster by the cationic stacks. e) Overlay of the experimental PXRD pattern of the bulk crystalline product (red) and the simulated PXRD pattern from the single-crystal X-ray data (blue).

Preliminary measurements indicated that aqueous PyBIG can act as a good sorbent for atmospheric CO_2. To quantify the sorption performance, an aqueous solution of PyBIG (5 mL, 9.6 mM) was placed in a 20 mL scintillation vial and left open to ambient air. Small crystals started to form within two days and were collected by vacuum filtration after one week. FTIR spectroscopic analysis of the crystals showed strong peaks at 1357 and 1327 cm^{-1} characteristic to the carbonate anion. The powder X-ray diffraction (PXRD) pattern of the bulk crystalline product matched well the powder pattern simulated from the single-crystal X-ray data for $PyBIGH_2(CO_3)(H_2O)_4$ (Fig. 1e), thereby confirming the identity and phase purity of the crystallized solid. The crystallization was run in duplicate, and the observed average yield was 50.3 ± 0.4%. While these preliminary data reveal a moderate reaction yield and relatively slow kinetics of crystallization, we note here that these CO_2 sorption measurements were done under completely passive conditions, with no efforts to maximize the contact between the air and the aqueous solution, or to optimize the reaction parameters (e.g., reaction time, temperature, concentration). We expect the optimization of the reaction conditions, especially increasing the airflow and the air-water interfacial area to enhance the CO_2 transport rate, will significantly improve the efficacy of CO_2 absorption. On the other hand, the recovery of the crystallized $PyBIGH_2(CO_3)(H_2O)_4$ from solution is greatly facilitated by its very low aqueous solubility. The solubility product of

$PyBIGH_2(CO_3)(H_2O)_4$, measured by UV-Vis spectroscopy, is estimated around $1.0(4) \times 10^{-8}$, which is comparable to the corresponding value of $CaCO_3$ ($K_{sp} = 3.4 \times 10^{-9}$).

Effective sorbent regeneration is critical for any CO_2 capture system to be of practical utility. We found that heating the $PyBIGH_2(CO_3)(H_2O)_4$ crystals at relatively low temperatures releases the CO_2 and the included water, and regenerates the PyBIG sorbent quantitatively (**Figure F.2**).

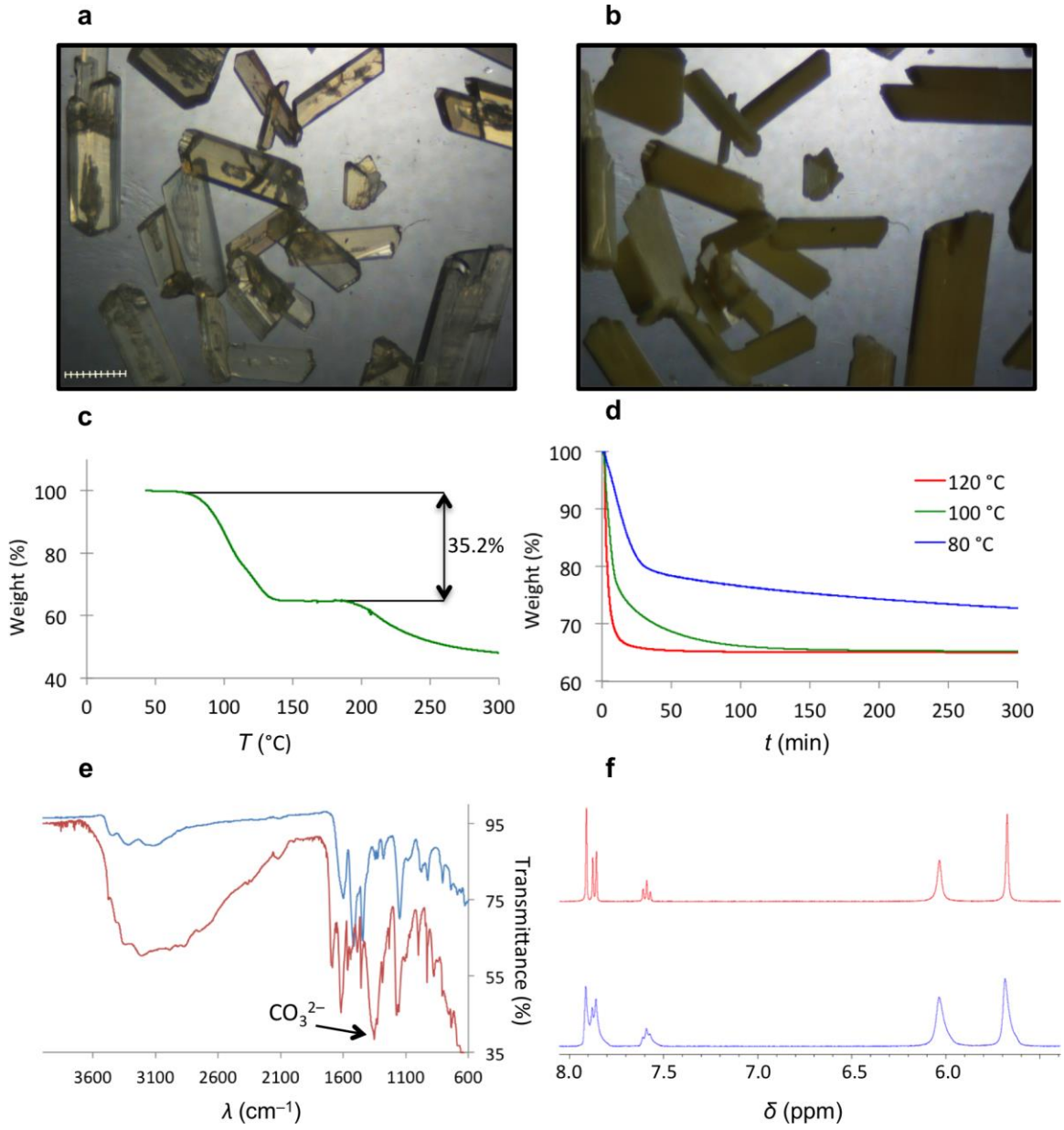

Figure F.2: Thermal decomposition of $PyBIGH_2(CO_3)(H_2O)_4$ crystals and regeneration of the PyBIG sorbent. a), b) Micrographs of the initial crystals (a) and after heating in air at 120 °C for one hour (b); scale bar: 100 μm. c), d) TGA plots from temperature-ramped (c) and isothermal (d) measurements. e) Overlaid FTIR spectra of the carbonate crystals (red) and the recovered PyBIG ligand (blue). f) ^{1}H NMR spectra (in DMSO-d_6) of the initial (red) and regenerated (blue) PyBIG.

Examination of the $PyBIGH_2(CO_3)(H_2O)_4$ crystals by optical microscopy revealed that upon heating in open air in an oven at 120 °C for one hour, the crystals changed their color from cream to yellow and became opaque (Fig. 2a,b). Thermogravimetric analysis coupled with mass spectrometry (TGA-MS) provided a more quantitative picture of the decomposition process. In a temperature-ramped TGA measurement (Fig. 2c), the $PyBIGH_2(CO_3)(H_2O)_4$ crystals lost 35.2% of their mass between 65 and 140 °C, and the MS analysis confirmed the simultaneous evolution of water and CO_2 (Supporting Information Fig. S4). These measurements are consistent with the loss of one carbonate and two protons (as CO_2 and H_2O), and four additional water molecules, as expected from the crystal structure of $PyBIGH_2(CO_3)(H_2O)_4$ (35.1% theoretical mass loss). Similarly, the mass loss of the crystals heated in open air in the oven for one hour at 120 °C (Fig.1b) was 34.3%, and the FTIR and NMR spectroscopic analysis of the resulting solid confirmed the complete disappearance of the carbonate peak and the regeneration of the anhydrous PyBIG ligand (Fig. 2e,f). The TGA-MS analysis showed no decomposition of the regenerated ligand up to 190 °C (Fig. 2c), which provides a thermal stability window of at least 50 °C for ligand recovery. Isothermal TGA runs at 120 and 100 °C (Fig. 2d) showed complete loss of carbon dioxide and water after 60 and 150 minutes, respectively, with no additional mass loss after 5 hours. On the other hand, at 80 °C the decomposition reached 77% completion after 300 minutes. This corresponds to about an order of magnitude reduction in the decomposition temperature compared to inorganic

carbonates, such as Na_2CO_3 or $CaCO_3$ (decomposition *T* of 800-900 °C) involved in traditional DAC technologies.[6,7]

An alternative approach to DAC with PyBIG is to combine the crystallization of $PyBIGH_2(CO_3)(H_2O)_4$ with the well-established carbonate/bicarbonate CO_2 capture cycle[12,22-24] (**Figure F.3**). In this approach, CO_2 sorption by an alkali carbonate solution (Eq.1) is followed by the reaction of the resulting bicarbonate with PyBIG to crystallize $PyBIGH_2(CO_3)(H_2O)_4$ and regenerate the carbonate sorbent (Eq.2). Finally, thermal decomposition of $PyBIGH_2(CO_3)(H_2O)_4$ regenerates the PyBIG ligand and releases the CO_2.

$$CO_3^{2-} + CO_2 + H_2O \longrightarrow 2\,HCO_3^- \quad \textbf{(Eq. 1)}$$

$$PyBIG_{(s)} + 2\,HCO_3^- + 4\,H_2O \longrightarrow PyBIGH_2(CO_3)(H_2O)_{4(s)} + CO_3^{2-} \quad \textbf{(Eq. 2)}$$

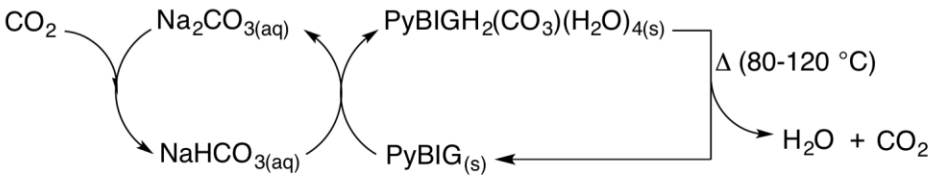

Figure F.3: Atmospheric CO_2 capture combining CO_2 sorption by an alkali carbonate solution (Eq. 1) and carbonate crystallization with PyBIG (Eq. 2). The overall CO_2 separation cycle is shown in the schematic diagram.

To demonstrate the feasibility of this approach, solid PyBIG (1 mol equiv) was suspended in a solution of 1 M $NaHCO_3$ (5-6 mol equiv) and the slurry was stirred at room temperature for four hours. The resulting mixture was filtered, and the separated

crystalline solid was confirmed by PXRD (Supporting Information Fig. S5) and FTIR (Supporting Information Fig. S6) to be $PyBIGH_2(CO_3)(H_2O)_4$. Subsequent heating of the carbonate crystals in the oven for one hour at 120 °C regenerated the PyBIG solid (Supporting Information Fig. S7), which was recycled back into the original sodium bicarbonate solution. The entire carbonate separation cycle was run three times, with observed yields for $PyBIGH_2(CO_3)(H_2O)_4$ crystallization of 99.0 ± 0.4%, 97.2 ± 0.6%, and 91.4 ± 0.4%, corresponding to the first, second, and third cycle, respectively. The regeneration of the PyBIG ligand was essentially quantitative in each cycle. The slight decrease in the crystallization yield observed in the later cycles is explained by the gradual increase in the solution alkalinity (initial pH 8.5, final pH 10.5) as a result of the increasing CO_3^{2-}/HCO_3^- ratio. As more bicarbonate is converted into carbonate in each subsequent cycle, according to Eq. 2, it is expected the pH of the solution should eventually become high enough to inhibit the protonation of PyBIG, thereby decreasing the driving force for the crystallization of $PyBIGH_2(CO_3)(H_2O)_4$. This is corroborated by the FTIR analysis of the isolated solid, which showed preponderantly the carbonate phase after the first two cycles, but a mixture of carbonate and free PyBIG ligand after the third cycle (Supporting Information Fig. S6).

The efficacy of the atmospheric CO_2 capture via crystallization of $PyBIGH_2(CO_3)(H_2O)_4$, and the ease of CO_2 release (compared to inorganic carbonate salts), can be attributed to a combination of factors. First, the guanidine groups of the PyBIG ligand are sufficiently basic to become protonated in moderately alkaline carbonate/bicarbonate solutions (pH 8.5-10.5), thereby driving the crystallization of the

bis-guanidinium carbonate salt. Second, the very low aqueous solubility of crystalline $PyBIGH_2(CO_3)(H_2O)_4$ facilitates its recovery from solution without the need of heating or evaporating water, which are energy intensive. Third, although the exact mechanism of $PyBIGH_2(CO_3)(H_2O)_4$ decomposition and CO_2 release has yet to be investigated, we surmise the close proximity of the carbonate and guanidinium groups, hydrogen-bonded within the crystal, facilitates proton transfer among them and the formation of H_2CO_3, which then decomposes into CO_2 and H_2O with the possible assistance of the included water molecules in the crystal.[25] Finally, as the PyBIG ligand can be quantitatively regenerated and recycled, the only chemical consumed in the overall CO_2 separation cycle is water, which could be easily recovered by condensation if desired. Furthermore, considering the relatively low temperature required for ligand regeneration is easily attainable using renewable energy such as concentrated solar power,[26] the overall separation process could be made energy sustainable, offering good prospects for the development of economical DAC technologies.

Acknowledgement

This research was supported by the U.S. Department of Energy, Office of Science, Basic Energy Sciences, Chemical Sciences, Geosciences, and Biosciences Division.

Supporting Information

Supporting information for this article is available online. CCDC 1509621 and 1509622 contain the supplementary crystallographic data for this paper. These data can be

obtained free of charge from The Cambridge Crystallographic Data Centre at http://www.ccdc.cam.ac.uk/data_request/cif.

References

1. D. S. Sholl, R. P. Lively, *Nature* **2016**, *532*, 435.
2. Lackner, K. S. *Science* **2003**, *300*, 1677.
3. D. M. Reiner, *Nature Energy* **2016**, *1*, 1.
4. D. W. Keith, *Science* **2016**, *325*, 1654.
5. K. S. Lackner, S. Brennan, J. M. Matter, A.-H. A. Park, A. Wright, B. van der Zwaan, *Proc. Natl. Acad. Sci.* **2012**, *109*, 13156.
6. E. S. Sanz-Perez, C. R. Murdock, S. A. Didas, C. W. Jones, *Chem. Rev.* **2016**, ***116,* 11840**.
7. Direct air capture of CO_2 with chemicals: A technology assessment for the APS Panel on Public Affairs. American Physical Society **2011**.
8. R. Baciocchi, G. Storti, M. Mazzotti, *Chem. Eng. Process.* **2006**, *45*, 1047.
9. F. Zeman, *Environ. Sci. Technol.* **2007**, *41*, 7558.
10. J. K. Stolaroff, D. W. Keith, G. V. Lowry, *Environ. Sci. Technol.* **2008**, *28*, 2728.
11. M. Mahmoudkhani, D. W. Keith, *Int. J. Greenhouse Gas Control* **2009**, *3*, 376.
12. T. Wang, K. S. Lackner, A. B. Wright, *Environ. Sci. Technol*. **2011**, *45*, 6670.
13. S. Choi, M. L. Gray, C. W. Jones, *ChemSusChem* **2011**, *4*, 628.
14. Choi, S., Drese, J. H., Eisenberger, P. M. & Jones, C. W. *Environ. Sci. Technol.* **2011**, *45*, 2420.

15. C. Gebald, J. A. Wurzbacher, P. Tingaut, T. Zimmermann, A. Steinfeld, *Environ. Sci. Technol.* **2011**, *45*, 9101.

16. A. Goeppert, M. Czaun, R. B. May, G. K. Surya Prakash, G. A. Olah, S. R. Narayanan, *J. Am. Chem. Soc.* **2011**, *133*, 20164.

17. T. M. McDonald, W. R. Lee, J. A. Mason, B. M. Wiers, C. S. Hong, J. R. Long, *J. Am. Chem. Soc.* **2012**, *134*, 7056.

18. A. Kumar, D. G. Madden, M. Lusi, K.-J. Chen, E. A. Daniels, T. Curtin, J. J. Perry IV, M. J. Zaworotko, *Angew. Chem. Int. Ed.* **2015**, *54*, 14372.

19. P. M. Bhatt, Y. Belmabkhout, A. Cadiau, K. Adil, O. Shekhah, A. Shkurenko, L. J. Barbour, M. Eddaoudi, *J. Am. Chem. Soc.* **2016**, *138*, 9301.

20. R. Custelcean, N. J. Williams, C. A. Seipp, *Angew. Chem. Int. Ed.* **2015**, *54*, 10525.

21. R. Custelcean, N. J. Williams, C. A. Seipp, A. S. Ivanov, V. S. Bryantsev, *Chem. Eur. J.* **2016**, *22*, 1997.

22. T. Wang, K. S. Lackner, A. B. Wright, *Phys. Chem. Chem. Phys.* **2013**, *15*, 504.

23. X. Shi, H. Xiao, K. S. Lackner, X. Chen, *Angew. Chem. Int. Ed.*, **2016**, *55*, 4026.

24. K. A. Mumford, K. H. Smith, C. J. Anderson, S. Shen, W. Tao, Y. A. Suryaputradinata, A. Qader, B. Hooper, R. A. Innocenzi, S. E. Kentish, G. W. Stevens, *Energy & Fuels* **2012**, *26*, 138.

25. C. S. Tautermann, A. F. Voegele, T. Loerting, I. Kohl, A. Hallbruker, E. Mayer, K. R. Liedl, *Chem. Eur. J.* **2002**, *8*, 66.

26. V. Nikulshina, C. Gebald, A. Steinfeld, *Chem. Eng. J.* **2009**, *146*, 244.

Appendix G: Chapter 3 - Crystallization Agents Based on Bis(Imino)Guanidiniums (SI)

1. Synthesis of PyBIG

Synthesis of 2,6-pyridinedicarboxaldehyde:

2,6-Pyridine dimethanol (6 g, 43 mmol) was added to 250 mL of dichloromethane. Dess Martin Periodinane (40 g, 95 mmol) was added slowly to the reaction mixture. After being allowed to stir for 10 minutes, 100 uL of water was added. After 3 hours, the reaction mixture was filtered to remove insoluble impurities. Aqueous sodium bicarbonate was added to neutralize the solution. The product was extracted into dichloromethane, and solvent was removed *in vacuo*. Column chromatography (Dichloromethane + 5% methanol) was used to purify the compound, giving 3 grams (50% yield) of product. . ^{1}H NMR (400 MHz, DMSO-d_6): δ 7.923 (2H, s), 7.869 (2H, d), 7.591 (1H, t), 6.047 (4H, bs), 5.723 (4H, bs).

Synthesis of PyBIG: 2,6-pyridinedicarboxaldehyde (3.8 g, 28 mmol) was dissolved in 70 mL of ethanol, and aminoguanidinium chloride (7.5 g, 68 mmol) was added to the solution. The round bottom flask was sealed, and the suspension was stirred overnight at 60 °C. Subsequently, the solution was placed into a freezer and allowed to sit at 0 °C for 24 hours. Vacuum filtration followed by subsequent rinsing with cold ethanol yielded 6.7 g of the crude PyBIG product as the hydrochloride salt (PyBIG-Cl). This product was used as obtained in the next step in a portion-wise manner. 1.12 g of the obtained PyBIG-Cl was dissolved in a minimal amount of water (~30 mL), and NaOH (50 mL, 2 M) was added in one portion. The resulting solution became deep goldenrod yellow and was stirred at room temperature until a creamy precipitate appeared and no more precipitate

could be observed forming (usually between 4 and 12 hours). The product was isolated by vacuum filtration, rinsed with water, and allowed to dry to give 650 mg (75% yield) of pure PyBIG·2.5H_2O. ^{1}H NMR (400 MHz, DMSO-d_6): δ 7.923 (2H, s), 7.869 (2H, d), 7.591 (1H, t), 6.047 (4H, bs), 5.723 (4H, bs). ^{13}C NMR (100 MHz, DMSO-d_6): δ 161.85, 155.69, 143.80, 136.18, 118.06. FTIR (cm^{-1}): 3345br, 3306br, 3077br, 1647w, 1582m, 1520vs, 1445s, 1420m, 1358w, 1328w, 1279w, 1156s, 1060w, 1004w, 989w, 959w, 938w, 910w, 812w, 748br, 737w, 687w. Elemental analysis: Anal. Calcd for $C_9H_{18}N_9O_{2.5}$: C, 36.98; H, 6.21; N, 43.13. Found*:* C, 37.10; H, 6.19; N, 43.52.

2. General Experimental Methods

CO2 capture from air using aqueous PyBIG: An aqueous solution of PyBIG (5 mL, 9.58 mM) was placed in a 20 mL scintillation vial and left open to ambient air for one week. Within two days, small crystals formed on the surface of the liquid as well as within clouds of fine precipitate floating in the solution. After one week the solution was filtered, rinsed with water, and allowed to dry. Yield 9.2 mg, 0.024 mmol (50.3% ± 0.4%) of PyBIG$H_2(CO_3)(H_2O)_4$. FT-IR (cm^{-1}): 1692m, 1619m, 1566w, 1485w, 1447 w, 1357bs, 1327s, 1286w, 1232w, 1156s, 999w, 929s, 876w, 808w, 753b, 687w. Elemental analysis: Anal. Calcd for $C_{10}H_{23}N_9O_7$: C, 31.50; H, 6.08; N, 33.06. Found: C, 31.59; H, 6.01; N, 33.32.

Crystallization of PyBIGH2(CO_3)(H_2O)4 from $NaHCO_3$ solution: All observed and theoretical yields are reported in the format "observed yield mg/mmol (theory mg/mmol)". PyBIG·2.5H_2O (502 mg, 1.72 mmol) was added to an aqueous solution of sodium bicarbonate (10 mL, 1M, pH 8.45). The resulting slurry was shaken at 1000 rpm on a vortex mixer for 4 hours, and the resulting white-cream solid was vacuum-filtered and washed with 1-2 mL of water. The remaining bicarbonate solution had a pH between 9 and 9.5 (measured with a pH strip). The solid was dried under vacuum, to yield 650 mg /1.70 mmol (655 mg/1.72 mmol) of PyBIG$H_2(CO_3)(H_2O)_4$ salt. This solid was placed in a vial and heated in the oven at 120 °C for one hour to give 420 mg/1.70 mmol (421 mg/1.70 mmol) of recovered PyBIG. The recovered ligand was added back to the original bicarbonate solution and allowed to vortex for another four hours, then it was filtered and dried to give 632 mg/1.66 mmol (647 mg/1.70 mmol) of PyBIG$H_2(CO_3)(H_2O)_4$ salt. Heating the carbonate salt for one hour at 120 °C gave 420 mg/1.70 mmol (410 mg/1.66 mmol) of the recovered PyBIG. The recovered ligand was added to the original bicarbonate solution once more, and allowed to vortex for four hours to give 590 mg/ 1.55 mmol (647 mg/1.70 mmol) of PyBIG$H_2(CO_3)(H_2O)_4$ salt. The final bicarbonate solution had a pH between 10.3 and 10.6 (measured with the pH meter).

PyBIG Regeneration: PyBIG$H_2(CO_3)(H_2O)_4$ crystals (35.0 mg, 0.09 mmol) were placed on a microscope slide and heated in the oven at 120 °C. After one hour, the slide was removed from the oven, allowed to cool to room temperature, and weighed. Yield 23.0 mg (0.09 mmol) of PyBIG (theory: 22.6 mg, 0.09 mmol). ^{1}H NMR (400 MHz,

DMSO-d_6): δ 7.912 (2H, s), 7.869 (2H, d), 7.591 (1H, t), 6.035 (4H, bs), 5.685 (4H, bs). FTIR (cm^{-1}): 3105bw, 1660 w, 1599m, 1523s, 1444s, 1433w, 1325w, 1279w, 1148m, 1079w, 974w, 920w, 806w, 737w, 662w, 633w.

Solubility measurements:

$PyBIGH_2(CO_3)(H_2O)_4$:

The solubility of $PyBIGH_2(CO_3)(H_2O)_4$ was determined by UV-Vis spectroscopy using the same methodology as previously described.[21] Saturated solutions were prepared by suspending excess of the crystalline solid in 10 mL of H_2O inside 15 mL polypropylene centrifuge tubes, and mixing the suspensions on a rotating wheel for 72 hours at 60 rpm inside an incubator set at 25 ºC. The pH of the equilibrated solutions (measured with the pH meter) were in the range of 8.33–8.37. The measurements were done in duplicate, and the obtained average solubility was $1.35 \pm 0.20 \times 10^{-3}$ M. Thus, considering the pK_a of HCO_3^- of 10.32, and the average pH of the saturated solution of 8.35, the concentration of the carbonate anion [CO_3^{2-}] was determined to be $1.4 \pm 0.2 \times 10^{-5}$ M. The solubility product of $PyBIGH_2(CO_3)(H_2O)_4$ was calculated using the following formula, where the activity coefficients ($\gamma_\pm$) were estimated at 0.74 using the Debye-Huckel limiting law:

$$K_{sp} = (\gamma_\pm)^2[PyBIGH_2^{2+}][CO_3^{2-}] = (0.74)^2\,[1.35 \times 10^{-3}][\,1.4 \times 10^{-5}] = 1.0 \pm 0.4 \times 10^{-8}$$

GBAH-Cl:

The solubility of the GBAH-Cl salt was determined gravimetrically. A saturated solution was obtained by allowing an aqueous suspension of the salt in deionized water to stir for 24 hours. One mL of the saturated solution was then pipetted into a pre-weighted glass vial containing a stir bar. The water was then removed under reduced pressure and gentle heating (~50 °C) while stirring. The resulting solid was left under vacuum overnight to ensure complete removal of the water, prior to weighting the vial. The weight of the recovered solid was 0.196 g, corresponding to an aqueous solubility of 0.88(8) M (average of three different measurements).

BBIG-Cl

The solubility of BBIG-Cl was determined gravimetrically. A saturated solution of BBIG-Cl was obtained by placing an excess of the salt in a 15mLpolypropylene centrifuge tube and adding 2 mL ofdeionized water. The suspension was mixed 2 days on a centrifugal contactor in an oven set at 25 °C. The suspension was centrifuged for 10 min at 3000 rpm to separate the aqueous and solid phases. The aqueous layer was then carefully removed using a 0.22 um syringe filter to remove leftover solid from the solution. A mL of the saturated salt solution was then pipetted into a pre-weighed glass vial containing a magnetic stir bar. The water was then re-moved under reduced pressure and gentle heating (~ 50 °C) while stirring. The resulting solid was left under vacuum overnight to ensure complete removal of the water prior to weighing the vial. The

solubility measurements were run in triplicate, and the average weight of the recovered chloride salt was 0.0202 g

Demonstration of the Recovery of BBIG:

BBIG-SO_4 (53.1 mg, 0.14 mmol) was added to a 2 mL solution of NaOH (10%) and stirred for 120 minutes at room temperature. This formed a thick yellow precipitate. The solid was filtered using vacuum filtration, rinsed with 0.2 mL of water, and then dried under vacuum. 93% recovery (31.8 mg) was observed. The yellow powder was dissolved in 1 M HCl, resulting in a clear solution. This could then be reused for sulfate separation, as demonstrated by precipitation of SO_4.

TGA Measurements: The TGA-MS was conducted under an argon atmosphere at 25 mL/min flow rate. The sample was held at ambient temperature for 1.5 min, then ramped at 5 °C/min to 300 °C and held for 0.5 min. The mass spectrometer collected the evolved gases under scanning mode of 2-200 amu, with the SEM detector at a speed of 200 ms/amu. For the isothermal runs, samples were first held at ambient temperature for 1.5 min, then jumped to the desired temperature (80, 100, or 120 °C) and held for 300 min.

Single crystal X-ray diffraction: Single crystals of PyBIG·2.5H_2O were obtained by slow evaporation of an aqueous ethanol solution of PyBIG. Single crystals of PyBIG$H_2(CO_3)(H_2O)_4$ were obtained by leaving an aqueous solution of PyBIG in open air for a few days, or by mixing it with an excess aqueous solution of $NaHCO_3$. The structures were solved by direct methods and refined on F^2 using the SHELXTL software

package (Bruker AXS, Inc., Madison, WI, 1997). Absorption corrections were applied using SADABS, part of the SHELXTL package. All non-hydrogen atoms were refined anisotropically.

Appendix H: Chapter 3 - Crystallization Agents Based on Bis(Imino)Guanidiniums (SI – PyBIG Complexes)

General Information: All reagents were purchased from commercial sources and used with no further purification. Single-crystal X-ray data were collected on a Bruker SMART APEX CCD diffractometer with fine-focus Mo Kα radiation (λ = 0.71073 Å), operated at 50 kV and 30 mA.

Solubility measurements: The solubility of PyBIGH was determined by UV-Vis spectroscopy using the same methodology as previously described.[21] Saturated solutions were prepared by suspending excess of the crystalline solid in 10 mL of H_2O inside 15 mL polypropylene centrifuge tubes, and mixing the suspensions on a rotating wheel for 72 hours at 60 rpm inside an incubator set at 25 ºC.

Ion Chromatography: A mixture of anions and PyBIG-Cl were mixing the suspensions on a rotating wheel for 72 hours at 60 rpm inside an incubator set at 25 ºC. The solid was filtered, and the remaining ion concentrations were determined by ion chromatography.

Appendix I: Present and Future Work – The "Bis(amide)guanidinium" (Supplementary Information)

1. Synthetic Methods

Synthesis of 3-nitro-2-isothiocyanatopyridine:[83]

5 g (32 mmol) of 2-chloro-3-nitropyridine was dissolved in 35 mL AcOH. Excess (4 g) potassium thiocyanate was added and the mixture was refluxed for three hours. The mixture was poured onto 200 mL of ice and water. The precipitate was filtered, washed with water, dissolved in ethyl acetate, and washed 4x with water. The ethyl acetate was dried with sodium sulfate, and evaporated to dryness to afford 3 grams of the desired isothiocyanate (43 % yield). ^{1}H NMR (400 MHz, $CDCl_3$): δ 8.934 (d, 1H), 8.659 (d, 1H), 7.573 (dd, 1H)

Synthesis of bis(2-nitrophenyl)methanediimine:[84]

2-nitrophenylisocyanate (4.00 g, 24 mmol) was added to 75 mL of cyclohexane. Several drops of 4-methyl-1-phenyl-2,3-dihydrophosphole 1-oxide was added to the solution, which was heated to 50 °C for three hours. The reaction was cooled to RT, and stirred over night. The precipitate was filtered and rinsed with 200 mL of cyclohexane to afford 4 g of pure product (93% yield). ^{1}H NMR (400 MHz, $CDCl_3$): δ 8.03 (2H, d), 7.61 (2H, t), 7.44 (2H, d), (2H, t). ^{13}C NMR (100 MHz, $CDCl_3$): δ 143.1, 134.3, 131.4, 127.8, 125.9, 125.6.

Synthesis of 1-(2-aminopyridin-3-yl)-3-phenylurea:

2 grams (18 mmol) of 2,3-diaminopyridine was dissolved in 20 mL dichloromethane. 1 mL (9 mmol) of phenylisocyanate was added slowly to the solution. After several hours, a thick white precipitate forms. The reaction was allowed to stir overnight before it was filtered and washed thoroughly with dichloromethane to afford 3.5 g (83% yield) of the desired urea. ^{1}H NMR (400 MHz, $CDCl_3$): δ8.70 (s, 1H), 7.77 (s, 1H), 7.70 (d, 1H), 7.64 (d, 1H), 7.43 (d, 2H), 7.24 (t, 2H), 6.925 (t, 1H), 6.56 (t, 1H), 5.602 (s, 2H).

Synthesis of *N*-(3-oxo-1-phenylbutan-2-yl)acetamide:

10 grams (60 mmol) of phenylalanine is dissolved in a mixture of 28.5 mL acetic anhydride and 5 mL of pyridine. This mixture is heated to reflux overnight. The solvent is removed *in vacuo*, and the thick oil is washed with saturated sodium bicarbonate and extracted into chloroform. Purification by column chromatography (0-100% EtOAc in Hexanes) yielded 8 grams (72%) of product. ^{1}H NMR (400 MHz, $CDCl_3$): δ 7.272 (m, 10H), 4.702 (t, 2H), 3.09 (dd, 2H), 2.93 (dd, 2H), 1.95 (s, 6H), 1.90 (s, 6).

Synthesis of the BAG 4,12-dibenzyl-5,11-dimethyl-2,14-dioxo-3,6,7,9,10,13-hexaazapentadeca-5,10-dien-8-iminium Chloride):

1 equivalent of *N*-(3-oxo-1-phenylbutan-2-yl)acetamide (5 g) was dissolved in a minimal amount of EtOH, and 0.5 equivalent (1.5 g) of aminoguanidinium chloride was added to the solution. The round bottom flask was sealed, and the suspension was stirred overnight at 60 °C. The solution was removed in vacuo, and the crude reaction mixture dissolved in water. 1N NaOH was added until a milky white precipitate formed and the pH remained

above 10. After stirring for six hours, the product was filtered to obtain the crude free base. The free base was shaken on a vortex mixture in 1M HCl in diethyl ether overnight and filtered to obtain the corresponding HCl salt in a 45% yield (3.5 g). ^{1}H NMR (400 MHz, $CDCl_3$): δ 7.264 (3H, m), 7.104 (2H, d), 6.210 (1H, d), 4.842 (1H, q), 3.080 (2H, ddd), 2.126 (3H, s), 1.946 (3H, s). ^{13}C NMR (100 MHz, $CDCl_3$): δ 169.30, 156.56, 152.01, 136.89, 129.53, 128.32, 126.63, 55.25, 38.72, 23.37, 15.49. HRMS (M+Na) Calculated: 486.258. Observed: 486.261).

Synthesis of *N*-(1-(4-phenylacetate)-3-oxobutan-2-yl)acetamide:

9 grams (49 mmol) of tyrosine was added to 30 mL of acetic anhydride and 30 mL of pyridine. The mixture was refluxed overnight. The solution was concentrated, and then excess ethyl acetate was added. The mixture was stirred vigorously for 4 hours until a thick white precipitate had formed. The precipitate was filtered, rinsed with ethyl acetate, and allowed to dry to afford pure compound (8.5 g, 65% yield). **^{1}H NMR (400 MHz, $CDCl_3$):** δ7.11 (d, 2H), 7.01 (d, 2H), 6.10 (bd, 1H), 4.85 (q, 1), 3.14 (dd, 1H), 3.042 (dd, 1H), 2.28 (s, 3H), 2.16 (s, 3H), 1.97 (s, 3H).

Synthesis of *N*-(1-(4-hydroxyphenyl)-3-oxobutan-2-yl)acetamide:

4.65 g (17.5 mmol) of *N*-(1-(4-hydroxyphenyl)-3-oxobutan-2-yl)acetamide was added to 100 mL of wet methanol. 4.65 g (55 mmol) sodium bicarbonate was added to the solution and refluxed over night. The solution was removed *in vacuo*, and the solid was suspended

in dichloromethane. The precipitate was filtered, and the dichloromethane was evaporated giving crude product. This product was subjected to column chromatography (0% - 10% methanol in dichloromethane) to afford 1.5 g of pure product. (38% yield). **^{1}H NMR (400 MHz, $CDCl_3$):** δ6.98 (dd, 2H), 6.74 (dd, 2H), 6.12 (bd, 1H), 5.78 (bs, 1H), 4.85 (q, 1H), 3.07 (dd, 1H), 2.93 (dd, 1H), 2.16 (s, 3H), 1.99 (s, 3H).

Synthesis of *N*-(1-(4-((3,7-dimethyloctyl)oxy)phenyl)-3-oxobutan-2-yl)acetamide: 1.5 g (6.6 mmol) of N-(1-(4-hydroxyphenyl)-3-oxobutan-2-yl)acetamide was added to a suspension of K_2CO_3 (2.34 g, 20 mmol) in 50 mL acetone and allowed to reflux over night. The residual bicarbonate was removed via filtration and the reaction was concentrated *in vacuo*. Column chromatography (0% - 50% ethyl acetate in hexanes) afforded 1.56 g (64% yield) of the desired product. **^{1}H NMR (400 MHz, $CDCl_3$):** δ7.00 (d, 2H), 6.80 (d, 2H), 6.07 (bd, 1H), 4.806 (q, 1H), 3.79 (d, 2H), 3.08 (m, 2H), 2.14 (s, 3H), 1.97 (s, 3H), 1.7-0.9 (bm, 18H) ^{13}C NMR (100 MHz, $CDCl_3$): δ206.7, 169.7, 158.2, 130.1, 127.6, 114.5, 66.2, 59.7, 39.2, 37.25, 36.1, 29.8, 28.1, 27.9, 24.6, 22.9, 22.7, 22.6, 19.65. **HRMS** *Calculated (m/z) (M+H)+*: 384.25090 *Observed (m/z) (M+H)+*: 384.25160.

Synthesis of the Lipophilic-BAG 4,12-bis(4-((3,7-dimethyloctyl)oxy)benzyl)-5,11-dimethyl-2,14-dioxo-3,6,7,9,10,13-hexaazapentadeca-5,10-dien-8-iminium chloride:

1.56 g (4.2 mmol) of *N*-(1-(4-((3,7-dimethyloctyl)oxy)phenyl)-3-oxobutan-2-yl)acetamide was taken up in 10 mL of ethanol. 273 mg (2.1 mmol) of diaminoguanidine

hydrochloride was added, and the mixture heated in a sealed round bottom flask over night at 60 °C. The solvent was removed *in vacuo*, and the product was purified by column chromatography (0% - 10% methanol in dichloromethane) to give 1.0 gram (29% yield) of pure product. **^{1}H NMR (400 MHz, $CDCl_3$):** δ7.00 (d, 4H), 6.80 (d, 4H), 6.07 (bd 2H), 4.806 (q, 2H), 3.79 (d, 4H), 3.08 (m, 4H), 2.14 (s, 6H), 1.97 (s, 6H), 1.7-0.9 (bm, 36H)^{13}C NMR (100 MHz, $CDCl_3$): δ 170.5, 158.1, 130.0, 128.2, 114.6, 66.3, 56.2, 39.3, 37.3, 36.2, 29.86, 27.97, 24.66, 23.11, 22.73, 22.62, 19.65, 16.07. HRMS (M+H) Calculated: 776.579 Observed: 776.580).

Synthesis of 1-(2-aminophenyl)-3-phenylurea:

5 g (46 mmol) of 2-3-diaminobenzene was added to 100 mL of dichloromethane. Phenyisocyanate (4 mL, 32 mmol) was added over several hours. The solution was allowed to stir over night. The precipitate was filtered and rinsed with dichloromethane, to afford pure urea in 43 % yield (4.5 g). ^{1}H NMR (400 MHz, DMSO-*d*6): δ 9.53 (bs, 1H), 9.02 (bs, 1H), 7.49 (d, 2H), 7.28 (t, 2H), 7.04 (q, 2H), 6.95 (t, 1H), 6.728 (d, 1H), 6.537 (t, 1H), 4.88 (bs, 2H).

References:

[1] *separation - definition of separation* https://en.oxforddictionaries.com/definition/separation (accessed Dec 22, 2016).
[2] Shim, H.; Kim, J.; Koo, K. *J. Cryst. Growth*, **2013**, *373*, 64-68.
[3] Alberts, B. *Essential cell biology*; Garland Science: New York, 2010.
[4] Luo, X.; Jiao, J. J. *Water Res.* **2016**, *102*, 11–31.
[5] Bader M. *Desalination* **2006,** 100-105.
[6] Moyer, B. A.; Custelcean, R.; Hay, B. P.; Sessler, J. L.; Bowman-James, K.; Day, V. W.; Kang, S.O. *Inorg. Chem.* **2013**, *52* (7), 3473–3490.
[7] *Vitrified high-level radioactive waste.* http://www.nwtrb.gov/facts/Vitrified_HLW.pdf (accessed Jan 1, 2017).
[8] Delmau, H.; Haverlock, T.; Sloop, F.; Moyer, B. A.; ORNL Technical Report *"Caustic-Side Solvent Extraction: Prediction of Cesium Extraction From Actual Wastes and Actual Waste Simulants"* **2003,** https://www.osti.gov/scitech/servlets/purl/944075-dk1tdq/
[9] Moyer, B. A.; Birdwell, J. F.; Bonnesen, P.; Bruffrey S.; Delmau, L.; Duncan, N.; Ensor, D.; Hill, T.; Lee, D. L.; Rajbanshi, A.; Roach, B.; Szczgiel, P.; Sloop, F.; Stoner, E.; Williams, N. J. ORNL Report, *Next Generation Solvent Development for Caustic-Side Solvent Extraction of Cesium*, **2014.**
[10] Peter, T. B.; Hobbs, D. T.; Fink, S. D. *Sep. Sci. Technol.* **2006,** 2447.
[11] Cantrell, K. J.; Krupka K. M.; Geisler, K. N.; Lindberg, M. J.; Arey, B. W.; Schaef, H. F.; PNNL Report "*Hanford Tank 241-S-112 Residual Waste Composition and Leach Test Data".*
[12] Marcus, Y. *J.; Chem. Soc., Faraday Trans.* **1991**, *87* (18), 2995–2999.
[13] Sessler, J. L.; Gale, P. A.; Cho, W.S. *Anion receptor chemistry*; Royal Society of Chemistry: Cambridge, 2006.
[14] Park, C.H.; Simmons, H. E. *J. Am. Chem. Soc*. **1968**, 90, 2431.
[15] Bell, R. A.; Christoph, G. G.; Fronczek, F. R.; Marsh, R. E. *Science* **1975**, *190* (4210), 151–152.
[16] Thodarson, P.; *Chem. Soc. Rev.* **2010,** 1305.
[17] Frassineti, C.; *et. al.; Anal. Biochem.* **1995,** 374-382.
[18] http://supramolecular.org/apps/
[19] Graf, E.; Lehn, J.M.; *J. Am. Chem. Soc.* **1975**, 97, 5022.
[20] Graf, E.; Lehn, J.M.; *J. Am. Chem. Soc.* **1976,** 98, 6403.
[21] Shannon, R. D.; *Acta Crystallographica* **1976,** A32, 751-767.
[22] Lehn, J. M. Supramolecular chemistry - scope and perspectives molecules - supermolecules - molecular devices https://www.nobelprize.org/nobel_prizes/chemistry/laureates/1987/lehn-lecture.pdf (accessed Jan 1, 2017).
[23] Schmidtchen, F. P. *Angew. Chem. Int. Ed.* **1977,** 10, 720.

[24] Jia, C.; Wu, B.; Li, S.; Yang, Z.; Zhao, Q.; Liang, J.; Li, Q.-S.; Yang, X.-J. *Chem. Commun.* **2010**, *46* (29), 5376.
[25] Processing of Used Nuclear Fuel http://www.world-nuclear.org/information-library/nuclear-fuel-cycle/fuel-recycling/processing-of-used-nuclear-fuel.aspx (accessed Dec 22, 2016).
[26] Crittenden, John; Trussell, Rhodes; Hand, David; Howe, Kerry and Tchobanoglous, George (2005). *Water Treatment Principles and Design*, Edition 2. John Wiley and Sons. New Jersey.
[27] Amy, G.; Ghaffour, N.; Li, Z.; Francis, L.; Valladares, R.; Missimer, T.; Lattemann, S.; *Desalination*, **2017**, 16.
[28] Rydberg, J.; Cox, M.; Misikas, C.; Choppin, G. *Solvent extraction principles and practice*; M. Dekker: New York, **2004**.
[29] Anderson, K.; Butler, E.; Anderson, D.; Woolley, E. *J. Phys. Chem.* 1**967**, *71*, 3566.
[30] Cram D. J. *J. Inclusion Phenom.* **1988**, *6*, 397.
[31] Schmidtchen, F. P. *Coord. Chem. Rev.* **2006**, *250* (23-24), 2918–2928.
[32] Gale, P. A.; Busschaert, N.; Haynes, C. J. E.; Karagiannidis, L. E.; Kirby, I. L. *Chem. Soc. Rev.* **2014**, *43* (1), 205–241.
[33] Blondeau, P.; Segura, M.; Perez-Fernandez, R.; Mendoza, J. D. *ChemInform* **2007**, *38* (20).
[34] Atwood, J. L.; Steed, J. W. *Encyclopedia of supramolecular chemistry*; M. Dekker: New York, 2004.
[35] Bregović, B.; Basarić, N.; Mlinarić-Majerski, K. *Coord. Chem. Rev.*, 2015, **295**, 80–124.
[36] Fowler, C. J.; Haverlock, T. J.; Moyer, B. A.; Shriver, J. A.; Gross, D. E.; Marquez, M.; Sessler, J. L.; Hossain, M. A.; Bowman-James, K. *J. Am. Chem. Soc.* **2008**, *130* (44), 14386–14387.
[37] C. Schmuck and H. Y. Kuchelmeister in *Artificial Receptors for Chemical Sensors*, ed. V. M. Mirsky and A. K. Yatsimirsky, Wiley-VCH, **2010**, pp. 270–313.
[38] Kurzmeier, H.; Schmidtchen, F. P. *J. Org. Chem.* **1990**, *55* (12), 3749–3755.
[39] Metzger, A.; Lynch, V. M.; Anslyn, E. V. *Angew. Chem. Int. Ed.* **1997**, *36* (8), 862–865.
[40] Schmuck, C. *Chem. Eur. J.* **2000**, *6* (4), 709–718.
[41] Wild, U.; Roquette, P.; Kaifer, E.; Mautz, J.; Hübner, O.; Wadepohl, H.; Himmel, H. J. *Eur. J. Inorg. Chem.* **2008**, 1248–1257.
[42] Reed, A. E.; Curtiss, L. A.; Weinhold, F. *Chem. Rev.* **1988**, *88* (6), 899–926.
[43] Usama, A. *J. Mol. Struc.* **2011**, 11-19.
[44] Saxena, A.; Pike, R. D. *J. Chem. Crystallogr.* **2007**, 755.
[45] Sharma, S. *Synthesis* **1978,** 803-820.
[46] Toptschiew. *Arch. Pharm.* **1934**, vol. 272, p.775-778.
[47] Katritzky, A.; Rogovoy, B. *Arkivoc*, **2005**, 49-87.
[48] Harris, R. L. N. *Aust. J. Chem,* **1972,** 993-1001.

[49] Huang, R.; Xin, L.; Nan-feng, Z.; You-Si, Z.; Shun-Liu, D.; Hui-Ping, Z.; Su-Yuan, X.; La-Sheng, L.; Lan-Sun, Z. *J. Mol. Struc.* **2002,** 265-270.
[50] Shi, L.; Zou, P.; Zhu, D.; Chang, D. *Tetrahedron*, **2015**, 1684-1693.
[51] Paixao, J. A.; Silva, P. S. P.; Beja, A. M.; Silva M. R.; Vega, L. A. *Acta Crystallogr. Sect. C: Cryst. Struct. Commun.* **1998**, 54, 805.
[52] Beja, A.M.; Paixao, J. A.; Silva, P. S. P.; Vega, L. A.; Gomes E. M.; Martin-Gil, J. *Z. Kristallogr.* **1998**, *213*, 655.
[53] Data was fit using the applications available at supramolecular.org based on Thordarson, P. *Chem Soc. Rev.* **2011**, *40*, 1305-1323
[54] Custelcean, R. *Chem. Commun.* **2013**, *49*, 2173–2182
[55] Ravikumar, I.; Ghosh, P. *Chem. Soc. Rev.* **2012**, *41*, 3077–3098.
[56] Jadhav, V. D.; Herdtweck, E.; Schmidtchen, F. P.; *Angew. Chem.* **2008,** 6098.
[57] Berger, M.; Schmidtchen, F. P. *J. Am. Chem. Soc.* **1999**, *121* (43), 9986–9993.
[58] Işıklan, M.; Saeed, M. A.; Pramanik, A.; Wong, B. M.; Fronczek, F. R.; Hossain, M. A. *Cryst. Growth Des.* **2011**, *11* (4), 959–963.
[59] Watt, M. M.; Zakharov, L. N.; Haley, M. M.; Johnson, D. W. *Angew. Chem.* **2013**, *125* (39), 10465–10470.
[60] Stephan, H.; Gloe, K.; Schiessl, P.; Schmidtchen, F. *Supramol. Chem.* **1995,** 273.
[61] Kotha, S.; Lahiri, K.; Kashinath, D. *Tetrahedron*, **2002,** 9633-9695.
[62] Buchwald, S.; Ruiz-Castillo, P. *Chem. Rev.* **2016,** 12564-12649.
[63] Bartoli, G.; Palmieri, G.; Bosco, M.; Dalpozzo, R. *Tetrahedron Lett.* **1989**, 2129-2132.
[64] Lide, David R., ed. (2009). *CRC Handbook of Chemistry and Physics* (90th ed.). Boca Raton, Florida: CRC Press. ISBN 978-1-4200-9084-0.
[65] Langmuir, D.; Riese, A. C. *Geochim. Cosmochim. Acta* **1985**, 49, 1593−1601.
[66] Custelcean, R.; Sloop, F. V.; Rajbanshi, A.; Wan, S.; Moyer, B. A. *Cryst. Growth Des.* **2015**, *15* (1), 517–522.
[67] Jia, C.; Hay, B. P.; Custelcean, R. *Inorg. Chem.* **2014**, *53* (7), 3893–3898.
[68] Custelcean, R. *Chem. Soc. Rev.* **2014**, *43* (6), 1813.
[69] Mardirossian, N.; Lambrecht, D.; McCaslin, L.; Xantheas, S.; Head-Gordon, M. *J. Chem. Theory and Comp.* **2013,** 1368.
[70] Crist, R. H.; Fuller, E. C. *J. Am. Chem. Soc.* **1941,** 1644-1650.
[71] House, K.; Baclig, A.; Ranjan, M.; Nierop, E.; Wilcox, J.; Herzog, H. *PNAS*, **2011**, 20428.
[72] Zeman, F. *Environ. Sci. Technol.* **2014,** 11730.
[73] Direct air capture of CO_2 with chemicals: A technology assessment for the APS Panel on Public Affairs. American Physical Society, **2011**.
[74] Biermann, C. J. *Essentials of pulping and papermaking*; Academic Press: San Diego, 1993.
[75] Wang, T.; Lackner, K. S.; Wright, A. B. *Phys. Chem. Chem. Phys.* **2013**, *15* (2), 504–514.

[76] Dubey, P. K.; Kumar, V. R. *Indian J. Chem.* **2000,** 746.
[77] Martin, D.; Tittelbach, F. *Tetrahedron* **1983**, *39*, 2311–2314.
[78] Cantos, L.; Conchita, F.; John, J. *Can. J. Chem.* **2004,** 1649.
[79] Dakin, H. D.; Randolph, W. *J. Biol. Chem.* **1928,** 91.
[80] Toptschiew. *Arch. Pharm.* **1934**, vol. 272, p.775-778.
[81] Thordarson, *P. Chem. Soc. Rev*. **2011,** 1305–1323.
[82] Fowler, C. J.; Haverlock, T. J.; Moyer, B. A.; Shriver, J. A.; Gross, D. E.; Marquez, M.; Sessler, J. L.; Hossain, M. A.; Bowman-James, K. *J. Am. Chem. Soc.* **2008,** *130*: 14386-14387.
[83] Eli Lilly and Company, US 5077287 A1, January 18 1991.
[84] Campbell, T. W.; Monagle, J.; Foldi, V. *J. Am. Chem. Soc.* **1962**, 3673-3677.